ฤทธิ์การยับยั้งของตัวยับยั้งซีรีนโปรทีเนสแบบคาซาลจากกุ้งกุลาดำ *Penaeus monodon* และเครย์ฟิช *Pacifastacus leniusculus*

นายสุเชาวน์ ดอนพุดซา

วิทยานิพนธ์นี้เป็นส่วนหนึ่งของการศึกษาตามหลักสูตรปริญญาวิทยาศาสตรดุษฎีบัณฑิต
สาขาวิชาชีวเคมี ภาควิชาชีวเคมี
คณะวิทยาศาสตร์ จุฬาลงกรณ์มหาวิทยาลัย
ปีการศึกษา 2552

INHIBITORY ACTIVITY OF KAZAL-TYPE SERINE PROTEINASE INHIBITOR FROM THE BLACK TIGER SHRIMP *Penaeus monodon* AND CRAYFISH *Pacifastacus leniusculus*

Mr. Suchao Donpudsa

A Thesis Submitted in Partial Fulfillment of the Requirements

for the Degree of Doctor of Science Program in Biochemistry

Department of Biochemistry

Faculty of Science

Chulalongkorn University

Academic Year 2009

Thesis Title	INHIBITORY ACTIVITY OF KAZAL-TYPE SERINE PROTEINASE INHIBITOR FROM THE BLACK TIGER SHRIMP *Penaeus monodon* AND CRAYFISH *Pacifastacus leniusculus*
By	Mr. Suchao Donpudsa
Field of Study	Biochemistry
Thesis Advisor	Associate Professor Vichien Rimphanitchayakit, Ph.D.
Thesis Co-Advisor	Professor Anchalee Tassanakajon, Ph.D.
	Professor Kenneth Söderhäll, Ph.D.

Accepted by the Faculty of Science, Chulalongkorn University in Partial Fulfillment of the Requirements for the Doctoral Degree

..... Dean of the Faculty of Science
(Professor Supot Hannongbua, Dr.rer.nat.)

THESIS COMMITTEE

..... Chairman
(Professor Aran Incharoensakdi, Ph.D.)

..... Thesis Advisor
(Associate Professor Vichien Rimphanitchayakit, Ph.D.)

..... Thesis Co-Advisor
(Professor Anchalee Tassanakajon, Ph.D.)

..... Thesis Co-Advisor
(Professor Kenneth Söderhäll, Ph.D.)

..... Examiner
(Associate Professor Siriporn Sittipraneed, Ph.D.)

..... Examiner
(Associate Professor Suganya Soontaros, Ph.D.)

..... External Examiner
(Associate Professor Apinunt Udomkit, Ph.D.)

สุเชาวน์ ดอนพุดซา : ฤทธิ์การยับยั้งของตัวยับยั้งซีรีนโปรทีเนสแบบคาซาลจากกุ้งกุลาดำ *Penaeus monodon* และเครย์ฟิช *Pacifastacus leniusculus*. (INHIBITORY ACTIVITY OF KAZAL-TYPE SERINE PROTEINASE INHIBITORS FROM THE BLACK TIGER SHRIMP *Penaeus monodon* AND CRAYFISH *Pacifastacus leniusculus*) อ. ที่ปรึกษาวิทยานิพนธ์หลัก : รศ.ดร.วิเชียร ริมพณิชยกิจ, อ. ที่ปรึกษาวิทยานิพนธ์ร่วม : ศ.ดร.อัญชลี ทัศนาขจร, ศ.ดร. Kenneth Söderhäll, 115 หน้า.

ตัวยับยั้งซีรีนโปรตีเนสถูกพบในสิ่งมีชีวิตหลายชนิด มีบทบาทเกี่ยวข้องในภาวะธำรงดุล (homeostasis) ที่มีโปรตีเนสอยู่ในระบบ และเกี่ยวข้องในระบบภูมิคุ้มกันที่มีมาแต่กำเนิด ตัวยับยั้งซีรีนโปรตีเนสแบบคาซาล (KPI) ชนิดสองโดเมน 2 ตัว (KPI2 และ KPI8) ถูกพบในห้องสมุด cDNA จากเซลล์เม็ดเลือดของเครย์ฟิช *Pacifastacus leniusculus* ซึ่งต่างจาก KPI ชนิดอื่น ๆ ใน *Pacifastacus leniusculus* KPI 2 ชนิดนี้มีความจำเพาะต่อเซลล์เม็ดเลือดและประกอบด้วยกรดอะมิโนตำแหน่ง P_2 เป็นไกลซีน เพื่อเปิดเผยฤทธิ์การยับยั้ง ได้ผลิต KPI ทั้ง 2 ชนิด และแต่ละโดเมนของ KPI ในปริมาณมาก เมื่อทดสอบฤทธิ์การยับยั้งต่อ subtilisin, trypsin, chymotrypsin และ elastase พบว่า KPI2 มีฤทธิ์การยับยั้งต่อ subtilisin และมีฤทธิ์อย่างอ่อนต่อ trypsin ขณะที่ KPI8 มีฤทธิ์การยับยั้งต่อ trypsin ขณะที่โดเมนสองของ KPI2 และ KPI8 ซึ่งมีกรดอะมิโนตำแหน่ง P_1 เป็นซีรีนและไลซีน มีฤทธิ์การยับยั้งต่อ subtilisin และ trypsin ตามลำดับ การกลายพันธุ์ที่โดเมนหนึ่งของ KPI8 ที่กรดอะมิโนตำแหน่ง P_2 จากไกลซีนเป็นโพรลีน ซึ่งเลียนแบบกรดอะมิโนตำแหน่ง P_2 ของโดเมนสองของ KPI8 พบว่า ตัวกลายพันธุ์มีฤทธิ์ยับยั้งต่อ trypsin แสดงให้เห็นว่า กรดอะมิโนตำแหน่ง P_2 มีบทบาทที่สำคัญต่อฤทธิ์การยับยั้งของ KPI นอกจากนี้ยังพบว่า มีเพียง KPI2 ที่พบว่า มีฤทธิ์การยับยั้งต่อโปรทีเนสที่อยู่นอกเซลล์ของเชื้อราที่ทำให้เกิดโรคในเครย์ฟิชน้ำจืด (*Aphanomyces astaci*)

KPI ขนาด 5 โดเมน (SPI*Pm*2) จากกุ้งกุลาดำ *Penaeus monodon* ซึ่งอาจเกี่ยวข้องกับระบบภูมิคุ้มกันที่มีมาแต่กำเนิด SPI*Pm*2 ประกอบด้วยกรดอะมิโนตำแหน่ง P_1 คือ ทรีโอนีน, อะลานีน, กรดกลูตามิก, ไลซีน และกรดกลูตามิกตามลำดับ ถูกแยกได้จากห้องสมุด cDNA จากเซลล์เม็ดเลือด และพบว่ามีฤทธิ์การยับยั้งต่อ subtilisin และ elastase และมีฤทธิ์อย่างอ่อนต่อ trypsin เพื่อเปิดเผยฤทธิ์การยับยั้ง ได้ผลิตแต่ละโดเมนของ SPI*Pm*2 ในปริมาณมาก และทำให้บริสุทธิ์ จากการทดสอบฤทธิ์การยับยั้งต่อ subtilisin, trypsin และ elastase พบว่า โดเมน 1 ไม่มีฤทธิ์การยับยั้ง โดเมน 2, 3 และ 5 มีฤทธิ์การยับยั้งต่อ subtilisin โดเมน 2 มีฤทธิ์ยับยั้งต่อ elastase โดเมน 4 มีฤทธิ์ยับยั้งอย่างอ่อนต่อ subtilisin และ trypsin นอกจากนี้ยังพบว่า SPI*Pm*2 มีฤทธิ์ยับยั้งการเจริญต่อ *Bacillus subtilis* แต่ไม่ส่งผลต่อ *Bacillus megaterium*, *Staphylococcus aureus*, *Vibrio harveyi* 639 และ *Escherichia coli* JM109 การกลายพันธุ์ของ SPI*Pm*2 ที่ตำแหน่ง P'_2 ของโดเมน 1 และ 3 แสดงให้เห็นว่า กรดอะมิโนตำแหน่ง P'_2 ของ SPI*Pm*2 เกี่ยวข้องกับประสิทธิภาพการจับต่อโปรตีเนส เพื่อศึกษาการจัดเรียงตัวของยีน SPI*Pm*2 ได้ออกแบบไพรเมอร์ที่มีความจำเพาะต่อ SPI*Pm*2 เพื่อเพิ่มปริมาณยีนจากจีโนมโดยวิธีปฏิกิริยาลูกโซ่พอลิเมอเรส (พีซีอาร์) หาลำดับเบสของผลิตภัณฑ์พีซีอาร์ และเทียบกับ cDNA จากผลการทดลองพบว่า SPI*Pm*2 ประกอบด้วย 7 เอ็กซอน และ 6 อินทรอน ผลของ western blot ต่อเนื้อเยื่อต่าง ๆ ของกุ้งกุลาดำ โดยใช้แอนติบอดีต่อ SPI*Pm*2 เป็นตัวทดสอบ พบว่า SPI*Pm*2 พบที่เซลล์เม็ดเลือดเป็นส่วนใหญ่ นอกจากนี้ยังพบในปริมาณต่ำที่เหงือก, หัวใจ, เฮพิโพไดต์, กระเพาะอาหาร และต่อมน้ำเหลือง รวมทั้งยังพบในพลาสมาอีกด้วย เพื่อดูผลกระทบของ SPI*Pm*2 ต่อการจำลองตัวของ WSSV ได้ฉีดกุ้งกุลาดำด้วยรีคอมบิแนนต์ SPI*Pm*2 กับ WSSV พบว่า SPI*Pm*2 มีฤทธิ์ยับยั้งต่อ WSSV

ภาควิชา..... ชีวเคมี..... ลายมือชื่อนิสิต .....

สาขาวิชา..... ชีวเคมี..... ลายมือชื่ออ.ที่ปรึกษาวิทยานิพนธ์หลัก .....

ปีการศึกษา ..... 2552..... ลายมือชื่ออ.ที่ปรึกษาวิทยานิพนธ์ร่วม .....

ลายมือชื่ออ.ที่ปรึกษาวิทยานิพนธ์ร่วม .....

4772523523: MAJOR BIOCHEMISTRY
KEYWORDS : KAZAL-TYPE/KAZAL-TYPE SERINE PROTEINASE INHIBITOR/ /BLACK TIGER SHRIMP/*Penaeus monodon*

SUCHAO DONPUDSA: INHIBITORY ACTIVITY OF KAZAL-TYPE SERINE PROTEINASE INHIBITORS FROM THE BLACK TIGER SHRIMP *Penaeus monodon* AND CRAYFISH *Pacifastacus leniusculus*. THESIS ADVISOR: ASSOC PROF. VICHIEN RIMPHANITCHAYAKIT, Ph.D., THESIS CO-ADVISOR: PROF ANCHALEE TASSANAKAJON, Ph.D., PROF. KENNETH SÖDERHÄLL, 115 pp.

Serine proteinase inhibitors are found ubiquitously in living organisms and involved in homeostasis of processes using proteinases as well as innate immune defense. Two two-domain Kazal-type serine proteinase inhibitors, KPI2 and KPI8, have been identified from the hemocyte cDNA library of the crayfish *Pacifastacus leniusculus*. Unlike other KPIs from *P. leniusculus*, they are found specific to the hemocytes and contain an unusual P_2 amino acid residue, Gly. To unveil their inhibitory activities, the two KPIs and their domains were over-expressed. By testing against subtilisin, trypsin, chymotrypsin and elastase, the KPI2 was found to inhibit strongly against subtilisin and weakly against trypsin, while the KPI8 was strongly active against only trypsin. With its P_1 Ser and Lys, the KPI2_domain2 and KPI8_domain2 were responsible for strong inhibition against subtilisin and trypsin, respectively. Mutagenesis of KPI8_domain1 at P_2 amino acid residue from Gly to Pro, mimicking the P_2 residue of KPI8_domain2, rendered the KPI8_domain1 strongly active against trypsin, indicating the important role of P_2 residue in inhibitory activities of the Kazal-type serine proteinase inhibitors. Only the KPI2 was found to inhibit against the extracellular serine proteinases from pathogenic fungus of the freshwater crayfish, *Aphanomyces astaci*

The five-domain Kazal-type serine proteinase inhibitor SPI*Pm*2 from the black tiger shrimp *Penaeus monodon* is presumably involved in innate immune response. The SPI*Pm*2 with the domain P_1 residues Thr, Ala, Glu, Lys and Glu was isolated from the hemocyte cDNA libraries and found to strongly inhibit subtilisin and elastase, and weakly inhibit trypsin. To unravel further the inhibitory activity of each domain, we subcloned, over-expressed and purified each individual SPI domain. Their inhibitory specificities against trypsin, subtilisin and elastase were determined. Domain 1 was found to be inactive. Domains 2, 3 and 5 inhibited subtilisin. Domain 2 inhibited also elastase. Domain 4 weakly inhibited subtilisin and trypsin. The intact SPI*Pm*2 inhibitor was found to possess bacteriostatic activity against the *Bacillus subtilis* but not the *Bacillus megaterium*, *Staphylococcus aureus*, *Vibrio harveyi* 639 and *Escherichia coli* JM109. Domains 2, 4 and 5 contributed to this bacteriostatic activity. Mutagenesis of the P_2' residue of the domain 1 and domain 3 of SPI*Pm*2 revealed that P_2' position of Kazal-type SPI might involve in binding efficiency against proteinase. To delineate the genomic organization of the SPI gene, the primers specific to SPI*Pm*2 were designed to PCR amplify the genomic version of the gene. The amplified DNAs were sequenced and aligned with the cDNA clone. The results showed that the open reading frame of the gene contained 7 exons and 6 introns. Western blot using anti-SPI*Pm*2 of total proteins from different shrimp tissues revealed that the SPI*Pm*2 was mainly produced in the hemocytes though lower amount was found in gill, heart, epipodite, stomach and lymphoid. In addition, SPI*Pm*2 was found in the plasma. To determine the effect of SPI*Pm*2 on WSSV replication, the shrimp were injected with rSPI*Pm*2 and WSSV. It was found that SPI*Pm*2 had the anti-viral activity against WSSV.

Department .....Biochemistry..... Student's signature .....
Field of study.....Biochemistry..... Advisor's signature .....
Academic year .....2009..... Co-advisor's signature .....
Co-advisor's signature .....

ACKNOWLEDGEMENTS

This study was carried out during the past six years at the Department of Biochemistry, Faculty of Science, Chulalongkorn university. I wish to express my deepest gratitude to my advisor Associate Professor Dr. Vichien Rimphanitchayakit, and my co-advisor Professor Dr. Anchalee Tassanakajon and Professor Dr. Kenneth Söderhäll for their excellent guidance, enthusiasm, supervision, encouragement and support from the very beginning to the very end of my thesis. Especially I thank Associate Professor Dr. Vichien Rimphanitchayakit for endless patience and advice.

My gratitude is also extended to Professor Dr. Aran Incharoensakdi, Associate Professor Dr. Siriporn Sittipraneed, Associate Professor Dr. Suganya Soontaros and Associate Professor Dr. Apinunt Udomkit for serving as thesis committees, for their valuable comments and also useful suggestions.

My appreciation is also expressed to Dr. Premruethai Supungul, Dr. Siriporn Pongsomboon, Dr. Piti Amparyap, Dr. Kunlaya Somboonwiwat and Miss Sureerat Tang for warm support, instruction, lending helping and interesting discussion. Many thanks to all my friends of the Department of Biochemistry, especially in Center of Excellence for Molecular Biology and Genomics of Shrimp for their helps in the laboratory and friendships that help me enjoy and happy throughout my study. Special thanks to all shrimps for sacrifice their lives for my research.

I thank the Commission on Higher Education and the Chulalongkorn University grant to me for a very generous research support.

Finally, I wish to thank my deepest gratitude to my parents and members of my family for their love, care, understanding and encouragement extended throughout my study family for keeping my feet tightly on the ground and my mind away from science when I was at home. It’s always good to be the family.

CONTENTS

Page

Page

Page

Page

Page

LIST OF TABLES

Page

LIST OF FIGURES

Page

Page

Page

LIST OF ABBREVIATIONS

bp	base pair
dATP	deoxyadenosine triphosphate
dCTP	deoxycytosine triphosphate
DEPC	diethylpyrocarbonate
dGTP	deoxyguanosine triphosphate
DNA	deoxyribonucleic acid
dTTP	deoxythymidine triphosphate
EtBr	ethidium bromide
h	hour
kb	kilobase
KPI	Kazal-type serine proteinase inhibitor
M	molar
mg	milligram
ml	millilitre
mM	millimolar
MT	metric ton
ng	nanogram
nm	nanometre
O.D.	optical density (absorbance)
^{o}C	degree Celcius

ORF	open reading frame
PCR	polymerase chain reaction
RNA	ribonucleic acid
RT	reverse transcription
sec	second
SPI	serine proteinase inhibitor
μg	microgram
μl	microlitre
μM	micromolar
UTR	untranslated region
WSSV	white spot syndrome virus

CHAPTER I

INTRODUCTION

1.1 Immunity

All multicellular organisms need to protect themselves from the invasion of potentially harmful non-self substances. Traditionally, the immune system can be divided into two parts, innate and adaptive immunity (Kim, 2006).

1.1.1 Adaptive immunity

Adaptive immunity is a newcomer in the evolutionary scene. It appeared about 500 million years ago in vertebrates (Kim, 2006). The adaptive immune system is composed of highly specialized, systemic cells and processes that eliminate or prevent pathogenic challenges. Thought to have arisen in the first jawed vertebrates, the adaptive or "specific" immune system is activated by the “non-specific” and evolutionarily older innate immune system (which is the major system of host defense against pathogens in nearly all other living things). The adaptive immune response provides the vertebrate immune system with the ability to recognize and remember specific pathogens (to generate immunity), and to mount stronger attacks each time the pathogen is encountered. It is adaptive immunity because the body's immune system prepares itself for future challenges.

1.1.2 Innate immunity

The innate immune system is the first line of defense against bacterial, fungal, and viral pathogens (Hoebe et al., 2004) that helps to limit infection at an early stage. This defense system is essential for the survival and perpetuation of all

multicellular organisms (Hoffmann et al., 1999; Salzet, 2001). The vertebrates possess both adaptive and innate immune system whereas the invertebrates have only the innate immunity. Nevertheless, the invertebrates survive in a pathogen-laden environment without an adaptive immune system. The recognition of pathogens depends on a limited number of germ-line encoded receptors, which recognize conserved pathogen-associated molecular patterns (PAMPs) found in microorganisms such as bacterial lipopolysaccharide (LPS), peptidoglycan and β-1, 3-glucan (Figure 1.1) (Janeway Jr, 1998). Innate immune responses include phagocytosis, complement, antimicrobial peptides and proteinase cascades, which lead to melanization and coagulation (Kim, 2006).

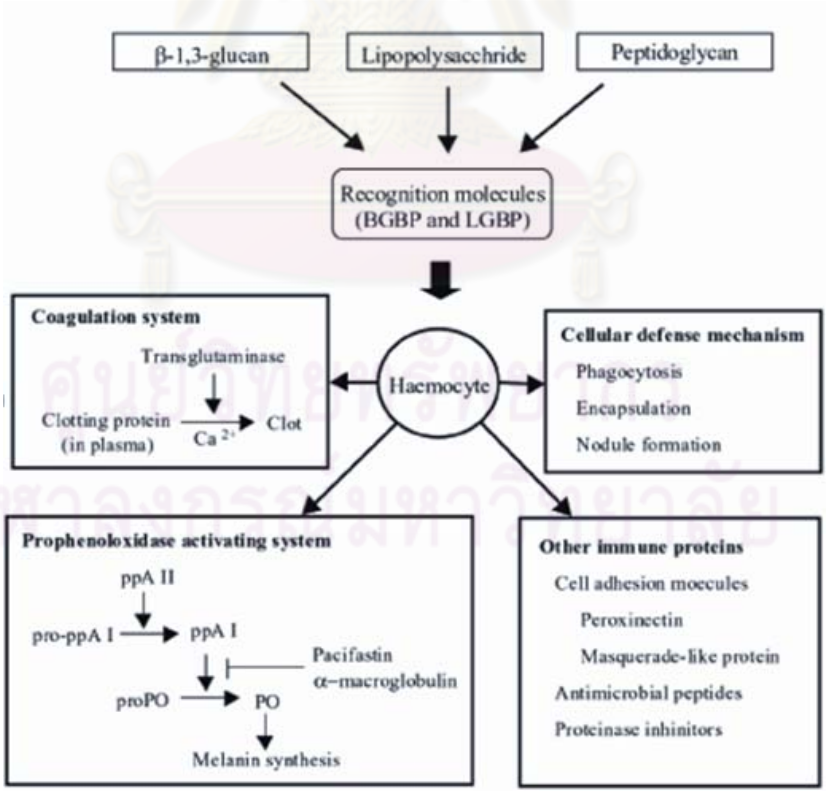

Figure 1.1 Schematic overview of crayfish defense reactions.

1.2 The crustacean immune system

The major defense systems of crustaceans are the innate immune response based on humoral and cellular components of the circulatory system. After pathogen infection, the recognition molecules may interact with and activate the haemocytes. Haemocytes are the effectors of the cellular immune response and they are also involved in the synthesis of the majority of humoral effectors (Figure 1.1). The direct participation of blood cells are demonstrated in phagocytosis, encapsulation, cell-mediated cytotoxicity and clotting. The humoral factors comprise molecules that act in the defense without direct involvement of cells, although many of the factors are originally synthesized and stored in the blood cells such as clotting proteins, agglutinins (e.g. lectins), hydrolytic enzymes and antimicrobial peptides.

1.2.1 Cell-mediated defense reactions

Cellular defense actions include phagocytosis, encapsulation and nodule formation (Millar, 1994). Phagocytosis is a phenomenon that appears to occur in all organisms, and includes attachment to the foreign body, ingestion and destruction. Encapsulation, a process wherein layers of cells surround the foreign material, occurs when a parasite is too large to be ingested by phagocytosis. Nodule formation, which appears similar to capsule formation, occurs when the number of invading bacteria is high. These structures, capsules and nodules, are always melanized in arthropods.

1.2.2 The prophenoloxidase (proPO) system

The proPO activating system consists of several proteins involved in melanin production, cell adhesion, encapsulation, and phagocytosis (Söderhäll et al., 1998; Sritunyalucksana et al., 2000).

In vitro studies have shown that phenoloxidase (PO) exists as an inactive precursor, prophenoloxidase (proPO), which is activated by a stepwise process involving serine proteases activated by microbial cell wall components, such as low quantities of lipopolysaccharides or peptidoglycans from bacteria and β-1,3-glucans from fungi, through pattern-recognition proteins (PRPs) (Ariki et al., 2004). An enzyme that is able to activate the proPO *in vivo* is termed prophenoloxidase activating enzyme (factor) (ppA, PPAE, PPAF) (Figure 1.2). In crayfish, ppA is a trypsin-like proteinase present as an inactive form in the haemocyte granules. After degranulation, the enzyme is released together with proPO and becomes an active form in the presence of microbial elicitors. The active ppA will convert proPO to an active form, phenoloxidase (PO) (Aspan et al., 1991; 1995). PO is a copper-containing protein and a key enzyme in melanin synthesis ((Söderhäll et al., 1998; Shiao et al., 2001). It both catalyses O-hydroxylation of monophenols to diphenols and oxidises diphenols to quinones, which can polymerise non-enzymatically to melanin. PO is a sticky protein and can adhere to the surface of parasites, which will lead to melanisation of the pathogen.

Melanisation is usually observed by blackening of the parasite in the hemolymph or black spots on the cuticle. The melanin and intermediates in the melanin formation can inhibit growth of microbial parasites, such as the crayfish plague fungus, *Aphanomyces astaci* (Söderhäll et al., 1982). The production of forming insoluble melanin deposits involving in the process of sclerotisation, wound healing and encapsulation of foreign materials (Theopold et al., 2004). To prevent excessive activation of the proPO cascade, proteinase inhibitors are needed for its regulation.

In the penaeid shrimp, enzymes of the proPO system are localized in the semigranular and granular cell (Perazzolo and Barracco, 1997). This is in agreement with a recent study showing that *P. monodon* proPO mRNA is expressed only in the haemocytes (Sritunyalucksana et al., 2000).

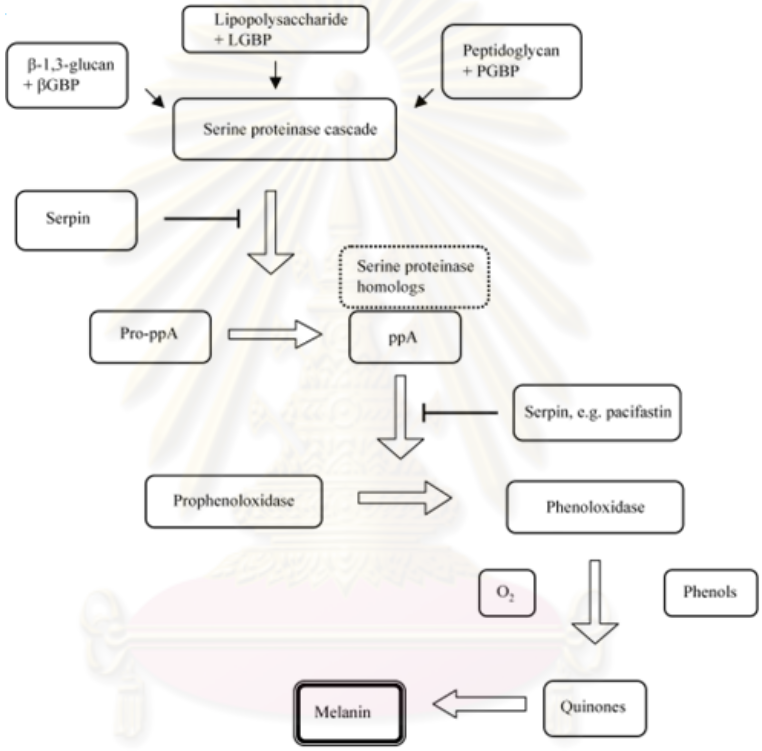

Figure 1.2 Overview of the arthropod prophenoloxidase (proPO)-activating system.

1.2.3 The coagulation system/the clotting system

Hemolymph coagulation is defense response of crustaceans that prevents both loss of hemolymph through breaks in the exoskeleton and the dissemination of bacteria throughout the body (Martin et al., 1991). It is a proteolytic cascade and is activated by microbial cell wall components. The coagulation system involves a plasma-clotting protein (CP) and a haemocyte-derived transglutaminase (TG)

(Kopacek et al., 1993; Yeh et al., 1998). The crayfish CP is a dimeric protein, whose subunits have both free lysine and glutamine residues for covalently linking to each other by TG. The CP is synthesized in the hepatopancreas and released into the hemolymph.

Transglutaminases (TG) are Ca^{2+}-dependent enzymes capable of forming covalent bonds between the side chains of free lysine and glutamine residues on clotting protein molecules in the presence of calcium ion to form a soft gel at the wound sites (Wang et al., 2001). In addition, they have assumed a wide variety of functions during development, differentiation and immune responses and post-translational protein remodeling (Greenberg et al., 1991; Aeschlimann and Pualsson, 1994).

In shrimp, TG is important for blood coagulation and post-translation remodeling of proteins. Synthesized and stored in young haemocytes (hyaline and semigranular cell), TG facilitates the instant release of TG and blood clotting following injury (Aono et al., 1996; Huang et al., 2004). TG activity was greatest in the hepatopancreas, then the heart, haemocytes and other organs (Huang et al., 2004). It sequence is homologous with that of factor XIIIa in the coagulation system. Recently, a shrimp second TG (STG II) was found from the tiger shrimp haemocyte cDNA. The STG II was characterized as a haemocyte TG that is involved in coagulation (Chen et al., 2005).

1.2.4 Antimicrobial peptides (AMPs)

The peptide antibiotics are defined as anti-microbial agents made by animals, including humans, with a function that is important for the innate immunity of that animal. Most of the AMPs are small in size, generally less than 150-200 amino

acid residues, amphipathic structure and cationic property. However, the anionic peptides also exist. For many of these peptides, there is evidence that one of the targets for the peptide is the lipid bilayer of the membrane. This is because these peptides can often increase the rate of leakage of the internal aqueous contents of liposomes. In addition, most of the antimicrobial peptides are cationic and their interaction with anionic phospholipids would provide a ready explanation for their specificity for bacterial membranes. With regard to the mechanism by which the peptide breaks down the membrane permeability barrier, it is possible that the peptide induces complete lysis of the organism by rupturing the membrane or perturbing the membrane lipid bilayer that allows the leakage of certain cellular components as well as dissipating the electrical potential of the membrane.

AMPs are active against a large spectrum of microorganisms; bacterial and filamentous fungi. In addition, some AMPs have antiviral or antiparasitic activities (Murakami et al., 1991; Hancock et al., 2000) and may also exhibit an anti-tumor property (Cruciani et al., 1991).

There are a few reports on antimicrobial peptides in shrimp. Penaeidins which act against Gram-positive bacteria and fungi were reported in *L. vannamei* (Destoumieux et al., 1997). The cDNA clones of penaeidin isoform were also isolated from the haemocytes of *L. vannamei*, *P. setferus* (Gross et al., 2001) and *P. monodon* (Supungul et al., 2004). Crustins, the antimicrobial peptides, were identified from *L. vannamei* and *L. setiferus*. Several isoforms of crustins were observed in both shrimp species. Like the 11.5 kDa antibacterial protein from *Carcinus maenas*, crustins from shrimp show no homology with other known antibacterial peptides, but possess sequence identity with a family of proteinase inhibitory proteins, the whey acidic

protein (WAP). Peptide derived from the hemocyanin of *L.vannamei, P. stylirostris* and *P. monodon* possessed antiviral activity has been identified (Destoumieux-Garzon et al., 2001; Patat et al., 2004; Zhang et al., 2004). Recently, the histones and histone-derived peptides of *L. vannamei* have been reported as an innate immune effectors because they can inhibit growth of Gram-positive bacteria (Patat et al., 2004).

1.3 Proteinase inhibitor

In multicellular organisms, serine proteinase inhibitors (SPIs) are essential factors involving in controlling the various proteinase mediated biological processes, such as the complement system, blood coagulation, melanization, apoptosis, etc. (Iwanaga et al., 2005; Jiravanichpaisal et al., 2006). Not only do they control the extent of deleterious protease digestion in such processes, they potentially fight as part of the humoral defence of the innate immune system against the invading pathogens (Christeller, 2005). Injury and microbial infection in vertebrates lead to activation of the blood coagulation and proPO systems. Both of these systems employ cascades of serine proteinases to amplify an initial signal (wounded tissue or the presence of microbial polysaccharides) resulting in rapid and efficient responses to the threats to health (O'Brien, 1993; Whaley, 1993). Blood clotting and phenoloxidase activation can also be harmful to the host if they are not limited as local and transient reactions. For this reason the proteinases in these systems are tightly regulated by proteinase inhibitors.

The SPIs are also involved in direct defense against proteinases from invading pathogens. For example, a subtilisin inhibitor, BmSPI, from *Bombyx mori* might function as an inhibitor to the microbial proteases and protected the silkworm pupae

from infection by pathogens (Zheng et al., 2007). Some microbial pathogens and parasites use the SPIs to counterdefense the host protective proteinases. For example, the oomycete *Phytophthora infestans*, a cause of disease in potato and tomato, produces an extracellular protease inhibitor to counter-defense the plant defensive proteinases (Tian et al., 2004; Tian et al., 2005). The obligate intracellular parasite of human *Toxoplasma gondii* produces a serine protease inhibitor to protect itself from the digestive enzymes during its residency in small intestine (Morris et al., 2002).

Some other SPIs are involved in reproductive processes. A male reproduction-related SPI is isolated from *Macrobrachium rosenbergii* with inhibitory activity on sperm gelatinolytic activity (Li et al., 2009). Another reproductive SPI was from the turkey male reproductive tract (Slowinska et al., 2008). For haematophagous insects such as *Dipetalogaster maximus* and *Triatoma infestans*, they secrete potent thrombin inhibitors dipetalogastin and infestin, respectively, to prevent blood clotting during blood meal (Campos et al., 2002; Mende et al., 2004).

Based on the primary and three-dimensional structures, topological functional similarities (Laskowski et al., 1980; Bode, 1992) and inhibition mechanisms, the proteinase inhibitors are classified into at least 18 families according to Laskowski and Qasim (Laskowski Jr et al., 2000). Among them, the following six families: Kazal, BPTI-Kunitz, α-macroglobulin, serpin, pacifastin and bombyx (Pham et al., 1996; Kanost, 1999; Simonet et al., 2002b) have been described in invertebrate haemolymph or also in saliva. Although the primary structure, with the number of amino acids ranging from 29 to approximately 400, and the structural properties of these inhibitors differ significantly, only two fundamentally different inhibiting mechanisms exist. Most inhibitors bind to their cognate enzyme(s) according to a common, substrate-like

standard mechanism. They are all relatively small (from 29 to 190 amino acids) and share an exposed, rigid binding loop with a very characteristic 'canonical' conformation (Laskowski et al., 1980; Bode, 1992).

One of the well-known SPIs is the Kazal-type SPIs (KPIs) which are grouped into family I1 (http://merops.sanger.ac.uk/) (Rawlings et al., 2004; Rawlings et al., 2008). The Kazal inhibitors are usually multi-domain proteins containing more than one Kazal domain. Each domain of 50–60 amino acid residues contains six well-conserved cysteine residues capable of forming three intra-domain disulphide bridges resulting in a characteristic three-dimensional structure (van de Locht et al., 1995). Each domain binds tightly and competitively via its reactive site loop to the active site of cognate proteinase rendering the proteinase inactive. Structural studies reveal that there are several contact positions responsible for the interactions between Kazal domains and the proteinases (Lu et al., 1997; Bode et al., 2000). However, the inhibitory specificity is determined mainly by the P1 amino acid residue resided at the second amino acid residue after the second cysteine residue of the domain.

1.4 Kazal-type SPIs (KPIs)

The invertebrate KPIs can be single or multiple domain proteins with one or more Kazal inhibitory domains linked together by peptide spacers of variable length. A typical or canonical Kazal domain is composed of 40–60 amino acid residues including some spacer amino acids. Generally, the vertebrate Kazal domains are slightly larger than the invertebrate ones but their domain architecture are quite similar. The Kazal motif has a general amino acid sequence of C-X_a-C-X_b-PVCG-X_c-Y-X_d-C-X_e-C-X_f-C where the subscripts *a*, *b*, *c*, *d*, *e* and *f* are integral numbers of

amino acid residues. Though a few amino acid residues in the Kazal motif are relatively conserved, most of them are quite variable both within and among the invertebrate species (Cerenius et al., 2010). Within the Kazal domain reside six well-conserved cysteine residues capable of forming three intra-domain disulfide bridges between cysteine numbers 1–5, 2–4, 3–6 resulting in a characteristic three-dimensional structure (Figure 1.3) (Krowarsch et al., 2003). There are one α-helix surrounded by an adjacent three-stranded beta-sheet and loops of peptide segments. The structure can be viewed as consisting of three loops A, B and C. The B loop harbours the specificity determining P_1 amino acid and the scissile peptide bond, and is, thus, called the reactive site loop. The convex reactive site loop is extended out providing easy access for the active site of the cognate proteinase to fit in and, then, get stuck. To emphasize on the scissile bond, a special numeral description of the primary structure of a Kazal domain is generally used. The numerals start from P_1, P_2, P_3, … to the N-terminus and P_1', P_2', P_3', … to the C-terminus (Schechter and Berger, 1967; Jering and Tschesche, 1976).

The Kazal proteinase inhibitory domain inhibits the proteinase by a standard mechanism (Laskowski and Kato, 1980). Each Kazal domain acts as a substrate analogue that stoichiometrically binds competitively through its reactive site loop to the active site of cognate proteinase forming a relatively stable proteinase–proteinase inhibitor complex, much more stable than the Michaelis enzyme–substrate complex. Though the binding is non-covalent, it is very tight as the association constant is extremely high (10^7–10^{13} M^{-1}) and, therefore, the inhibition is very strong. In invertebrate, the typical inhibition constants (K_is) are in the range of nanomolar compared to the millimolar range of K_m values of the synthetic proteinase substrates

(Somprasong et al., 2006; Wang et al., 2009; Visetnan et al., 2009; Li et al., 2009a; Li et al., 2009b; González et al., 2007a; González et al., 2007b; Campos et al., 2002).

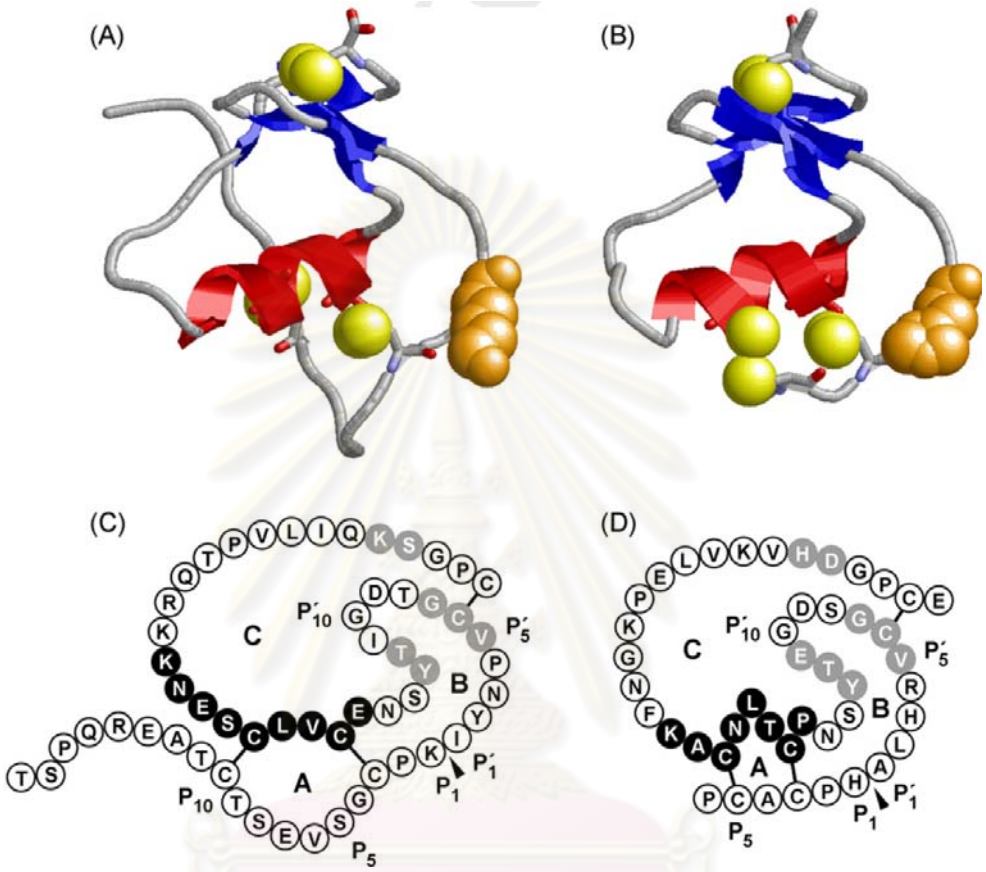

Figure 1.3. Structural comparison of Kazal proteinase inhibitors from vertebrate and invertebrate. The structure of porcine pancreatic secretory inhibitor derived from the PDB file 1TGS (Bolognesi et al., 1982) (A) with its covalent primary structure (C) is a representative of vertebrate KPIs. The structure of rhodniin domain 1 derived from the PDB file 1TBQ (van de Locht et al., 1995) (B) and its covalent primary structure (D) is used as representative for invertebrate KPIs. The structures are derived from their complexes with cognate proteinases. Helices and sheets are shown in red and blue but in black and gray circles in the covalent primary structures, respectively. The sulphur atoms are presented as yellow balls. The space-filled side chains of the P1 amino acids are in orange colour. The scissile peptide bonds are indicated by arrows.

1.5 Biological and physiological functions of KPIs

The KPIs are believed to play regulatory roles in the processes that use serine proteinases. However, it is not easy to define their biological functions in a complex

biological system like in the higher eukaryotes. Also very little work has been done to pursue the roles of these KPIs. Nevertheless, the origin of KPIs, the target proteinases and the inhibitory specificities can be used as clues to the actual functions of the KPIs.

1.5.1 Blood feeding

Hematophagous animals such as leeches, mosquitoes, ticks and bugs, feed on blood and are in need of anticoagulants to prevent the blood from clotting during their blood meal drawn from their prey or digestion of blood in their gut. They actively synthesize the anticoagulants and secreted into the saliva or stomach juice.

The European medical leech *Hirudo medicinalis* and some other leech species have been used for clinical bloodletting for thousands of years because they can prevent blood clotting, thereby stimulate the blood circulation. Nowadays, they are used in medicine to stimulate blood flow in the area of injuries or surgeries where the blood veins are damaged. The ability to prevent blood clotting of the leeches has been investigated extensively in search for the anticoagulants to be used for medical therapy. Besides the hirudin, a non-Kazal specific thrombin inhibitor, which is a potent anticoagulant and now used in medicine to prevent thrombosis in patients (Nowak et al., 2007), two one-domain "non-classical" Kazal-type proteinase inhibitors, namely the bdellin B-3 and leech-derived tryptase inhibitor (LDTI) are also isolated from the medical leech *Hirudo medicinalis* (Sommerhoff et al., 1994; Fink et al., 1986). The bdellin B-3 with it P_1 Lys is able to inhibit trypsin, plasmin and sperm acrosin while the LDTI with the same P_1 Lys inhibits trypsin and chymotrypsin. The LDTI is not involved in the blood coagulation since it does not inhibit any of the proteases in the cascade (Fritz and Sommerhoff, 1999). The bdellin B-3 with its inhibitory activity against plasmin prevents the plasmin-mediated platelet activation

that leads to platelet clot (Quinton et al., 2004). The bdellin B-3, thus, helps the hirudin to completely block the coagulation.

The blood-sucking triatomine bug *Rhodnius prolixus* synthesizes a double-headed Kazal-type proteinase inhibitor, rhodniin, to prevent the host blood coagulation. It is a high affinity inhibitor highly specific for thrombin (Friedrich et al., 1993). Another blood-sucking insect *Dipetalogaster maximus* produces a cDNA coding for a six-domain Kazal-type thrombin inhibitor, dipetalogastin. The natural dipetalogastin is double-headed of domains 3 and 4 with the P_1 Arg and Asp, respectively. The natural inhibitor strongly inhibits thrombin (Mende et al., 1999; 2004). The domain 3 is responsible for the inhibitory activity against thrombin (Schlott et al., 2002).

Still another blood-sucking bug *Triatoma infestans* which is the most important vector of Chagas disease expresses a Kazal-type thrombin inhibitor infestin in the midgut. The full-length cDNA encodes seven Kazal domains but the natural infestins identified so far are the one-domain KPI, named the infestin 1R, corresponding to domain 1 and the double-headed KPI, named the infestin 1-2, corresponding to domains 4 and 5 (Campos et al., 2002; Lovato et al., 2006). The native infestin 1R with its P_1 Leu does not have anticoagulation activity. It inhibits neutrophil elastase, subtilisin A, proteinase K and chymotrypsin but not thrombin (Lovato et al., 2006). The native infestin 1-2 with its P_1 Arg and Asn inhibits thrombin and trypsin (Campos et al., 2002). The recombinant infestin 3-4 and 4 with the P_1 Lys and Arg corresponding to domains 6 and 7 inhibit trypsin, plasmin, factor XIIa and factor Xa. Particularly, the recombinant infestin 4 exhibits very strong

anticoagulant activity (Campos et al., 2004b). Thus, the infestin in the midgut plays an important role as anticoagulant during the ingestion of blood meal in *T. infestans*.

Brasiliensin, an eight-domain KPI from a related blood-sucking bug *Triatoma brasiliensis*, is very similar to infestin (Araujo et al., 2007). The reduction of brasiliensin in the midgut by RNA interference reduces the ingestion of blood stressing the important role of anticoagulant in blood feeding in these *Triatoma* bugs.

1.5.2 Reproduction

In the male reproductive tract especially the vas deferens of the prawn *Macrobrachium rosenbergii*, a Kazal-type peptidase inhibitor (MRPINK) is expressed (Cao et al., 2007). By using suppression subtractive hybridization technique, a cDNA of the MRPINK was cloned. The cDNA sequence indicated that the MPPINK was a double-headed KPI with the P_1 Leu and Pro. As expected from the P_1 amino acids, the MRPINK inhibits chymotrypsin but not trypsin or thrombin. Domain 2 (MRTKPIa-1) is solely responsible for this inhibition and domain 1 (MRTKPIa-1) seems to be inactive (Li et al., 2009a). The MRPINK also has an inhibitory effect on the gelatinolytic activity of sperms supposedly catalyzed by a *M. rosenbergii* sperm gelatinase (MSG) (Li et al., 2008). Therefore, the MRPINK may be involved in the male reproductive process and further investigation is needed.

1.5.3 Prevention of excessive autophagy

A tightly regulated process that cell degrades and recycles its own components using lysosome is called autophagy. Excessive autophagy was observed in gland cells and endodermal digestive cells of *Hydra magnipapillata* when the expression of an evolutionarily conserved gene *Kazal1* was silenced through double-stranded RNA feeding (Chera et al., 2006). The *Kazal1* is a three-domain KPI (P_1 Met,

Arg and Arg) expressed from the gland cells. The *Kazal1* silencing affects homeostatic conditions, for instances disorganization and death of gland cells and highly vacuolation of digestive cells. The final result of prolonged *Kazal1* silencing is death. Therefore, the *Kazal1* gene is required for the modulation of autophagy like the pancreatic secretory trypsin inhibitor *SPINK1* and *SPINK3* genes in human and mice, respectively (Masaki et al., 2009).

1.5.4 Protection from microbial destruction

To protect their cocoons from predators and microbial degradation, the wax moth *Galleria mellonella* produces two types of proteinase inhibitors from the silk glands, which are found as components in the cocoon silk besides the major silk proteins, fibroins and sericins, and a few other proteins. The two serine proteinase inhibitors belong to the Kunitz and Kazal families named silk proteinase inhibitors 1 (GmSPI 1) and 2 (GmSPI 2), respectively (Nirmala et al., 2001a). Both serine proteinase inhibitors are single-domain proteins, which inhibit subtilisin and proteinase K. Two similar serine proteinase inhibitors, a Kunitz-type BmSPI 1 and Kazal-type BmSPI 2, are also present in the cocoon silk of *Bombyx mori* (Nirmala et al., 2001b). The Kazal domain of GmSPI 2 is atypical lacking the 1–5 disulfide bridge. The presence of serine proteinase inhibitors and their activities against the bacterial subtilisin and fungal proteinase K in the cocoon silk suggests the protection of silk cocoon from the microbial proteinases.

1.5.5 Protection against pathogen proteinases and antimicrobial activity

It is well known that many invasive pathogens produce extracellular proteinases as virulent factors during the development of the infectious diseases for they help to penetrate through physical barrier of their hosts (Travis eet al., 1995;

Christeller, 2005). To defend against such pathogens, the host organisms produce the proteinase inhibitors to combat the microbial proteinases. Some of these inhibitors also exhibit antimicrobial activity.

One of the four KPIs from the hepatopancreas of Chinese white shrimp, *Fenneropenaeus chinensis*, namely FcSPI-1, is able to inhibit the microbial proteinases, subtilisin and proteinase K, indicating that the KPI may participate in the immune defense response (Wang et al., 2009). Besides, the FcSPI-1 can also inhibit the chymotrypsin from the Chinese white shrimp suggesting that it may function as a regulator of the shrimp proteinase activity.

In *Hydra magnipapillata*, the endodermal gland cells are involved in innate immunity by producing a three-domain KPI, kazal2 (Augustin et al., 2009). The KPI strongly inhibits trypsin and subtilisin, and possesses bactericidal activity against *Staphylococcus aureus*. The observations that the KPIs can inhibit or even kill the bacteria may indicate another mechanism of host defense led by the KPIs as well as other serine protease inhibitors.

The potential role of several KPIs in invertebrate immunity can also be implied from their responses against microbial challenge. Semi-quantitative RT-PCR or quantitative real time RT-PCR analysis were performed and showed that the mRNA expression of invertebrate KPIs was up-regulated upon bacteria or viral challenges. Nevertheless, the actual functions of the up-regulated KPIs are to be confirmed by further investigation. A few examples are as follows. A mollusk KPI (AISPI) mRNA from the bay scallop *Argopecten irradians* which encodes a six-domain KPI is up-regulated after *Vibrio anguillarum* injection (Zhu et al., 2006). A twelve-domain KPI gene from the Zhikong scallop *Chlamys farreri* (CfKZSPI) is

highly expressed after *V. anguillarum* challenge (Wang et al. 2008). A double-headed KPI from the hemocyte cDNA library of the oriental white shrimp *Fenneropenaeus chinensis* is up-regulated in shrimp infected with the white spot syndrome virus (WSSV) (Kong et al., 2009).

1.5.6 Protection from host proteinases

Toxoplasma gondii is an obligate intracellular parasitic protozoon which infects almost all warm blooded animals as intermediate hosts. The definitive host, however, is the feline. The infection occurs via oral route when a person ingests meat contaminated with the oocysts or the parasites. The parasites pass through the digestive system where the epithelial cells of intestine are infected. The parasites in the infected intestinal epithelium produce more oocysts for new infection and spreading through faeces. Being transit through and multiply in the digestive tract, the parasite produces protease inhibitors to protect itself from the proteolytic enzymes found within the lower intestine. The parasite produces a four-domain KPI, namely the *Toxoplasma gondii* protease inhibitor 1 (TgPI-1) which strongly inhibits trypsin, chymotrypsin, pancreatic elastase and neutrophil elastase (Pszenny et al., 2000; Morris et al., 2002). The natural TgPI-1 probably functions as two double-headed KPIs. The protection against digestive enzymes gives the parasite an opportunity to proliferate in the intestine before disseminating to other host tissues. The parasite also produces another four-domain KPI, namely TgPI-2, which inhibits only trypsin. The actual function of TgPI-2 is not known (Morris and Carruthers, 2003).

In *Neospora caninum*, a closely related species of *T. gondii*, the parasite produces a single-domain KPI, NcPI-S, that inhibits potently the subtilisin but has no

or low inhibitory activities against trypsin, chymotrypsin and elastase (Morris et al., 2004; Bruno et al., 2004). The function of NcPI-S is not known either.

1.6 Objectives of the thesis

In *Penaeus monodon*, Kazal proteinase inhibitors were found at least nine types from the expressed sequence tag (EST) database (http://pmonodon.biotec.or.th/) particularly the hemocyte libraries (Supungul et al., 2002; Tassanakajon et al., 2006; Visetnan et al., 2009). The most abundant SPI is the five Kazal-domain SPI*Pm*2. SPI*Pm*2, SPI*Pm*4 and SPI*Pm*5 were over-expressed and its activity has been studied (Somprasong et al., 2006; Visetnan et al., 2009). The recombinant SPI*Pm*2 exhibits strong inhibitory activity against subtilisin and elastase, weak inhibitory activity against trypsin, and no activity against chymotrypsin. SPI*Pm*5 showed inhibitory activities against subtilisin and elastase. SPI*Pm*4 inhibited subtilisin. It turns out that the inhibitory specificities can not be assigned to all Kazal SPI domain of the SPI*Pm*2. It is then interesting to find out the inhibitory specificity of each Kazal domain. In this study, each domain of SPI*Pm*2 was individually over-expressed and tested for their inhibitory specificities. As compared to the intact recombinant SPI*Pm*2 inhibitor, their growth inhibition on bacteria were also elucidated and reported herein. Therefore, we have investigated SPI*Pm*2 for tissue distribution, anti-viral activity and genomic organization. The site directed mutagenesis of the domain1 and 3 of SPI*Pm*2 of the $P_{2'}$ residues was also carried out to show its essence for the inhibitory activity.

In the freshwater crayfish *P. leniusculus*, there are about 12 KPI transcripts present (Cerenius et al., 2010) and, interestingly, one of these, KPI2, is a marker for one type of blood cells, namely the semigranular cells. Another KPI, KPI8, is found in only mature hemocytes (semigranular and granular cells). Those KPIs have, therefore,

been used to track the hemocyte synthesis along the lineage from hematopoietic stem cells to the mature blood cells (Wu et al., 2008; Cerenius et al., 2010). The two major extracellular serine proteinases, subtilisin and trypsin-like enzymes, were found in *Aphanomyces astaci* (Bangyeekhun et al., 2001). Three proteinase inhibitors from crayfish inhibited the extracellular proteinase from *Aphanomyces spp* (Dieguez-Uribeondo and Cerenius, 1998). In this thesis, we have investigated two KPIs, KPI2 and KPI8, from the freshwater crayfish *Pacifastacus leniusculus* for their inhibitory specificities and the kinetics of their inhibition. These KPIs were characterized by their unusual P_2 residues and site directed mutagenesis of one of the P_2 residues was also carried out to show its essence for the inhibitory activity. Therefore, these KPIs were tested the inhibitory activities against extracellular fungal proteinase from *Aphanomyces astaci*.

CHAPTER II

MATERIALS AND METHODS

2.1 Materials

2.1.1 Equipments

Autoclave model # LS-2D (Rexall industries, Taiwan)

Automatic micropipettes P10, P100, P200 and P1000 (Gilson Medical Electrical S.A., France)

Balance Satorius 1702 (Scientific Promotion)

Gel documentation (Syngene)

Innova 4080 incubator shaker (New Brunswick Scientific)

LABO Autoclave (Sanyo)

Laminar Airflow Biological Safety Cabinets Class II Model NU-440-400E (NuAire, USA)

Microtiter plate reader (BMG Labtech)

PCR thermal cycler: DNA Engine (MI Research, USA)

PD-10 column (GE Healthcare)

pH meter model # SA720 (Orion)

Pipette tips 10, 20, 200, and 1000 µl (Bio-RAD, USA)

Refrigerated microcentrifuge Kubota 1300 (Kubota, Japan)

Refrigerated microcentrifuge MIKRO 22R (Hettich Zentrifugen, Germany)

Spectrophotometer: Spectronic 2000 (Bausch & Lomb)

Spectrophotometer DU 650 (Beckman, USA)

Transilluminator 2011 Macrovue (LKB)

Trans-Blot® SD (Bio-Rad, USA)

Vacuum blotter Model # 785 (Bio-RAD, USA)

Vacuum pump (Bio-RAD, USA)

Vertical electrophoresis system (Hoefer™ miniVE)

Whatman® 3 MM Chromatography paper (Whatman International, England)

White/UV transilluminator: UVP ImageStore 7500 (Mitsubishi Electric Corporation, Japan)

2.1.2 Chemicals and Reagents

100 mM dATP, dCTP, dGTP, and dTTP (Fermentas)

5-bromo-4-chloro-indolyl phosphate (BCIP) (Fermentas)

Agarose (Sekem)

Alkaline phosphatase-conjugated rabbit anti-mouse IgG (Jackson ImmunoResearch Laboratories)

Anti-His antiserum (GE Healthcare)

GeneRuler™ 100bp DNA ladder (Fermentas)

Isopropyl-β-D-thiogalactoside (IPTG) (Fermentas)

Trizol reagent (Gibco BRL)

2.1.3 Kits

ImProm-II™ Reverse Transcription system kit (Promega)

NucleoSpin® Extract II kit (Macherey-Nagel)

QIAprep spin miniprep kit (Qiagen)

QuickChange Site-Directed Mutagenesis Kit (Stratagene)

RevertAid™ First Strand cDNA Synthesis Kits (Fermentas)

T & A Cloning Vector kit (RBC)

2.1.4 Enzymes

Ampli*Taq* DNA Polymerase (Fermentas)

*Bam*HI (Biolabs)

α-Chymotrypsin, bovine pancreas (Sigma)

DyNAzyme_II DNA Polymerase (Finnzymes)

Elastase, porcine pancreas (Pacific Science)

*Eco*RI (Biolabs)

Enterokinase, light chain (Biolabs)

*Hin*dIII (Biolabs)

*Nco*I (Biolabs)

*Not*I (Biolabs)

RNase A (Sigma)

RQ1 RNase-free DNase (Promega)

*Sal*I (Biolabs)

subtilisin Carlsberg, *Bacillus licheniformis* (Sigma)

T4 DNA Ligase (Fermentas)

T4 DNA Polymerase (Fermentas)

Trypsin, bovine pancreas (Sigma)

*Xho*I (Biolabs)

2.1.5 Substrate

N-benzoyl-Phe-Val-Arg-*p*-nitroanilide (Sigma)

N-succinyl-Ala-Ala-Ala-*p*-nitroanilide (Sigma)

N-succinyl-Ala-Ala-Pro-Phe-*p*-nitroanilide (Sigma)

2.1.6 Antibiotic

Ampicillin

Chloramphenicol

Kanamycin

Tetracycline

2.1.7 Bacterial strains

Bacillus megaterium

Bacillus subtilis

Escherichia coli JM109

Escherichia coli XL-1 Blue MRF´

Escherichia coli Rosetta(DE3)pLysS

Staphylococcus aureus

Vibrio harveyi 639

2.1.8 Software

BlastX (http://www.ncbi.nlm.nih.gov/blast/Blast.cgi)

Clustal X (Thompson, 1997)

ExPASy ProtParam (http://au.expasy.org/tools/protparam.html)

GENETYX version 7.0 program (Software Development Inc.)

SECentral (Scientific & Educational Software)

SignalP 3.0 Server (http://www.cbs.dtu.dk/services/SignalP/)

SMART (http://smart.embl-heidelberg.de/smart/set_mode.cgi.GENOMIC=1)

Penaeus monodon EST database (http://pmonodon.biotec.or.th/home.jsp)

2.1.9 Vector

pET28b(+)

pVR500, a pET32a(+) derivative

2.2 Recombinant protein expression for Kazal-typed serine proteinase inhibitors SPI*Pm*2, KPI2, KPI8, and their domains

2.2.1 Construction of the expression plasmid

For the sake of protein purification, a modified expression vector pVR500 was constructed from an expression vector pET-32a(+) by deleting the His·Tag and S·Tag between *Msc*I and *Kpn*I sites (Figure 2.1). The only His·Tag left was at the 3' side of the reading frame and used for the protein purification as described below. The pET-32a(+) was digested with *Msc*I and *Kpn*I, treated with T4 DNA polymerase to blunt the DNA ends and religated. The resulting pVR500 was sequenced to confirm the correct construction. By using the expression vector pVR500, the cloned gene was fused with the thioredoxin Trx·Tag at the N-terminal side and His·Tag at the C-terminal end.

For protein expression of each domain of SPI*Pm*2, PCR primers were designed for the PCR amplification of SPI domains from the pSPI*Pm*2-NS2, a

pET22b(+) containing the SPI*Pm*2 gene (Somprasong et al., 2006). The forward and reverse primers contain *Nco*I and *Xho*I sites at their 5' terminal ends, respectively. The restriction sites were for the cloning of SPI domain into the expression vector. The primer sequences and their annealing sites are depicted in Table 2.1 and Figure 2.2. The PCR reaction was carried out in a final volume of 30 µl containing 25 ng of DNA

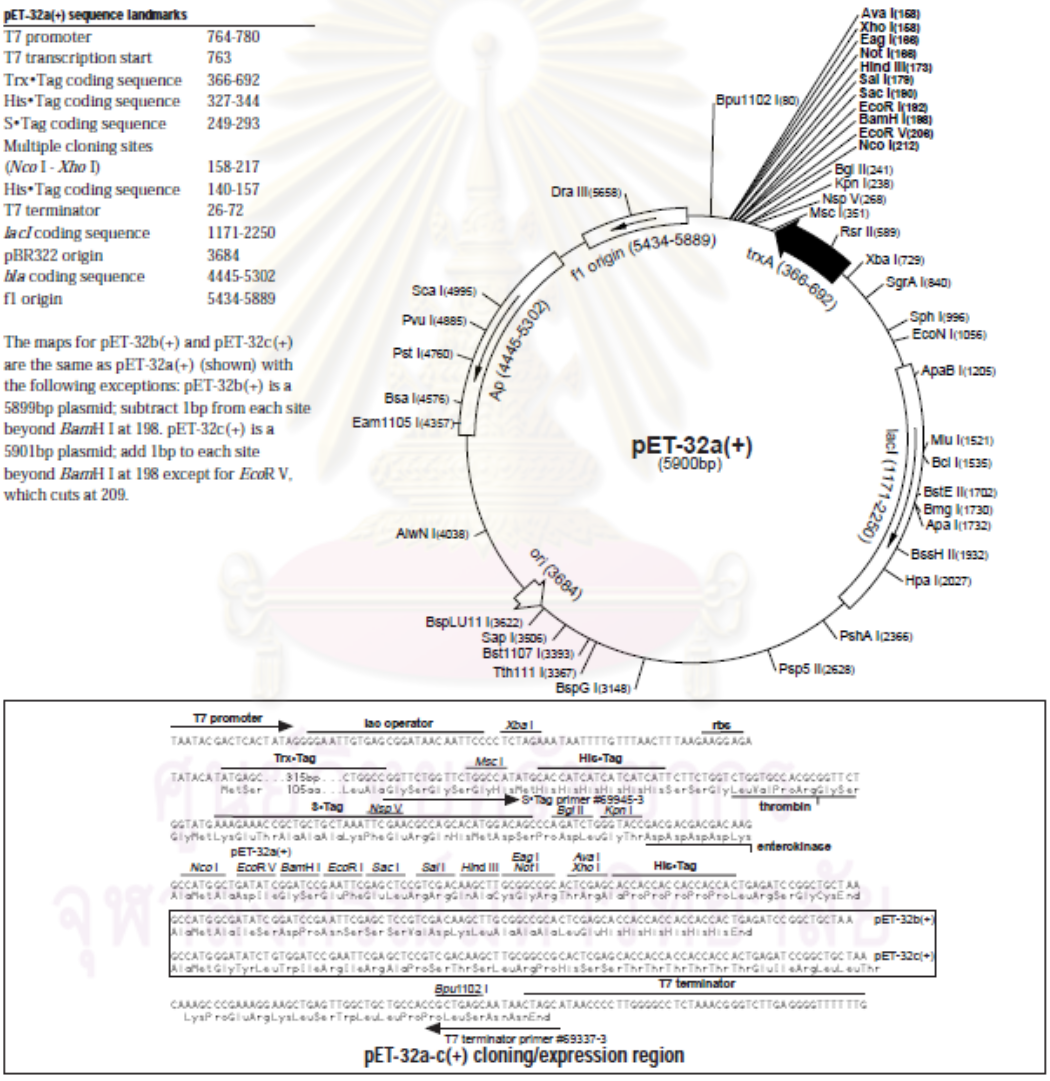

Figure 2.1 The pET-32a(+) vector map (Novagen®, Germany). The pVR500 was constructed by deleting the His_Tag and S_Tag between MscI and KpnI sites. The only His_Tag left was at the 30 side of the reading frame and used for the protein purification as described below. The pET-32a(+) was digested with MscI and KpnI, treated with T4 DNA polymerase to blunt the DNA ends and relegated.

template, 0.45 μM of each primer, 0.2 mM of each dNTP and 0.45 units of *Pfu* polymerase (Promega). The PCR amplification was run for 30 cycles of 45 s at 94 °C, 45 s at 55 °C and 60 s at 72 °C. The PCR product was gel-purified, digested with *Nco*I and *Xho*I and cloned into the pVR500 vector at the same restriction sites. The sequences of the domain clones were verified by DNA sequencing. Each recombinant plasmid was transformed into an *E. coli* Rosetta(DE3)pLysS for over-production of the recombinant protein.

For protein expression of KPI2, KPI8 and their domains, total RNA and cDNA from the hemocytes of *P. leniusculus* was prepared as described by Liu et al. (2006). The two Kazal-type serine protienase inhibitor genes, KPI2 (GenBank Accession EU433325) and KPI8 (GenBank Accession CF542313) and their domains were amplified by PCR technique using the KPI-specific primers. The primers were designed such that the signal peptides predicted by the online Signal Peptide Prediction (http://bmbpcu36.leeds.ac.uk/prot_analysis/Signal.html) were excluded. Each forward primer contained *Nco*I site at its 5' terminal end. Each reverse primer contained the 6×His tag, stop codon and *Not*I site, respectively. The primer sequences and their annealing sites are depicted in Table 2.2 and Fig. 2.3. The PCR reactions were carried out in a final volume of 25 μl containing 150 ng of cDNA template, 0.2 μM of each primer, 0.2 mM of each dNTP and 1 units of Phusion DNA polymerase (Finnzymes). The reactions were pre-heated at 98 °C for 2 min before the PCR amplification was run for 34 cycles of 10 s at 98 °C, 20 s at 50 °C and 30 s at 72 °C. The final extention was at 72 °C for 5 min. The PCR product was gel purified, digested with *Nco*I and *Not*I and cloned into the *Nco*I and *Not*I linearized pVR500

vector. The recombinant plasmids were verified by DNA sequencing. Each recombinant plasmid was transformed into an *E. coli* Rosetta gami B (DE3) for over-production of the recombinant protein.

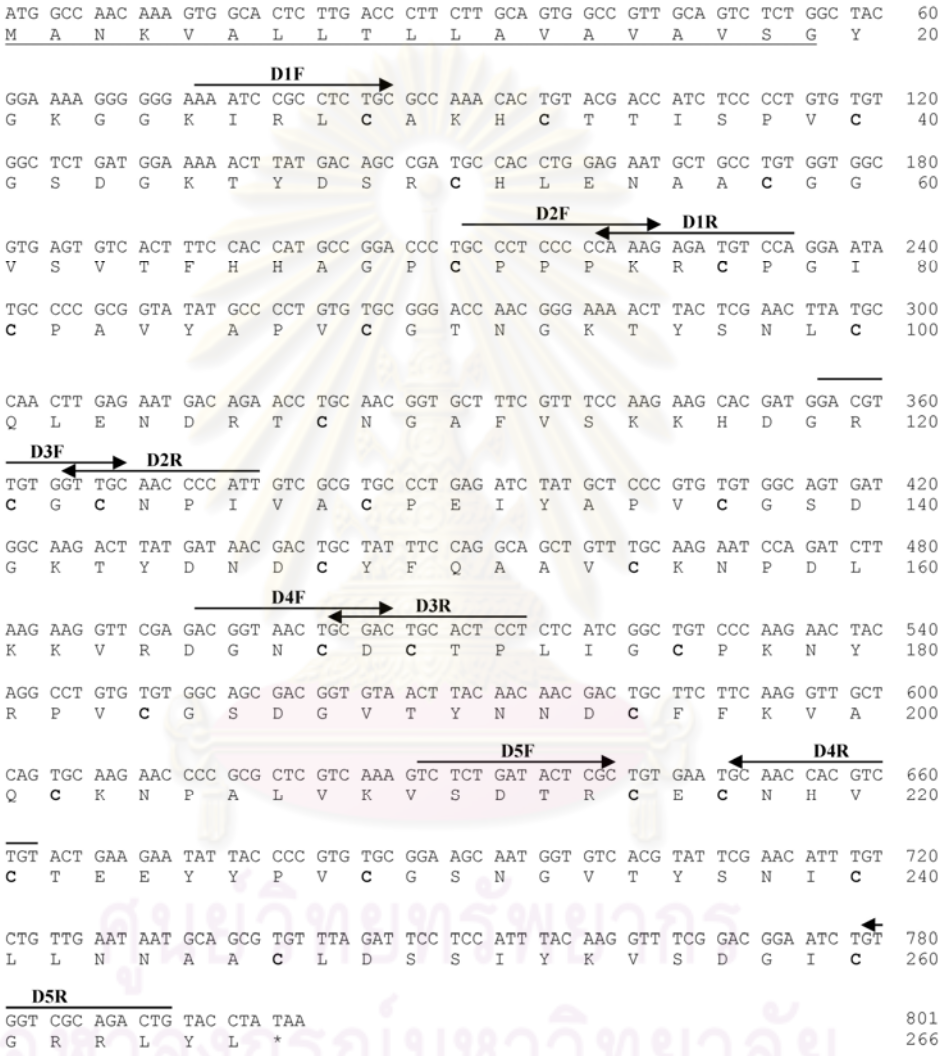

Figure 2.2. The nucleotide and amino acid sequences of SPI*Pm*2. The annealing sites of primers used to amplify each inhibitory domain for the cloning into an expression vector. The SPI domains 1-5 are represented by D1-D5. The F and R letters indicate forward and reverse direction as also represented by the directions of arrows. The cysteine residues and signal sequence are bold-faced and underlined, respectively.

Table 2.1. Nucleotide sequences of primers for PCR amplification of the Kazal domains of SPI*Pm*2.

Primer[a]	Sequence (5'-3')[b]
1F	AAAGCCATGGAAATCCGCCTCTGC
1R	GGCACTCGAGTGGACATCTCTTTG
2F	GCCGCCATGGGCCCTCCCCCAAAG
2R	GGCACTCGAGAATGGGGTTGCAAC
3F	AAGCCCATGGGACGTTGTGGTTGC
3R	AGCCCTCGAGAGGAGTGCAGTCGC
4F	AAGGCCATGGACGGTAACTGCGAC
4R	ATTCCTCGAGACAGACGTGGTTGC
5F	CTCGCCATGGTCTCTGATACTCGC
5R	CGACCTCGAGCAGTCTGCGACCAC

[a] F and R are forward and reverse, respectively.
[b] Restriction sites are underlined.

Table 2.2. Nucleotide sequences of primers for PCR amplification of the two KPIs and their domains from crayfish *Pacifastacus leniusculus*.

Primer name	Sequence (5'-3')*	Recombinant protein	Forward or reverse primer
KPI2F	CATGCCATGGGAACAAGCCCTACGCGTCCCATTG	KPI2	F
KPI2_D1F	CATGCCATGGGACGTCCCATTGGTGGGCTATG	Domain1 of KPI2	F
KPI2_D1R	ATTCTTATGCGGCCGCTTAGTGGTGGTGGTGGTG GTGTCCTCCTCCTGTTGCACATG	Domain1 of KPI2	R
KPI2_D2F	CATGCCATGGGAGGAAGGAGGTTGTGTG	Domain 2 of KPI2	F
KPI2_D2R	ATTCTTATGCGGCCGCTTAGTGGTGGTGGTGGTG GTGACCTGTGCATTCACCGTTATAG	KPI2 and Domain2 of KPI2	R
KPI8_D1F	CATGCCATGGGAAAAGTTAGGCCTTGTAAAAAG	KPI8 and Domain1 of KPI8	F
KPI8_D1R	ATTCTTATGCGGCCGCTTAGTGGTGGTGGTGGTG GTGCGTCTTCGCTTGACATGG	Domain1 of KPI8	R
KPI8_D2F	CATGCCATGGGACAAGCGAAGACGTGCTCG	Domain2 of KPI8	F
KPI8_D2R	ATTCTTATGCGGCCGCTTAGTGGTGGTGGTGGTG GTGATCTCTGCATTTACCATTATAG	KPI8 and Domain2 of KPI8	R

* The *Nco*I and *Not*I sites are shaded.

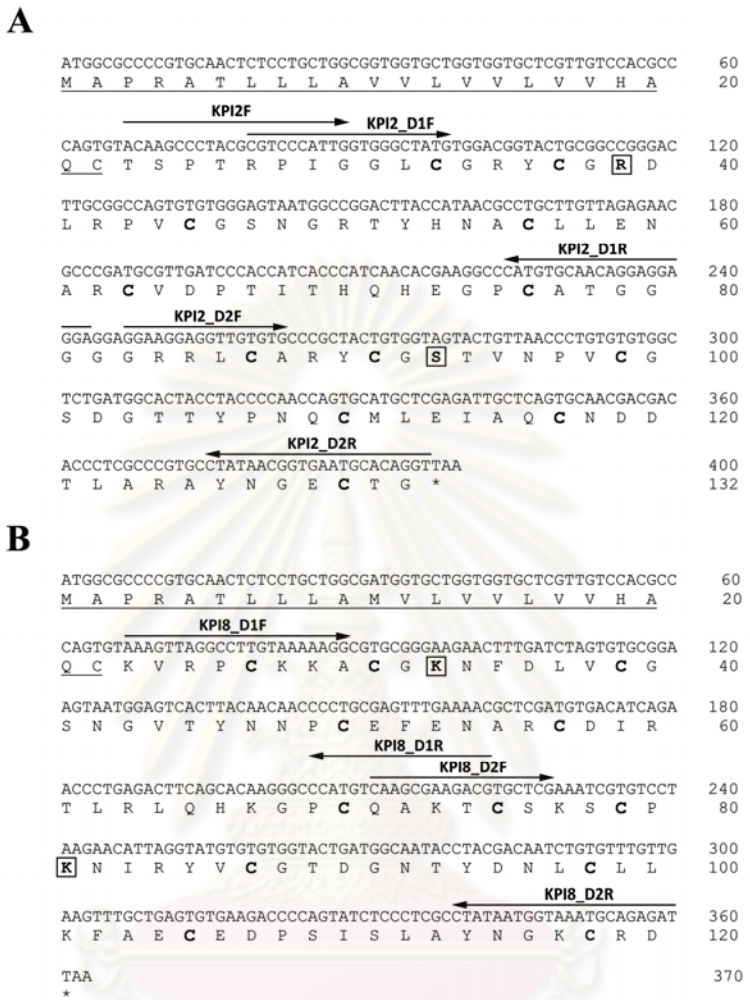

Fig. 2.3. The nucleotide and amino acid sequences of KPI2 (A) and KPI8 (B). Arrows indicate the annealing sites of primers used to amplify the KPI2, KPI8 and their domains for the cloning into an expression vector. The cysteine residues and signal sequence are bold-faced and underlined, respectively. The P_1 residues are boxed.

2.2.2 Recombinant protein expression

All expression plasmids were transformed into the expression host, *Escherichia coli* Rosetta(DE3)pLysS for the Kazal-type SPI from the black tiger shrimp and *E. coli* Rosetta gami B (DE3) for the Kazal-type SPI from the crayfish. The starter culture was prepared by inoculating a single colony from a freshly streaked plate into a 2 ml LB medium containing 100 μg/ml of ampicillin and 34

μg/ml of chloramphenicol for the Kazal-type SPI from the black tiger shrimp or 100 μg/ml of ampicillin, 34 μg/ml of chloramphenicol, 15 μg/ml of kanamycin and 12.5 μg/ml of tetracycline for the Kazal-type SPI from the crayfish and incubating at 37 ºC overnight with shaking at 250 rpm.

The starter was diluted 1:100 into the culture supplemented with antibiotics and incubated at 37 ºC with shaking at 250 rpm until the OD_{600} reached 0.6. Protein expression was induced by the addition of 1 M isopropyl-β-D-thiogalactopyranoside to a final concentration 1 mM. The culture was incubated at 37 ºC further with shaking for 0, 1, 2 and 3 h (the Kazal-type SPI from the black tiger shrimp) and for 0, 1, 2 and 4 (the Kazal-type SPI from the crayfish). The 1 ml culture was aliquot at each time point and the pellets collected by centrifugation at 10,000g for 5 min at 4 ºC. The cell pellets were stored at -80 ºC for further analysis. The expression of the recombinant proteins was checked by sodium dodecyl sulfate polyacrylamide gel electrophoresis (SDS-PAGE).

The cell pellet at 3 or 4 h was resuspended in phosphate-buffered saline, pH 7.4 (1× PBS; 137 mM NaCl, 2.7 mM KCl, 10 mM Na_2HPO_4, 2 mM KH_2PO_4) and sonicated for 2-4 min. The cell lysate was centrifuged at 10,000g for 10 min at 4 °C. The pellet and supernatant were collected and analyzed using SDS-PAGE in order to test the inclusion body formation.

2.3 Purification of recombinant proteins

The *E. coli* transformants were cultured under vigorous shaking at 37 °C. When the OD_{600} of the culture reached about 0.6, the expression was induced by

adding IPTG to the final concentration of 1 mM and the incubation was continued for additional 3 h. Cells were harvested by centrifugation, resuspended in 1× PBS and sonicated for 2–4 min. The cell lysate was centrifuged at 8,000g for 10 min at 4 °C to collect the supernatant. The soluble recombinant protein was purified using a Ni-NTA agarose column and eluted stepwise with the 1× PBS buffer pH 7.4 containing 500 mM imidazole. Consequently, the fractions containing the eluted protein were dialyzed against the enterokinase buffer (20 mM Tris-HCl, pH 8.0, 50 mM NaCl, 2 mM $CaCl_2$) followed by incubation with enterokinase (0.00001 g enterokinase/g fusion protein) at 23 °C for 16 h in order to cleave the Kazal-type SPI away from the Trx·Tag. The final step was to purify the SPI domain using a Ni-NTA agarose column as described above. The purified SPI domain was dialyzed against 50 mM Tris-HCl, pH 8.0 and analyzed using SDS-PAGE. The concentration of eluted protein was determined using the Bradford method (Bradford, 1976).

The intact SPI*Pm*2 was prepared according to Somprasong et al. (2006).

2.4 Protein analysis

2.4.1 Sodium dodecyl sulfate-polyacrylamide gel electrophoresis (SDS-PAGE)

A discontinuous system of SDS-PAGE was used. The gel solutions were prepared as shown in the Appendix B. After the glass plates and spacers were assembled, the components of the separation gel solution were mixed thoroughly and pipetted into the gel plate setting. Then, a small amount of distilled water was careful layered over the top of the separation gel solution to ensure that a flat surface of gel

be obtained. When the polymerization was complete, water was poured off. The stacking gel solution was prepared, mixed thoroughly and poured on top of the separating gel. A comb was placed in position with excess gel solution overflowing the front glass plate. After the stacking gel was polymerized, the comb was removed and the wells were rinsed with distilled water to remove excess unpolymerized acrylamide.

Protein samples were prepared by resuspending the proteins in 1× sample buffer (12 mM Tris-HCl, pH 6.8, 5% glycerol, 0.4% SDS, 2.88 mM 0.02% bromophenol blue, 2-mercaptoethanol). The samples were then boiled for 10 min and either held at room temperature or kept at 0 ºC until loaded into the gel.

After boiling, the protein samples and the prestained protein marker were loaded into the wells. Electrophoresis was conducted in 1× running buffer [25 mM Tris-HCl, pH 8.3, 192 mM glycine, 0.1% (w/v) SDS] at a constant current of 20 mA until the tracking dye (bromophenol blue) reached the bottom of the separating gel.

The gel was placed in Coomassie blue staining solution [0.1% (w/v) Coomassie brillian blue R250, 10% (v/v) acetic acid, 45% (v/v) methanol] at room temperature with gentle shaking for 1 h, immersed in destaining solution [10% (v/v) acetic acid, 10% (v/v) methanol] and incubated at room temperature with agitation for 1-3 h. Destaining solution was replaced regularly to assist the removal of stain. The gel was then placed between the two sheets of cellophane over the glass plate before air-dried at room temperature.

2.4.2 Western blot detection of the His-tagged protein

After running the SDS-PAGE, the SDS-gel slab was removed from the glass plates. The nitrocellulose membrane, gel and filter paper were soaked in a transfer buffer (25 mM Tris base, 150 mM glycine and 20% methanol) for 30 min before they were consequently laid on Trans-Blot® SD (Bio-Rad). The filter paper was placed on the platform, followed by the membrane, the gel and the filter paper, respectively, as shown in Figure 2.4.

Protein transfer was performed at constant 90 mA for 90 min from cathode towards anode. After transferring the proteins from the gel to the membrane, the orientation of the gel was marked on the membrane. Transfer the membrane to an appropriate container (petri dish). The membrane was incubated in blocking buffer (1× PBS buffer [10 mM phosphate buffer, 150 mM NaCl, pH 7.4, 0.05% (v/v) Tween™-20 and 5% (w/v) non-fat dry milk)] at room temperature for an overnight with gentle shaking. The membrane was washed 3 times for 10 min each in washing buffer (PBS-Tween buffer [1× PBS buffer (10 mM phosphate buffer, 150 mM NaCl, pH 7.4, 0.025% (v/v) Tween™-20) and incubated in an anti-His antibody solution, 1:3000 dilution in washing buffer with 1% (w/v) non-fat dry milk, at ambient temperature with gentle mixing for 3 h. Then, the membrane was washed 3 times for 10 min each in washing buffer and then incubated in a secondary antibody solution, 1:2500 dilutions in washing buffer with 1% (w/v) non-fat dry milk with agitation for 1 h. The membrane was washed 3 times for 10 min each in washing buffer at room temperature. The bound antibody was detected by color development using

NBT/BCIP (Fermentas) as substrate dissolving in 100 mM Tris-HCl, 100 mM NaCl and 50 mM $MgCl_2$, pH 9.5.

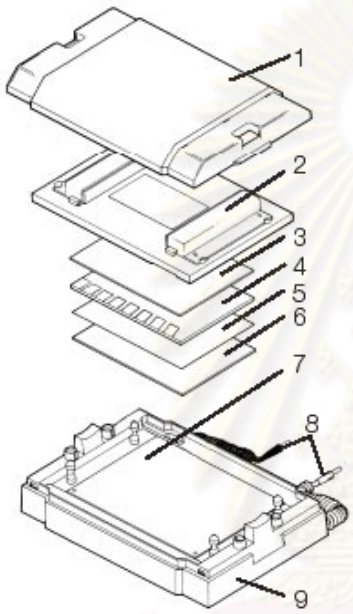

1. Safety lid
2. Cathode assembly with latches
3. Filter paper
4. Gel
5. Membrane
6. Filter paper
7. Spring-loaded anode

Figure 2.4 Exploded view of the Trans-Blot® SD (Bio-Rad).

2.5 Molecular mass determination of recombinant domains of SPI*Pm*2 by using MALDI-TOF mass spectrometry

The molecular masses of each domain of SPI*Pm*2 were accurately determined by MALDI-TOF mass spectrometry and used for the calculation in inhibitory activity and kinetic studies. It was performed in the commercial facility of the Proteomic Service Center, Bioservice Unit (BSU) (BIOTEC, Pathumthani, Thailand).

2.6 Proteinase inhibition assay

The inhibitory activity of each domain of *SPIPm*2 towards serine proteinases; trypsin (bovine pancreas, Sigma), subtilisin Carlsberg (*Bacillus licheniformis*, Sigma) and elastase (porcine pancreas, Pacific Science), was assayed using a procedure of Hergenhahn et al. (1987). The reaction mixture consisted of 50 mM Tris-HCl, pH 8; 146.8 and 293.6 μM of *N*-benzoyl–Phe–Val–Arg–*p*-nitroanilide (Sigma) for trypsin and subtilisin and 886.1 μM of *N*-succinyl–Ala–Ala–Ala–*p*-nitroanilide (Sigma) for elastase; and 0.02, 0.04 and 0.08 μM of subtilisin, trypsin and elastase, respectively, in a total volume of 100 μl. The final concentrations of SPI*Pm*2 inhibitory domains in the reaction mixtures were listed in Table 2.3. The reaction was incubated at 30 °C for 15 min and then terminated by adding 50 μl of 50% acetic acid. The absorbance of *p*-nitroaniline formed was measured at 405 nm. The percentages of remaining activity were calculated and plotted against the molar ratios of inhibitor domain to proteinase.

The inhibitory activities of the KPIs and their domains towards serine proteinases; trypsin (bovine pancreas, Sigma), chymotrypsin (bovine pancreas, Sigma), subtilisin Carlsberg (*Bacillus licheniformis*, Sigma) and elastase (porcine pancreas, Sigma), were assayed using a modified procedure from Hergenhahn et al. (1987). The reaction mixture consisted of 50 mM Tris-HCl pH 8; 5 and 9 mM of S-2222 (Chromogenix) for trypsin and subtilisin, 0.7 mM of S-2586 (Chromogenix) for chymotrypsin and 0.9 mM of *N*-succinyl–Ala–Ala–Ala–*p*-nitroanilide (Sigma) for elastase; and 0.04 μM of subtilisin, trypsin, chymotrypsin and elastase, in a total volume of 100 μl. The final concentrations of the recombinant proteins in the reaction mixtures were listed in Table 2.4. The reaction was incubated at 37 °C for 15 min and

then terminated by adding 50 µl of 50% acetic acid. The absorbance of *p*-nitroaniline formed was measured at 405 nm. The percentages of remaining activity were calculated and plotted against the molar ratios of the inhibitors to proteinase.

Table 2.3. The final concentrations of SPI*Pm*2 inhibitory domains (D) in the inhibition assay reactions.

	Concentration of inhibitory domain (µM)	
	Subtilisin reactions	**Elastase (D2) and trypsin (D4) reactions**
D1	0, 0.013, 0.026, 0.051, 0.103, 0.205, 0.410, 0.820	
D2	0, 0.002, 0.004, 0.007, 0.014, 0.028, 0.056, 0.112, 0.224, 0.449, 0.897	0, 0.009, 0.017, 0.034, 0.068, 0.136, 0.272, 0.544, 1.089, 2.178
D3	0, 0.027, 0.055, 0.109, 0.219, 0.438, 0.875	
D4	0, 0.013, 0.026, 0.053, 0.105, 0.210, 0.420, 0.840	0, 0.013, 0.025, 0.050, 0.100, 0.200, 0.400, 0.800, 1.600, 3.200
D5	0, 0.028, 0.056, 0.113, 0.226, 0.452, 0.904	

Table 2.4. The final concentration of the two KPIs and their domains in the inhibition assay.

	Concentration of inhibitory domain (µM)			
	Subtilisin reaction	**Trypsin reaction**	**Chymotrypsin reaction**	**Elastase reaction**
KPI2	0, 0.0018, 0.0036, 0.0072, 0.014, 0.029, 0.058, 0.115, 0.23, 0.46, 0.92, 1.84	0, 0.46, 0.92, 1.84	0, 0.92, 1.84	0, 0.92, 1.84
KPI2_domain1	0, 0.34, 0.68, 1.35	0, 0.46, 0.92, 1.85	0, 0.92, 1.85	0, 0.92, 1.85
KPI2_domain2	0, 0.0008, 0.0016, 0.0031, 0.0062, 0.012, 0.024, 0.05, 0.1, 0.2, 0.4, 0.8, 1.6	0, 0.4, 0.8, 1.6	0, 0.8, 1.6	0, 0.8, 1.6
KPI8	0, 0.8, 1.6	0, 0.0062, 0.012, 0.025, 0.05, 0.1, 0.2, 0.4, 0.8, 1.6	0, 0.8, 1.6	0, 0.8, 1.6
KPI8_domain1	0, 0.71, 1.42	0, 0.187, 0.375, 0.75, 1.5	0, 0.71, 1.42	0, 0.71, 1.42
KPI8_domain2	0, 0.75, 1.5	0, 0.0055, 0.0111, 0.022, 0.044, 0.089, 0.18, 0.355, 0.71, 1.42	0, 0.75, 1.5	0, 0.75, 1.5
KPI8_domain1 G32P	0, 1.72, 3.44	0, 0.0034, 0.0067, 0.013, 0.027, 0.054, 0.108, 0.215, 0.43, 0.86, 1.72, 3.44	0, 1.72, 3.44	0, 1.72, 3.44

2.7 Kinetics of serine proteinase inhibition

2.7.1 Kinetics of serine proteinase inhibition from each domain of SPI*Pm*2

The experiment was composed of four sets of reactions for different concentrations of each inhibitory domain. Each set consisted of four concentrations of substrate in the presence of fixed amounts of serine proteinase and three different concentrations of SPI*Pm*2 inhibitory domain (Table 2.5). For subtilisin: 10 nM of subtilisin; 0, 0.11, 0.22, 0.44 and 0.88 mM *N*-benzoyl–Phe–Val–Arg–*p*-nitroanilide were used. For elastase: 77.2 nM of elastase; 0, 0.22, 0.44, 0.89, 1.77 mM *N*-succinyl–Ala–Ala–Ala–*p*-nitroanilide were used.

The reactions were made a total volume of 100 µl with 50 mM Tris-HCl, pH 8, and initiated by the addition of proteinase. After incubating at 30 °C for 15 min, they were stopped by adding 50 µl of 50% acetic acid. The absorbance of *p*-nitroaniline formed was measured at 405 nm. The amount of *p*-nitroaniline was calculated using a millimolar extinction coefficient of 9.96 $mM^{-1}cm^{-1}$. The activity was calculated as nmole of *p*-nitroaniline/min. The activities were plotted against the concentrations of substrates as a substrate saturation curve and a Lineweaver–Burk plot. The apparent K_Ms at different concentrations of inhibitor and V_{max} were determined. The apparent K_Ms were re-plotted against the concentrations of inhibitor. The latter plotting was constructed for the calculation of inhibition constant (K_i).

Table 2.5. The final concentrations of SPI*Pm*2 inhibitory domains (D) in the kinetic assay.

	Concentration of inhibitory domain (μM)	
	Subtilisin reactions	**Elastase reactions**
D2	0, 0.003, 0.006, 0.013	0, 0.011, 0.021, 0.043
D3	0, 0.014, 0.028, 0.056	-
D5	0, 0.045, 0.090, 0.181	-

2.7.2 Kinetics of serine proteinase inhibition from KPI2, KPI8 and their domains

The experiment was composed of four sets of reactions for different concentrations of the recombinant proteins. Each set consisted of six concentrations of substrate in the presence of fixed amounts of serine proteinase and three different concentrations of the recombinant protein (Table 2.6). For subtilisin: 0.04 μM of subtilisin; 0, 1.15, 2.29, 4.59, 9.18 and 18.36 mM S-2222 were used. For trypsin: 0.04 μM of trypsin; 0, 0.765, 1.35, 2.7, 5.4 and 10.8 mM S-2222 were used. The reactions were made a total volume of 100 μl with 50 mM Tris-HCl pH 8, and initiated by the addition of proteinase. After incubating at 30 °C for 15 min, they were stopped by adding 50 μl of 50% acetic acid. The absorbance of *p*-nitroaniline formed was measured at 405 nm. The amount of *p*-nitroaniline was calculated using a millimolar extinction coefficient of 9.96 $mM^{-1}cm^{-1}$. The activity was calculated as nmole of *p*-nitroaniline/min. The activities were plotted against the concentrations of substrates as a Lineweaver–Burk plot. The apparent K_Ms and V_{max} at different concentrations of inhibitor and were determined. The apparent K_Ms or V_{max} were re-plotted against the concentrations of inhibitor. The latter plotting was constructed for the calculation of inhibition constant (K_i).

Table 2.6. The final concentrations of the recombinant KPIs and their domains in the kinetic assay.

	Concentration of inhibitory domain (μM)	
	Subtilisin reaction	**Trypsin reaction**
KPI2	0, 0.11, 0.22, 0.44	-
KPI2_domain2	0, 0.033, 0.065, 0.13	-
KPI8	-	0, 0.015, 0.03, 0.06
KPI8_domain2	-	0, 0.0053, 0.01, 0.02

2.8 Bacterial growth inhibition of SPI*Pm*2 and its domains

Bacteriostatic activities of SPI*Pm*2 and its domains were assayed based on the procedure by Han et al. (2008) on Gram-positive bacteria, *Bacillus subtilis*, *Bacillus megaterium*, *Staphylococcus aureus*, and Gram negative bacteria, *Vibrio harveyi* 639, *E. coli* JM109. For each bacterium, the assay was done in duplicate. An overnight culture of bacterium was diluted a hundred-fold, and grew in a shaking incubator in the presence of 0, 3.5 and 7 μM of SPI*Pm*2 or 7 μM of each domain at 30 °C for *B. megaterium* and *V. harveyi* 639 and 37 °C for *B. subtilis*, *S. aureus* and *E. coli* JM109. The bacterial growth was measured by monitoring the optical density at 595 nm from 0 to 18 h.

2.9 Mutagenesis of Kazal-type SPI

2.9.1 Mutagenesis of KPI8_domain1 at P_2 residue

The P_2 residue (Gly32) of KPI8_domain1 was replaced by proline using QuickChange Site-Directed Mutagenesis kit (Stratagene). The forward and reverse mutagenic primers were 5' AGGCCTTGTAAAAAGGCGTGCCCAAAGAACTT TGATCTAGTGTGC 3' and 5' GCACACTAGATCAAAGTTCTTTGGGCACGCC TTTTTACAAGGCCT 3', respectively. The mutagenesis was performed according to

the manufacturer's protocol. The resulting mutant, KPI8_domain1G32P, was over-expressed, purified and determined the inhibitory activities comparing with the wild type, KPI8_domain1 as described above (Table 2.4).

2.9.2 Mutagenesis of domain1 of SPI*Pm*2 at $P_{2'}$ residue

Tyrosine was replaced between Ile36 and Ser37 of domain 1 of SPI*Pm*2 using QuickChange Site-Directed Mutagenesis kit (Stratagene). The forward and reverse mutagenic primers were 5' CCAAACACTGTACGACCATCtatTCCCCTG TGTGTGGCTCTG 3' and 5' CAGAGCCACACACAGGGGAataGATGGTCGTAC AGTGTTTGG 3', respectively. The mutagenesis was performed according to the manufacturer's protocol. The resulting mutant, SPI*Pm*2_domain1Tyr, was over-expressed, purified and determined the inhibitory activities comparing with the wild type, domain1 of SPI*Pm*2 as described above (Table 2.7).

2.9.3 Mutagenesis of domain3 of SPI*Pm*2 at $P_{2'}$ residue

The $P_{2'}$ residue (Tyr132) of domain 3 of SPI*Pm*2 was deleted and replaced by Glycine using QuickChange Site-Directed Mutagenesis kit (Stratagene). The forward and reverse mutagenic primers for the deletion were 5' GTCGCGTGCCCT GAGATCGCTCCCGTGTGTGGCAGTG 3' and 5' CACTGCCACACACGGGAGC GATCTCAGGGCACGCGAC 3', respectively. The forward and reverse mutagenic primers for the replacement were 5' GTCGCGTGCCCTGAGATCGGCGCTCCCG TGTGTGGCAGTG 3' and 5' CACTGCCACACACGGGAGCGCCGATCTCAGGG CACGCGAC 3', respectively. The mutagenesis was performed according to the manufacturer's protocol. The resulting mutants, SPI*Pm*2_domain3Del for the deletion and SPI*Pm*2_domain3Gly, was over-expressed, purified and determined the inhibitory

activities comparing with the wild type, domain 3 of SPI*Pm*2 as described above (Table 2.7).

Table 2.7. The final concentration of the mutant domain 1 and 3 of SPI*Pm*2 and their wild types in the inhibition assay.

	Concentration of inhibitory domain (µM)			
	Subtilisin reaction	**Trypsin reaction**	**Chymotrypsin reaction**	**Elastase reaction**
SPI*Pm*2_domain1 (wild type)	0, 1.2, 2.4, 4.8	0, 1.2, 2.4, 4.8	0, 1.2, 2.4, 4.8	0, 1.2, 2.4, 4.8
SPI*Pm*2_domain1Tyr	0, 0.05, 0.1, 0.2, 0.4, 0.8, 1.6, 3.2, 6.4	0, 1.2, 2.4, 4.8	0, 1.2, 2.4, 4.8	0, 1.2, 2.4, 4.8
SPI*Pm*2_domain3 (wild type)	0, 0.18, 0.36, 0.72, 1.44	0, 1.44, 2.88	0, 1.44, 2.88	0, 1.44, 2.88
SPI*Pm*2_domain3Del	0, 0.18, 0.36, 0.72, 1.44	0, 1.44, 2.88	0, 1.44, 2.88	0, 1.44, 2.88
SPI*Pm*2_domain3Gly	0, 0.18, 0.36, 0.72, 1.44	0, 1.44, 2.88	0, 1.44, 2.88	0, 1.44, 2.88

2.10 Parasite proteinase inhibition assay of KPI2 and KPI8

Mycelia of *Aphanomyces astaci* isolated from the *P. clarkii* were grown in 500 ml Erlenmeyer flasks for 3-4 days at 20 °C in a peptone-glucose medium, PG-1. The culture was filtered. The filtered culture medium containing the extracellular proteinase was assayed for its proteolytic activities against chromogenic peptide substrates: S-2222 (*N*-benzoyl-Ile-Glu-Gly-Arg-*p*-nitroanilide, Chromogenix), S-2586 (MeO-succinyl-Arg-Pro-Tyr-*p*-nitroanilide, Chromogenix) and S-7388 (*N*-succinyl-Ala-Ala-Pro-Phe-*p*-nitroanilide, Sigma) with or without the presence of Kazal inhibitors. The reaction mixture consisted of 50 mM Tris-HCl pH 8; chromogenic peptide substrates, 5 mM of S-2222, 0.7 mM of S-2586 and 0.5 mM of S-7388; 10 µl of the extracellular proteinase from the culture medium (5 U for S-7388 and 1 U for S-2222 and S-2586, U is Δ405/min/mg) and 7 µM KPI2, 7 µM KPI8 or 1× PBS buffer, in a total volume of 100 µl. The reaction was incubated at 37 °C for 35 min

and, then, terminated by adding 50 µl of 50% acetic acid. The absorbance of *p*-nitroaniline formed was measured at 405 nm. The percentages of remaining activity were calculated.

2.11 Genomic organization of SPI*Pm*2 gene

2.11.1 Preparation of *P. monodon* genomic DNA

Genomic DNA was prepared from the pleopods of *P. monodon* using phenol-chloroform extraction. The pleopods were homogenized in 700 µl of extraction buffer (100 mM Tris buffer pH 8.0, 100 mM EDTA pH 8.0, 250 mM NaCl, 1% (w/v) SDS, and 100 µg/ml Proteinase K) and incubated overnight at 65 ºC. Then, 5 µg of RNase A were added into the lysate and incubated for 30 min at 37 ºC, extracted with phenol:chloroform:isoamyl alcohol (25:24:1) by inverting and mixing for 20 min and centrifuged for 10 min at 5,000 rpm. The upper phase was transferred to a new tube, extracted with chloroform:isoamyl alcohol (24:1) by inverting and mixing for 20 min and centrifuged for 10 min at 5,000 rpm. The upper phase was transferred to a new tube. The genomic DNA was precipitated with two volumes of cold absolute ethanol. The mixture was centrifuged at 5,000 rpm for 1 min. The genomic DNA was washed with 70% ethanol, air-dried, and then dissolved in 50 µl of TE buffer (10 mM Tris-HCl pH 8.0 and 1 mM EDTA pH 8.0).

2.11.2 Quality of genomic DNA

The quality of genomic DNA was checked by 0.6% agarose gel electrophoresis. One µl of experimental genomic DNA (0.1 µg/µl) and 1 µl of control genomic DNA (0.1 µg/µl) were loaded and run on 0.6% agarose gel in 1× TBE buffer.

The gel was stained with ethidium bromide and visualized under the UV light to estimate the size of product. A good genomic DNA preparation should contain DNA larger than 50 kb with minimum smearing.

2.11.3 Amplification of genomic SPI*Pm*2 gene

The sequence of the SPI*Pm*2 gene was determined by PCR amplification technique using genomic DNA as a template and six primers (Table 2.8), designed from cDNA of SPI*Pm*2 (EST) so as to amplify from the start codon to the second domain, the second domain to the third domain and the third domain to the stop codon of SPI*Pm*2.

Table 2.8. Nucleotide sequences of primers for PCR amplification of SPI*Pm*2 from *P. monodon* genomic DNA.

PRIMER NAME	SEQUENCE (5'-3')	POSITION	FORWARD (F) OR REVERSE (R) PRIMER
SD3F	GATGGCCAACAAAGTGGCAC	SIGNAL PEPTIDE (START CODON)	F
SPIPm2_D2R	GCACCGTTGCAGGTTCTGTC	DOMAIN 2	R
SPIPm2_D2F_2	CGAACTTATGCCAACTTGAG	DOMAIN 2	F
SPIPm2_D3R	GCTGCCTGGAAATAGCAGTC	DOMAIN 3	R
SPIPm2_D3F	TGTGGCAGTGATGGCAAGAC	DOMAIN 3	F
SD2	CCACATCTCTCTTTAATATC	Downstream of stop codon	R

Approximately 50-100 ng of template DNA was used for the PCR amplification in 50 µL reaction containing one unit Advantage 2 Polymerase Mix (Clonetech), 1× Advantage 2 buffer, 0.4 mM each dNTP, 0.2 mM each primer with an initial denaturation step at 94 ºC for 2 min, followed by: 30 cycles at 94 ºC for 30 s, 55 ºC for 30 s and 68 ºC for 3 min. The expected DNA fragment was cloned into the

T-A vector (RBC) and sequenced. The sequences of PCR products were compared with cDNA of SPI*Pm*2 in order to determine introns, exons and 5'-3' splicing site.

2.12 Preparation of SPI*Pm*2 protein

An *E. coli* Rosetta(DE3)pLysS transformant containing a rSPI*Pm*2 expression plasmid, pSPIPm2-NS2 (Somprasong et al., 2006), was cultured under vigorous shaking at 37 °C until the optical density at 600 nm reached 0.6–0.8, the protein expression was induced by adding IPTG to the final concentration of 1 mM and the incubation was continued for 4 h. The cell pellet was collected by centrifugation at 8,000g for 10 min, frozen completely at −80 °C, thawed at room temperature and resuspended by pipetting up and down in a lysis buffer (50 mM Tris-HCl, pH 8, 5% glycerol and 50 mM NaCl). The suspension was shaken for an hour at room temperature, sonicated with a Bransonic 32 (Bandelin) for 4 min and centrifuged at 10,000g for 20 min to remove the supernatant liquid. The pellet containing the inclusion bodies was washed twice with 0.5 M NaCl, 2% Triton X-100, twice with 0.5 M NaCl and twice with distilled water. The inclusion bodies were solubilized with 50 mM sodium carbonate, pH 10, at room temperature overnight. The insoluble material was removed by centrifugation. The soluble protein was purified using a Ni-NTA agarose column. The purified rSPI*Pm*2 was dialyzed against distilled water. The purity of the protein was analyzed using SDS-PAGE. The concentration of protein was determined using the Bradford method (Bradford, 1976).

2.13 The effect of SPI*Pm*2 on the WSSV replication

Two groups of three individual black tiger shrimp were injected with with WSSV (1:10,000,000 dilution from purified WSSV purified stock; die in 6 days) plus saline, WSSV plus 10 μM rSPI*Pm*2 and saline. After 48 h of the injection, gills were removed from the shrimp for total RNA preparation. The cDNAs were prepared and analyzed by RT-PCR for the replication of WSSV via the expression of vp28 gene.

Each total RNA preparation from the shrimp was extracted from the gills using the TRI Reagent® (Molecular Research Center). The synthesis of first strand cDNA was done using the First Strand cDNA Synthesis Kit (Fermentas). Total RNA 5 μg were mixed with the oligo(dT)18 primer for the reverse transcription reaction performed according to the manufacturer's protocol. Then, 0.5 μl and 2 μl of each cDNA preparation were, respectively, used for the PCR amplification of β-actin and vp28 in a 25 μl reaction volume containing 2.5 unit Taq DNA polymerase (Fermentas), 1× buffer, 200 μM of dNTP and 0.2 μM each of the forward and reverse primers (Table 1), respectively. The reactions were carried out using the following conditions: an initial denaturation step of 94 ºC for 2 min; followed by 25 cycles of 94 ºC for 30 s, 55 ºC for 30 min and 72 ºC for 1 min; and the final extension phase of 72 ºC for 5 min. The PCR products were analyzed by electrophoresis using 2.0% agarose gel. The band intensity of the PCR products were recorded and analyzed using the Genetools analysis software. The expression of vp28 was reported relative to that of the internal control, β-actin. Statistic analysis of the RT-PCR results was performed using the independent samples t-test as indicated in the results. Data differences were considered significant at $P < 0.05$.

2.14 Production of anti-SPI*Pm*2 immune serum

Rabbit polyclonal antiserum was raised against SPI*Pm*2 using 2.0 mg of purified recombinant protein. It was performed in the Biomedical Technology Research Unit, Faculty of Associated Medical Sciences, Chiang Mai University, Thailand.

2.15 Localization of SPI*Pm*2 in different tissues of normal and WSSV-infected shrimp

The whereabouts of SPI*Pm*2 protein expression was determined from normal and WSSV-infected shrimp at 48h. The nine tissues were collected: hemocyte, plasma, lymphoid, gill, epipodite, heart, stomach, intestine, and eye stalk. Hemocyte protein sample was prepared by collecting the hemolymph from three shrimp using 1/10 volume of 10% sodium citrate, pH 7, as an anticoagulant. The hemocytes were separated by centrifugation at 800g for 5 min at 4 ºC. The cell pellets were washed with 450 mM NaCl solution, resuspended in a homogenizing buffer (50 mM Tris–HCl, pH 7.5, 150 mM NaCl and 3 mM EDTA) and vigorously vortexed. The mixture was centrifuged at 14,000g for 20 min at 4 ºC to clarify the hemocyte lysate.

The other tissues were homogenized on ice in the homogenizing buffer and then centrifuged at 10,000g for 10 min according to Shi et al. (2008). The supernatants from all tissue homogenates were measured the protein content according to the method of Bradford (Bradford, 1976). The supernatant liquids were analyzed using 12% SDS-PAGE. Western blot analysis was also performed to detect the SPI*Pm*2 and β-actin using the rabbit anti-SPI*Pm*2 and mouse anti-actin.

The proteins separated by the SDS-PAGE were electro-transferred onto a nitrocellulose membrane (Bio-Rad) in a semi-dry electrophoretic transfer cell (Trans-blot SD, Bio-Rad) at 10 V for 30 min. The membrane was incubated in a blocking buffer (5% skim milk powder in phosphate buffer saline (PBS) containing 0.05% (v/v) Tween20) at room temperature for overnight. The membrane was subsequently washed three time with PBS containing 0.05% (v/v) Tween20 at room temperature for 10 min and incubated with anti-SPI*Pm*2 (1:5000 dilution) and anti-actin (1:20,000 dilution) antibodies at 55 °C for 2 h. After washing the membrane, goat anti-rabbit antibodies conjugated with alkaline phosphatase (1:15,000 dilution) and goat anti-mouse antibodies conjugated with horseradish peroxidase (1:20,000 dilution) were then added. The protein was visualized as a color band with the substrate as DAB solution and NBT/BCIP solution, respectively.

CHAPTER III

RESULTS

3.1 Kazal-type SPI from *Penaeus monodon*

3.1.1 Construction of the expression plasmids for SPI*Pm*2 domains

In an attempt to study each domain of the SPI*Pm*2 separately, five PCR primer pairs were designed for the amplification of the domains such that there would be *Nco*I and *Xho*I sites at the 5' and 3' sides of the PCR products. A few amino acid residues were left on both sides of each SPI domain as well (Figure 2.2). The pET-32a(+) was then chosen since the SPI domain sequence would fused with the thioredoxin tag and expressed as fusion protein. To simplify the purification of SPI domains, the His·Tag at the 5' side in pET-32a(+) was removed along with the S·Tag leaving the His·Tag at the 3' side intact. The resulting expression vector pVR500 was, then, used for the cloning of SPI domain sequences. The SPI domain sequences were fused to the 5' thioredoxin tag and 3' His·Tag. The recombinant clones were sequenced to verify the correct SPI domain sequences. The recombinant expression plasmids obtained were named pSPI*Pm*2-D1 to pSPI*Pm*2-D5 for domains 1 to 5, respectively.

3.1.2 Over-expression of the Kazal-type SPIs in the *E. coli*

All SPIs were over-expressed in an *E. coli* system using as expression vectors. The five expression clones, pSPI*Pm*2-D1 to pSPI*Pm*2-D5, were transformed into an *E. coli* Rosetta(DE3)pLysS. The recombinant proteins were produced. The results showed that the protein expression was continuously increased after 3 h of

IPTG induction (Figure 3.1). In addition, all SPIs were expressed mostly in soluble forms (Figure 3.2).

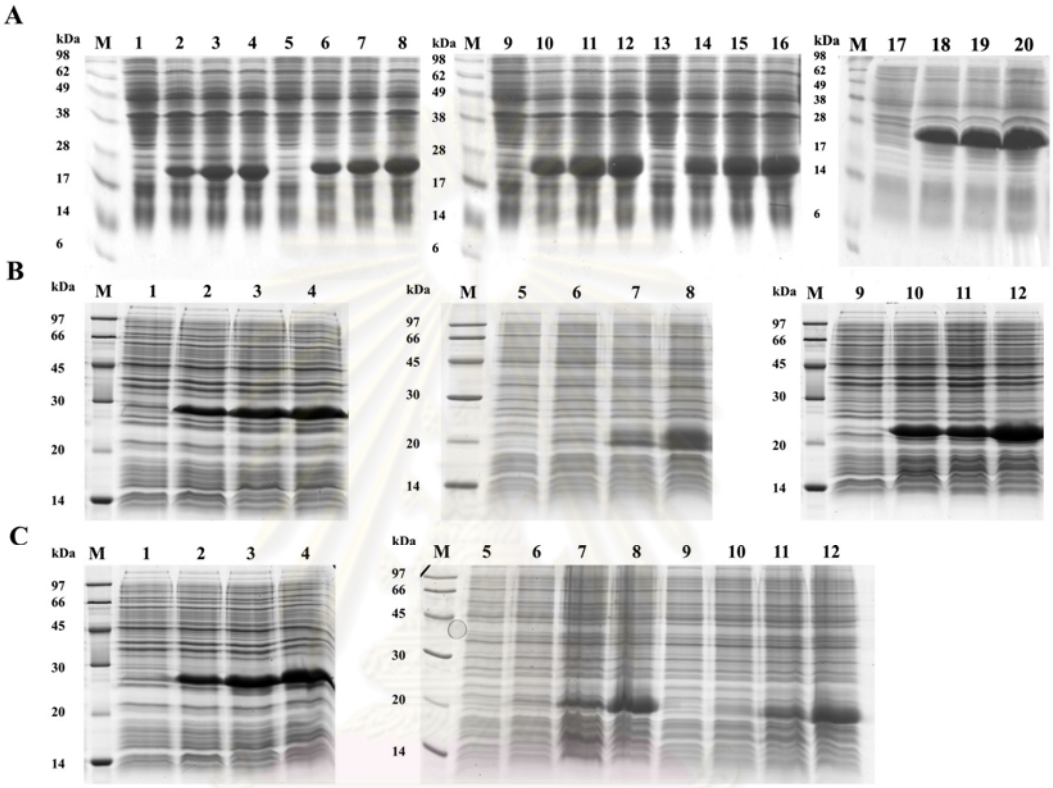

Figure 3.1. SDS-PAGE analysis of the rKazal domains of SPI*Pm*2 (A), rKPI2 and its domains (B) and rKPI8 and its domains (C) expressed in *E. coli* system at various times of induction, respectively. For rKazal domains of SPI*Pm*2 (A), lanes 1-4, lanes 5-8, lanes 9-12, lanes 13-16 and lanes 17-20 are the lysate of cells carrying pSPI*Pm*2-D1 to pSPI*Pm*2-D5 from induced cells at 0, 1, 2 and 3 h, respectively. Lanes M are SeeBlue® Plus2 standard marker (Invitrogen). For rKPI2 and its domains (B), lanes 1-4, lanes 5-8 and lanes 9-12 are the lysate of cells carrying pKPI2, pKPI2_domain1 and pKPI2_domain2 from induced cells at 0, 1, 2 and 4 h, respectively. Lanes M are LMW standard marker (Invitrogen). For rKPI8 and its domains (C), lanes 1-4, lanes 5-8 and lanes 9-12 are the lysate of cells carrying pKPI8, pKPI8_domain1 and pKPI8_domain2 from induced cells at 0, 1, 2 and 4 h, respectively. Lanes M are LMW standard marker (Invitrogen).

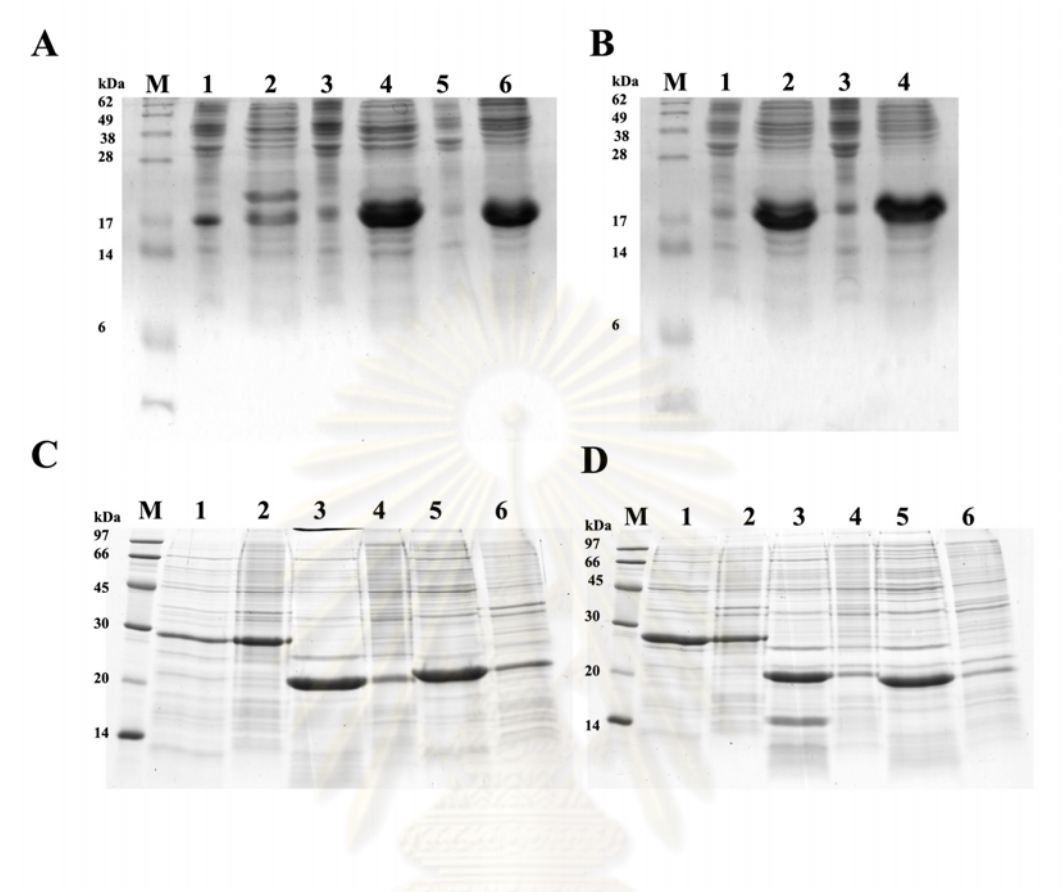

Figure 3.2. SDS-PAGE analysis of pSPI*Pm*2-D1 to pSPI*Pm*2-D3 (A), pSPI*Pm*2-D4 and pSPI*Pm*2-D5 (B), rKPI2 and its domains (C) and rKPI8 and its domains (D) showing the expressed proteins in *E.coli* host cells containing the recombinant proteins in the soluble and inclusion fraction. For pSPI*Pm*2-D1 to pSPI*Pm*2-D3 (A), lanes 1, 3 and 5 are the inclusion fraction. Lanes 2, 4 and 6 are the soluble fraction of pSPI*Pm*2-D1 to pSPI*Pm*2-D3, respectively. For pSPI*Pm*2-D4 and pSPI*Pm*2-D5 (B), lanes 1 and 3 are the inclusion fraction. Lanes 2 and 4 are the soluble fraction of pSPI*Pm*2-D4 and pSPI*Pm*2-D5, respectively. For rKPI2 and its domains (C), lanes 1, 3 and 5 are the soluble fraction. Lanes 2, 4 and 6 are the inclusion fraction of pKPI2, pKPI2_domain1 and pKPI2_domain2, respectively. For rKPI8 and its domains (D), lanes 1, 3 and 5 are the soluble fraction. Lanes 2, 4 and 6 are the inclusion fraction of pKPI8, pKPI8_domain1 and pKPI8_domain2, respectively.

3.1.3 Purification of recombinant protein

The recombinant proteins were efficiently purified by two purification steps using a nickel-NTA affinity column under nondenaturing condition. All SPIs were expressed as the soluble fusion proteins. They were purified with nickel-NTA column (Figure 3.3). Then, the thioredoxin was removed by enterokinase digestion. The digested proteins were purified again by nickel-NTA column and analyzed for the identity and purity on 15% SDS-PAGE (Figure 3.4).

Analysis of the recombinant SPI domains of SPI*Pm*2 using 15% SDS-PAGE revealed 2-3 more minor bands of proteins besides the major band in each SPI domain sample (Figure 3.4A). Western blot analysis indicated that these bands were actually the SPI domains whose sizes were corresponding to dimer or trimer of the SPI domains (Figure 3.4B). The molecular masses of the SPI domains 1-5 were determined by MALDI-TOP mass spectrometry to be 6977.09, 7148.63, 7038.239, 7453.13 and 7253.52, respectively, which were agreed well with the calculated ones. The SPI domains on SDS-PAGE, however, gave anomalous mobility probably due to their small sizes so that the mobility was not related only to the size but also the amino acid sequences. Relatively to other SPI domains, the SPI domain 5 was notably less detectable with western blot analysis.

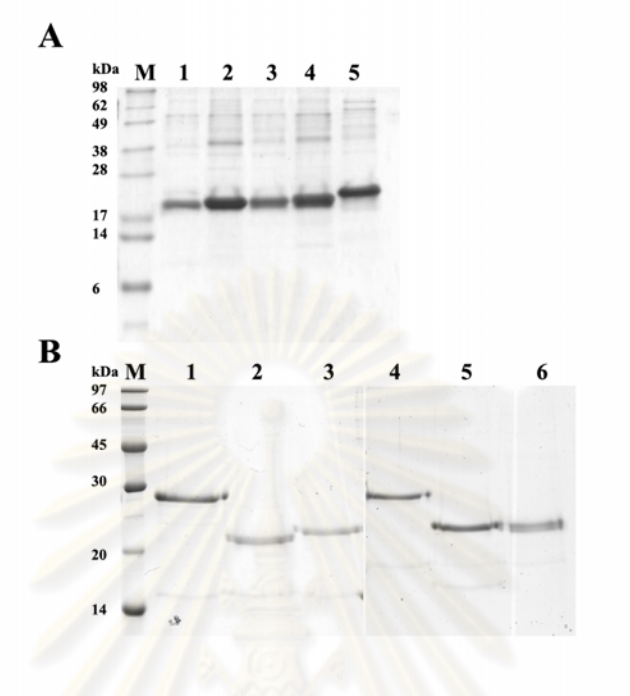

Figure 3.3. SDS-PAGE analysis of the first purification using nickel-NTA column of the fusion proteins (rKazal domains of SPI*Pm*2 (A) and rKPI2, rKPI8 and their domains (B)). For rKazal domains of SPI*Pm*2 (A), lanes 1-5 are pSPI*Pm*2-D1 to pSPI*Pm*2-D5, respectively. For rKPI2, rKPI8 and their domains (B), lanes 1-6 are pKPI2, pKPI2_domain1, pKPI2_domain2, pKPI8, pKPI8_domain1 and pKPI8_domain2, respectively.

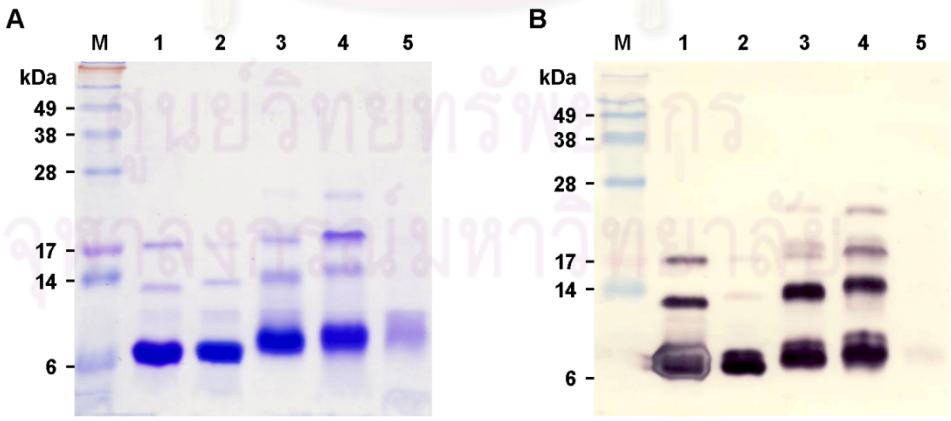

Figure 3.4. SDS-PAGE (A) and western blot (B) analysis of the purified SPI domains of SPI*Pm*2 after digesting with enterokinase. A 15% polyacrylamide gel was used. Lane 1 is the size marker. Lanes 1-5 are SPI domains 1-5, respectively.

3.1.4 Serine proteinase inhibitory assay

The SPI*Pm*2 with the domain P_1 residues T, A, E, K and E was isolated from the hemocyte cDNA libraries and found to strongly inhibit subtilisin and elastase, and weakly inhibit trypsin. To unravel further the inhibitory activity of each domain, we subcloned, over-expressed and purified each individual SPI domain. Their inhibitory specificities against trypsin, subtilisin and elastase were determined. All but SPI domain 1 inhibited subtilisin with variable activity (Figure 3.5A). Domain 1 has no inhibitory activity against subtilisin. Domains 2, 3 and 5 strongly inhibited subtilisin while domain 4 weakly inhibited subtilisin. Only domains 2 and 4 were active against elastase and trypsin, respectively (Figure 3.5B). Domain 2 strongly inhibited elastase while domain 4 weakly inhibited trypsin.

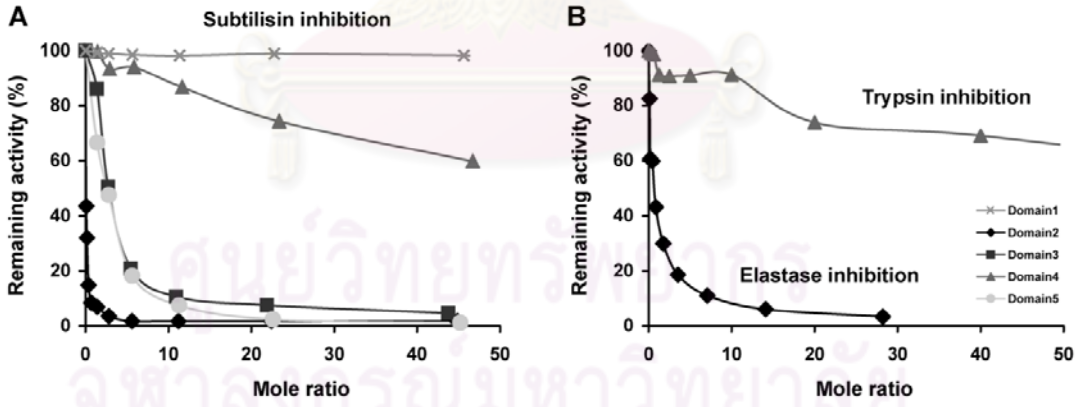

Figure 3.5. Inhibition assays of the SPI domains of SPI*Pm*2 against subtilisin (A), trypsin (B) and elastase (B). All 5 SPI domains were tested against subtilisin at various mole ratio of inhibitor to protease. Symbols ✕, ◆, ■, ▲ and ● were for domains 1 to 5, respectively. Domains 2 and 4 were also tested against elastase and trypsin, respectively.

3.1.5 Determination of inhibition constant of each domain of SPI*Pm*2

The inhibition against proteinases of the SPIs were studied further for their kinetics. To gain more insight on the inhibition of proteinases by the serine proteinase inhibitor, the inhibition reactions were performed by varying the substrate concentrations with fixed amount of proteinase in the presence of different inhibitor concentrations. The inhibition constant was determined by measuring its inhibitory effect on enzymatic hydrolysis of the chromogenic substrate at 30°C for 15 min as described in section 2.7. The Lineweaver-Burk plots or the inverted substrate saturation curves were constructed (Figure 3.6). The following Michaelis-Menten equation was applied to determine the dissociation constant of the inhibitor complex, K_i.

The strong inhibitory domains 2, 3 and 5 were assayed for their kinetic parameters against subtilisin and only domain 2 against elastase. Figure 3.6 shows the Lineweaver-Burk plots of proteinase inhibition of the SPI domains. The apparent K_Ms obtained from the plots were used to calculate the inhibition constants (K_is). The values of V_{max}s, K_Ms and K_is are summarized in Table 3.1 as well as those of the SPI*Pm*2. The three SPI domains were shown to be strong inhibitors with the K_is in the range of 10^{-8}-10^{-9} M. The V_{max}s and K_Ms were both varied with the SPI domains as compared to those of SPI*Pm*2.

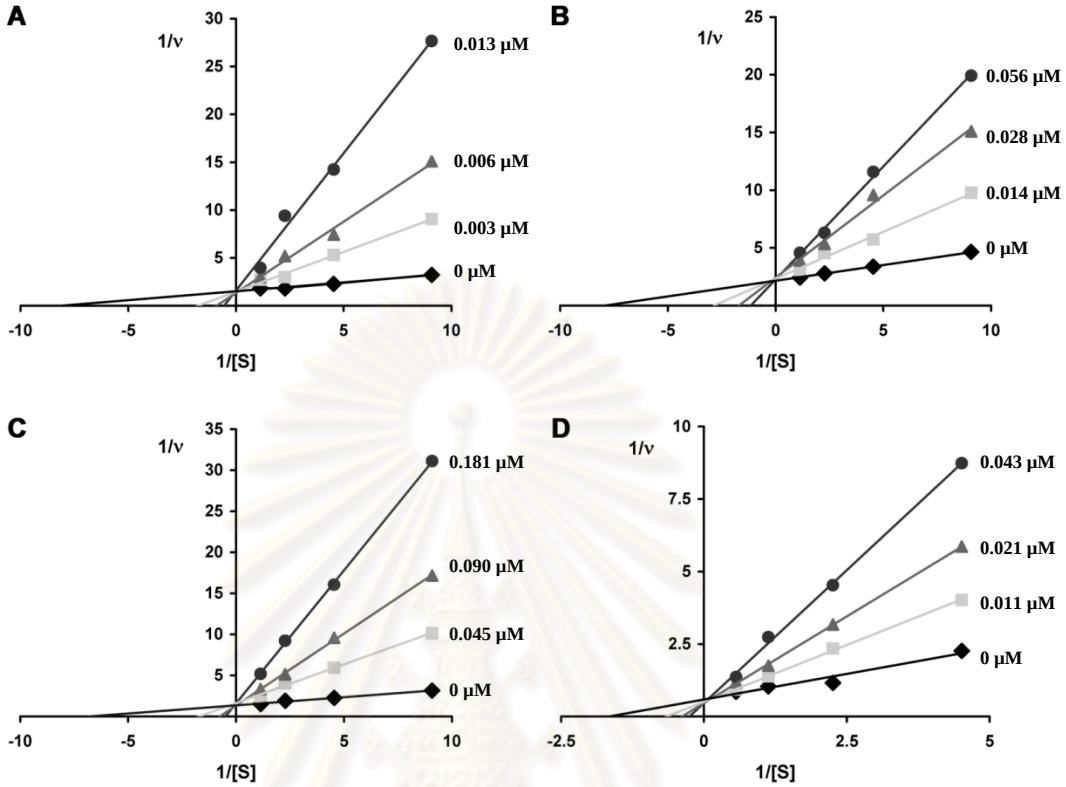

Figure 3.6. Lineweaver-Burk plots of proteinase inhibition assays of SPI domains of SPI*Pm*2. The inhibition of subtilisin activity was assayed with domains 2 (A), 3 (B) and 5 (C). The inhibition of elastase activity was assayed with domain 2 (D).

Table 3.1. The values of V_{max}s, K_Ms and K_is of SPI*Pm*2 for subtilisin and elastase.

	Subtilisin				**Elastase**	
	Domain 2	**Domain 3**	**Domain 5**	**SPI*Pm*2[a]**	**Domain 2**	**SPI*Pm*2[a]**
V_{max} (nmole/min)	0.6818	0.4373	0.6781	1.25	1.9877	1.49
K_M (M) × 10^{-3}	0.1611	0.1588	0.1755	0.22	0.7073	1.73
K_i (M) × 10^{-9}	1.2547	12.0303	16.4019	0.52	8.9873	3.27

[a] Data from Somprasong et al., 2006.

3.1.6 Bacterial growth inhibition of SPI*Pm*2 and its domains

It had been a thought that a potent subtilisin inhibitor might have negative effect on bacterial growth particularly that of *B. subtilis* as those observed with a serine proteinase inhibitor from frog eggs, ranaserpin (Han et al., 2008). Since the SPI*Pm*2 strongly inhibits subtilisin, an enzyme produced by several bacteria particular *B. subtilis*, the effect of inhibitor on the growth of Gram-positive bacteria, *B. subtilis*, *B. megaterium*, *S. aureus*, and Gram-negative bacteria, *V. harveyi* 639, *E. coli* JM109, was tested.

The diluted culture of bacteria was grown in the presence of SPI*Pm*2 and the growth was monitored. It was found that only the growth of *B. subtilis* (Figure 3.7A) but not *B. megaterium*, *S. aureus*, *V. harveyi* 639 and *E. coli* JM109 (data not shown) was inhibited. Greater growth inhibition was observed with higher concentration of SPI*Pm*2. The growth inhibitory activity was bacteriostatic since the cells continued to grow at slower pace or stopped growing. Testing the growth of *B. subtilis* with the SPI domains, domains 2 and 5 exerted stronger inhibition on growth while domains 4 had lower activity and domains 1 and 3 were relatively neutral (Figure 3.7B). The SPI domains exhibited lesser growth inhibitory effect than the intact SPI*Pm*2, and the inhibition took effect quite late in the growing culture.

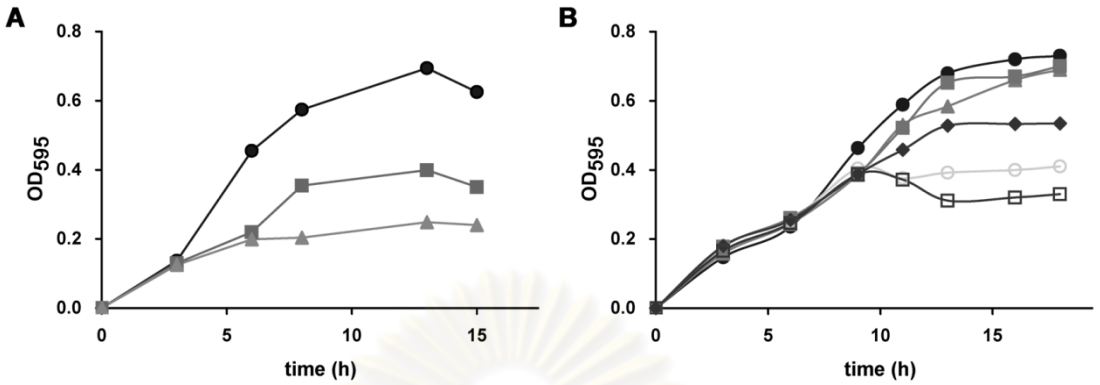

Figure 3.7. Bacteriostatic activity of SPI*Pm*2 and its five domains on *B. subtilis*. (A) The *B. subtilis* cultures were grown in the absence (●) and presence of 3.5 μM (■) and 7.0 μM (▲) SPI*Pm*2. (B) The *B. subtilis* cultures were grown in the absense (●) and presence of 7 μM SPI domain 1 (▲), domain 2 (○), domain 3 (■), domain 4 (◆) and domain 5 (□).

3.1.7 Mutagenesis of domain1 of SPI*Pm*2 at $P_{2'}$ residue

When each domain of SPI*Pm*2 was determined the inhibitory activity against the proteinases, it showed that only domain 1 was inactive against the proteinases. From the amino acid sequence alignment of each domain of SPI*Pm*2 (Figure 3.8), it was found that amino acid length between C_2 and C_3 residues of domain 1 was less than those of other domains. Tyrosine was not found in only $P_{2'}$ residue of domain 1. We reasoned that if the $P_{2'}$ Tyr was inserted into domain 1, the domain1 might then be active. We, thus, inserted the $P_{2'}$ Tyr into domain1 and the resulting mutant was called SPI*Pm*2_domain1Tyr. The inhibitory activity of the mutant was determined and compared with that of the wild type domain1. As predicted, the SPI*Pm*2_domain1Tyr had the weak inhibitory activity against subtilisin (Fig. 3.9A).

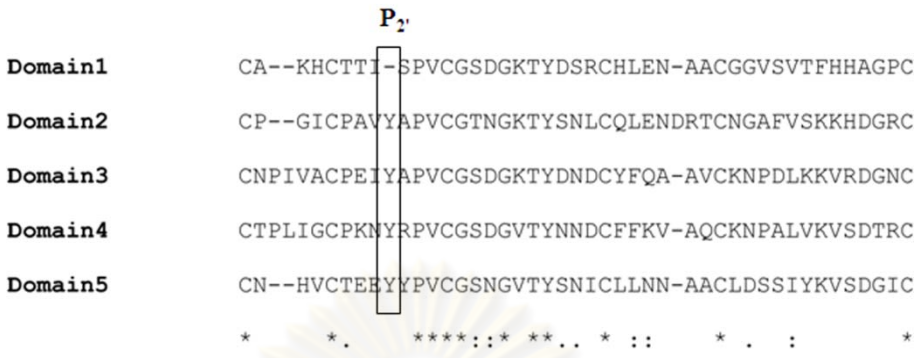

Figure 3.8. Amino acid alignment between SPI domains of SPI*Pm*2. The $P_{2'}$ residue was in the box.

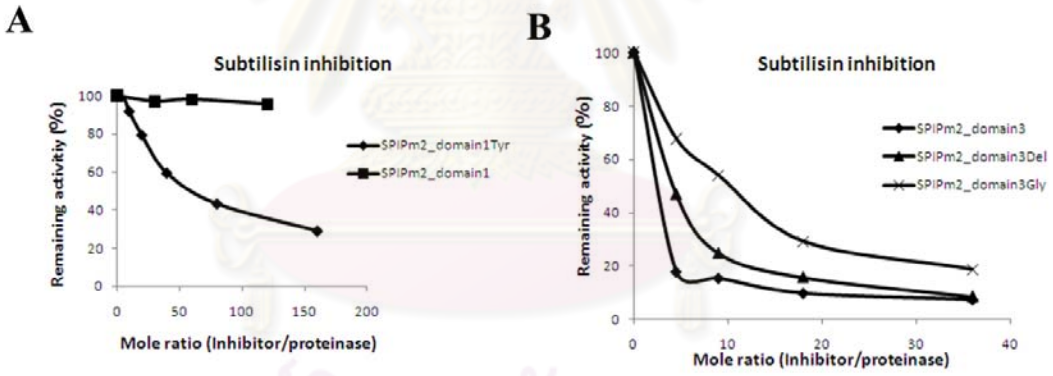

Figure 3.9. Inhibition assays of the domain 1 (A) and domain 3 (B) of SPI*Pm*2 and their mutants against subtilisin. The SPIs were tested against the proteinases at various mole ratio of inhibitor to proteinase.

3.1.8 Mutagenesis of domain3 of SPI*Pm*2 at $P_{2'}$ residue

When the domain 1 of SPI*Pm*2 was mutagenized, it was found that the mutant the weak inhibitory activity against subtilisin. The importance of $P_{2'}$ residue against Kazal domain was proved. The domain 3 of SPI*Pm*2 was the choice for study. We reasoned that if the $P_{2'}$ Tyr of domain 3 was changed, the domain1 might then be less active. We, thus, replaced the $P_{2'}$ Tyr132 of the domain 3 with a glycine and deleted the $P_{2'}$ Tyr132 of the domain 3 and the resulting mutants were called SPI*Pm*2_domain3Gly and SPI*Pm*2_domain3Del, respectivefully. The inhibitory activity of the mutant was determined and compared with that of the wild type domain 3. As predicted, the SPI*Pm*2_domain3Gly and SPI*Pm*2_domain3Del were less active against subtilisin than the wild type (Fig. 3.9B).

3.1.9 Genomic organization of SPI*Pm*2 gene

To unveil the genomic organization of SPI*Pm*2 gene, the primers were designed from the cDNA sequences were used for genomic amplification. The SPI*Pm*2 gene was amplified to determined exon and intron sequences. The PCR products were obtained. The genomic sequences were analyzed as compared to the corresponding cDNA sequences. The results showed that the size of the SPI*Pm*2 was about 3.7 kb. This gene consisted of seven exons interrupted by six introns which were between each domain of SPI*Pm*2 (Figure 3.10).

Figure 3.10. Genomic nucleotide sequences of SPI*Pm*2. The coding sequence (exon) of SPI*Pm*2 was shaded. The start and stop codon were in the boxes.

3.1.10 The effect of SPI*Pm*2 on the WSSV replication

Two groups of three individual black tiger shrimp were injected with WSSV (1:10,000,000 dilution from purified WSSV purified stock; die in 6 days) plus saline, WSSV plus 10 μM rSPI*Pm*2 and saline. After 48 h of the injection, gills were removed from the shrimp for total RNA preparation. The cDNAs were prepared and analyzed by RT-PCR for the replication of WSSV via the expression of vp28 gene. The β-actin, housekeeping gene, was used as an internal control. The results showed that the 10 μM of rSPI*Pm*2 exhibited the antiviral activity against the white spot syndrome virus (WSSV) by inhibiting WSSV propagation (Figure 3.11).

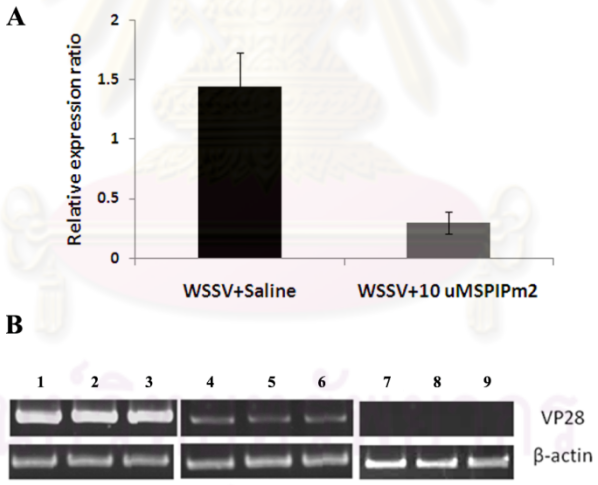

Figure 3.11. Effect of SPI*Pm*2 on WSSV replication in black tiger shrimp. Relative expression levels of VP28 (A) and the RT-PCR analysis (B) of VP28 normalized with β-actin expression were carried out. For the RT- PCR analysis (B), lanes 1-3 were shrimp injected with WSSV and saline. Lanes 4-6 were shrimp injected with WSSV and 10 μM of purified SPI*Pm*2. Lanes 7-9 were shrimp injected with only saline.

3.1.11 Localization of SPI*Pm*2 in different tissues of normal and WSSV-infected shrimp

The whereabouts of SPI*Pm*2 protein expression was determined from normal and WSSV-infected shrimp at 48 h. The nine tissues were collected: hemocyte, plasma, lymphoid, gill, epipodite, heart, stomach, intestine, and eye stalk. Total proteins from each tissue were prepared and analyzed using 12% SDS-PAGE. Western blot analysis was also performed to detect the SPI*Pm*2 and β-actin (internal control) using the rabbit anti-SPI*Pm*2 and mouse anti-actin. The result showed that SPI*Pm*2 was mainly found in hemocyte of normal shrimp (Figure 12A). It was also found in gill, heart, epipodite, stomach and lymphoid, but the protein level was not high in those tissues, which is corresponding to mRNA expression of SPI*Pm*2 in different tissues obtain from normal shrimp (data unpublished). When shrimp were infected by WSSV, it seemed that the SPI*Pm*2 protein level of all tissues was decreased (Figure 12B), whereas, mRNA expression level of SPI*Pm*2 was increased after WSSV infection (data unpublished). Possibly, SPI*Pm*2 might be used for shrimp defense against WSSV. In addition, SPI*Pm*2 was found in the plasma of shrimp (Figure 12C). It was suggested that SPI*Pm*2 was secreted for anti-WSSV. Because of secretion of SPI*Pm*2, the protein level of SPI*Pm*2 in tissues was decreased when shrimp was infected by WSSV.

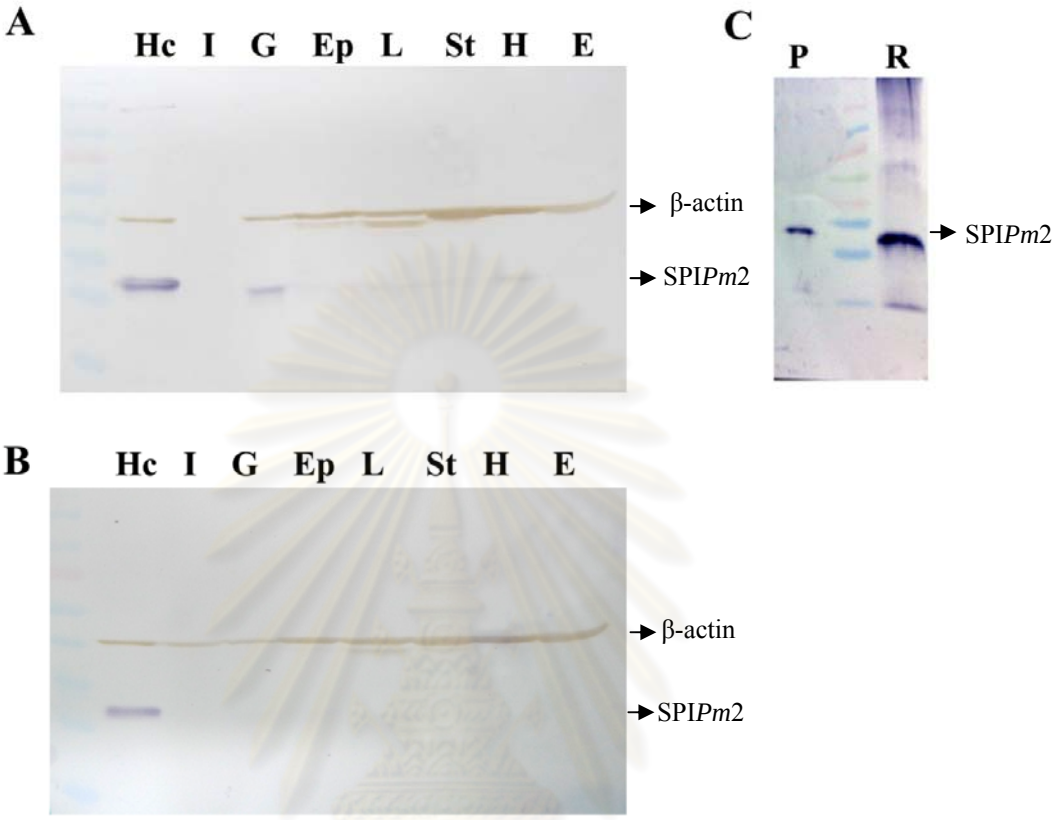

Figure 3.12. Western blot analysis of SPI*Pm*2. Expression of SPI*Pm*2 in different tissues obtained from normal shrimp (A) and WSSV-infected shrimp (B) at 48 h. Lanes Hc, I, G, Ep, L, St, H, E were extracted protein from hemocyte, intestine, gill, epipodite, lymphoid, stomach, heart and eye stalks, respectively. SPI*Pm*2 was detected in plasma from normal shrimp by Western blot technique comparing with the recombinant SPI*Pm*2 (C). Lanes P and R were plasma and the recombinant SPI*Pm*2, respectively. 200 µg of the protein from the plasma and tissues and 1 µg of the recombinant SPI*Pm*2 were loaded in the SDS-gel.

3.2 Kazal-type SPI from *Pacifastacus leniusculus*

3.2.1 Construction of the recombinant plasmid for KPI2, KPI8 and their domains

The KPI2 and KPI8 (GenBank Accession EU433325 and CF542313), consisting of two Kazal domains, was isolated from the hemocyte cDNA libraries of *P. leniusculus* (Cerenius et al., 2010). The KPI2 and KPI8 contain the open reading frames (ORFs) of 399 bp encoding a putative protein of 132 amino acid residues and 363 bp encoding a putative protein of 120 amino acid residues, respectively (Figure 2.3). Putative signal peptides of the KPI2 and KPI8 were identified using the online Signal Peptide Prediction with the predicted cleavage sites between Cys22-Thr23 and Cys22-Lys23, resulting in the 110 and 98 residue mature proteins with the calculated molecular masses of 11,586 and 10,905 Da and the predicted p*I*s of 7.3 and 8.3.

To determine the inhibitory activities of these two KPIs and their domains, the KPI genes and their domains were amplified by PCR technique from cDNA of the crayfish. The PCR primers were designed such that the PCR gene fragments contained the *Nco*I and *Not*I restriction sites, respectively, at their 5′ and 3′ ends. After digesting with *Nco*I and *Not*I restriction enzymes, the PCR gene fragments were cloned into an *E. coli* expression vector, pVR500. The KPI sequences were fused to the 5' thioredoxin tag and 3' His·Tag. The recombinant clones were sequenced to verify the correct KPI domain sequences. The recombinant expression plasmids obtained were named pKPI2, pKPI2_domain1, pKPI2_domain2, pKPI8, pKPI8_domain1 and pKPI8_domain2 for KPI2, domain1 of KPI2, domain2 of KPI2, KPI8, domain1 of KPI8 and domain2 of KPI8, respectively.

3.2.2 Over-expression of the Kazal-type SPIs in the *E. coli*

All SPIs were over-expressed in an *E. coli* system using as expression vectors. The six expression clones, pKPI2, pKPI2_domain1, pKPI2_domain2, pKPI8, pKPI8_domain1 and pKPI8_domain2, were transformed into an *E. coli* Rosetta gami B (DE3). The recombinant proteins were produced. The results showed that the protein expression was continuously increased after 4 h of IPTG induction (Figure 3.1). In addition, all SPIs were expressed mostly in soluble forms (Figure 3.2).

3.2.3 Purification of recombinant protein

The recombinant proteins were efficiently purified by two purification steps using a nickel-NTA affinity column under nondenaturing condition. All SPIs were expressed as the soluble fusion proteins. They were purified with nickel-NTA column (Figure 3.3B). Then, the thioredoxin was removed by enterokinase digestion. The digested proteins were purified again by nickel-NTA column and analyzed for the identity and purity on 15% SDS-PAGE (Figure 3.13). The predicted sizes of KPI2, KPI8, KPI2_domain1, KPI2_domain2, KPI8_domain1 and KPI8_domain2 were about 12.7, 12, 6.9, 6.4, 6.9 and 6.6 kDa, respectively.

3.2.4 Serine proteinase inhibitory assay

The recombinant inhibitors were assayed for their inhibitory activities against trypsin, chymotrypsin, elastase and subtilisin A. The mole ratios up to 50 of inhibitor against proteinase were used. For a strong inhibitor, the inhibition was readily seen at the mole ratios less than 10.

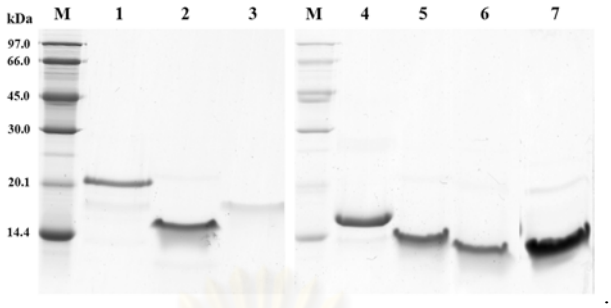

Figure 3.13. SDS-PAGE of the purified KPI2, KPI8 and their domains after digesting with enterokinase. A 15% polyacrylamide gel was used. Lane M is the size marker. Lanes 1–7 are KPI2, KPI2_domain1, KPI2_domain2, KPI8, KPI8_domain1, KPI8_domain2 and KPI8_domain1G32P, respectively.

We found that the KPI2 and KPI8 inhibited the subtilisin and trypsin, respectively, but not the chymotrypsin and elastase. The KPI2 also weakly inhibited trypsin. Its domain1 with the P_1 Arg weakly inhibited both the subtilisin and trypsin while the domain2 with the P_1 Ser inhibited strongly the subtilisin but not the trypsin (Fig. 3.14A and B). The KPI8_domain2 with the P_1 Lys strongly inhibited trypsin while the KPI8_domain1 with also the P_1 Lys was inactive against the proteinases tested (Fig. 3.14C).

3.2.5 Determination of inhibition constant of KPI2, KPI8 and their domains

The inhibition against subtilisin of the KPI2 and KPI2_domain2 as well as that against trypsin of the KPI8 and KPI8_domain2 was studied further for their kinetics. By varying the substrate concentrations with fixed amount of proteinase in the presence of different inhibitor concentrations, Lineweaver–Burk plots were constructed. The KPI2 and KPI2_domain2 were found to be competitive inhibitors whereas KPI8 and KPI8_domain2 were non-competitive inhibitors. The V_{max}s, K_Ms and K_is were calculated and shown in Figure 3.15 and Table 3.2. The inhibition

constants (K_is) were in the range of nanomolar while the K_Ms were in the range of millimolar.

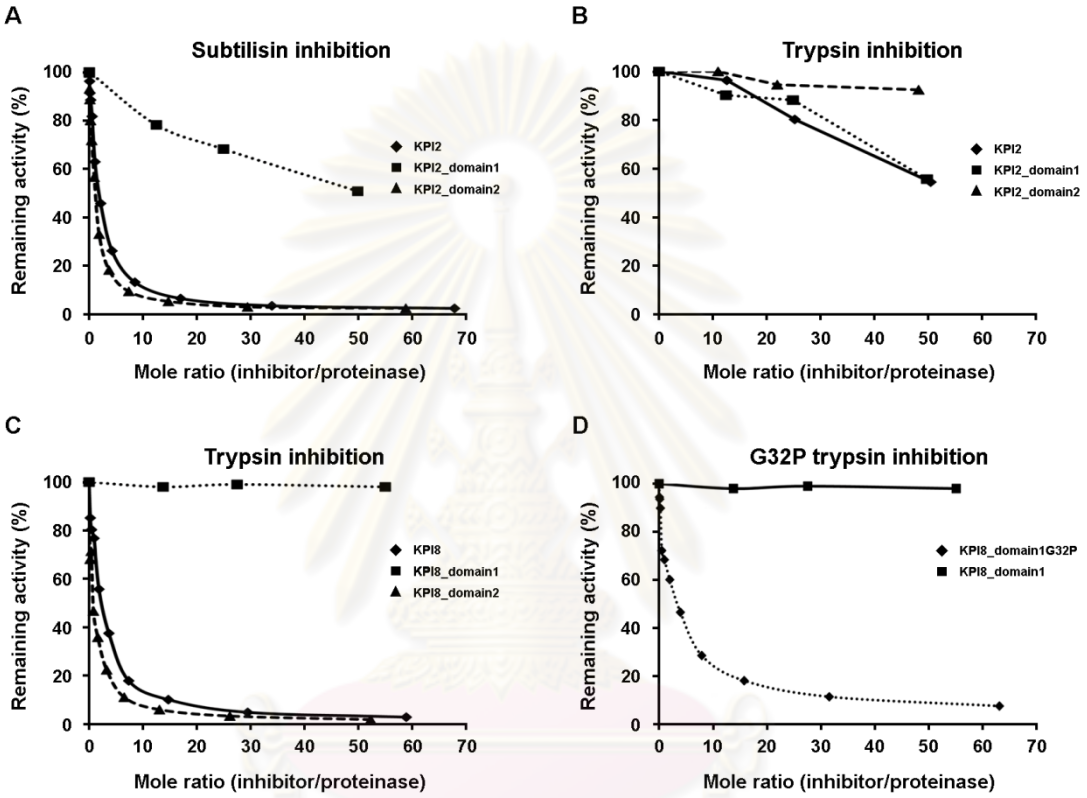

Figure 3.14. Inhibition assays of the KPI2 and its domains against subtilisin (A) and trypsin (B), KPI8 and its domains against trypsin (C) and KPI8_domain1G32P against trypsin (D). All KPIs were tested against the proteinases at various mole ratio of inhibitor to proteinase.

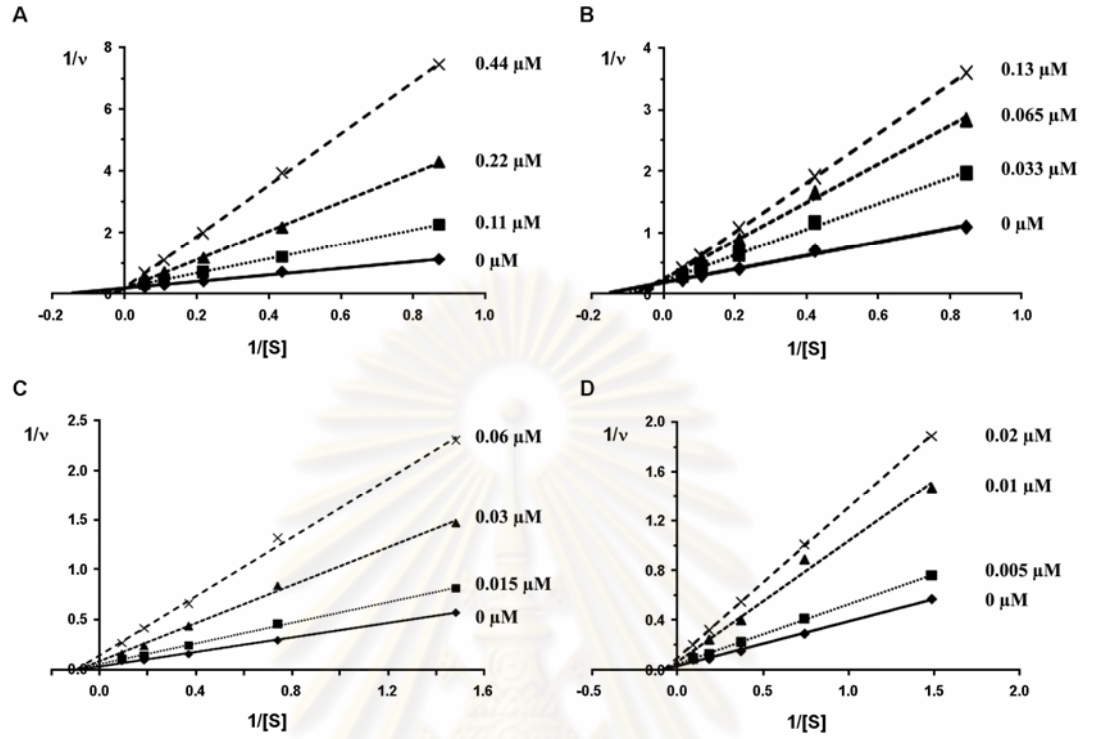

Figure 3.15. Lineweaver-Burk plots of proteinase inhibition assays. The inhibition of subtilisin activity was assayed with KPI2 (A) and KPI2_domain 2 (B). The inhibition of trypsin activity was assayed with KPI8 (C) and KPI8_domain 2 (D).

Table 3.2. The values of V_{max}s, K_Ms and K_is for subtilisin and trypsin.

	Subtilisin		**Trypsin**	
	KPI2	**KPI2_domain2**	**KPI8**	**KPI8_domain2**
V_{max} **(nmole/min)**	5.58	5.03	37.31	34.48
K_M **(M)** $\times 10^{-3}$	6.02	6.70	11.09	12.85
K_i **(M)** $\times 10^{-9}$	71.26	61.45	14.10	9.35

3.2.6 Mutagenesis of KPI8_domain1 at P_2 residue

The proteinase inhibition of the KPI8 was interesting owing to the fact that while the two domains of KPI8 had the same P_1 Lys residue, their proteinase inhibition was different. When the two domains of KPI8 were determined for their

inhibitory activities against proteinases, it was found that only domain2 had a strong inhibitory activity against trypsin. The result suggested that the amino acid residues around the P_1 residue of domain1 might negatively influence the inhibitory activity of the domain and were of interest. From the amino acid sequence alignment of the two KPI8 domains (Fig. 3.16), several amino acids along the sequence were different including the P_2 residue. That in domain2 was Gly32. We reasoned that if the P_2 Gly was changed to Pro like that in domain2, the domain1 might then be active. We, thus, replaced the P_2 Gly32 of KPI8 domain1 with a proline and the resulting mutant was called KPI8_domain1G32P (Figure 3.13). The inhibitory activity of the mutant was determined and compared with that of the wild type domain1. As predicted, the KPI8_domain1G32P was active against trypsin (Fig. 3.14D).

Figure 3.16. Amino acid alignment between KPI8_domain1 and KPI8_domain2. The P_1 and P_2 residues were indicated.

3.2.7 Inhibition of parasite-derived extracellular proteinases

Extracellular proteinases play important roles for the invasion of crayfish pathogenic oomycetes, such as *Aphanomyces astaci*, into the host. To determine if the KPI2 and KPI8 might be involved in the protection of host against such parasitic invasion, the KPIs were tested *in vitro* for their inhibitory activity against the

extracellular proteinases from the *A. astaci*. Since the KPI2 and KPI8 strongly inhibited subtilisin and trypsin, three chromogenic substrates, S-2222 for trypsin- and subtilisin-like activities and S-2586 and S-7388 for chymotrypsin- and subtilisin-like activities, were used for the assay. The three substrates also had different P_1 amino acids, Arg for S-2222, Tyr for S-2586 and Phe for S-7388. We observed that the proteinase activity using the S-2222 and S-2586 but not the S-7388 was decreased by about 20% and 60%, respectively, when the extracellular proteinase was incubated with KPI2 (Fig. 3.17). The KPI8 was inactive against extracellular *A. astaci* proteinase.

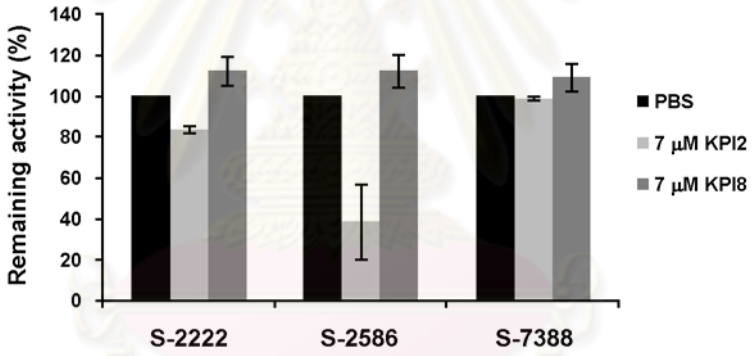

Figure 3.17. Inhibition assays of the KPI2 and KPI8 against the extracellular proteinase from the crayfish parasite *Aphanomyces astaci* using the three proteinase substrates, S-2222, S-2586 and S-7388.

From its strong inhibition against subtilisin and the extracellular fungal proteinase using S-2586, it was suggested that the KPI2 might inhibit against Tyr-specific subtilisin-like proteinase from the oomycete. In addition, the KPI2 also weakly inhibited the extracellular fungal proteinase reaction using S-2222 corresponding to its weak inhibition against trypsin. Thus, there might be a trypsin-like proteinase from the fungus.

CHAPTER IV

DISCUSSION

Kazal-typed proteinase inhibitors are extensively spread among all living organisms from bacteria to human. Since the first invertebrate Kazal-type inhibitor was reported in *R. prolixus* in 1993, followed by the isolation of a four-domain Kazal proteinase inhibitor from the hemocytes of *P. leniusculus* in 1994, the interest in these abundant proteins have increased, mainly for their possible function in immune defense (Rimphanitchayakit and Tassanakajon, 2010). We have recently reported that considerable sequence polymorphisms exist among crustacean Kazal inhibitors and a high number of different Kazal variants are expressed in *P. leniusculus* (Cerenius et al., 2010). Like other invertebrate KPIs, *P. leniusculus* KPIs are single or multiple domain proteins with one or more Kazal inhibitory domains. Common to all KPIs are six well-conserved cysteine residues responsible for three intra-domain disulfide bridges, and the active proteinase inhibitory site resides in amino acids around the P_1 residue. Specificity of the KPIs is mainly dependent on the P_1 residue although the surrounding amino acid residues influence the binding and specificity too (Krowarsch et al., 2003).

The KPIs, investigated in more detail in our present work, were chosen for KPI2 and KPI8 are exclusively expressed in the hemocytes while most other KPIs are widely expressed in different tissues of *P. leniusculus*. They also have an unusual sequence around the active sites for both Kazal domains of KPI2 and one domain of KPI8 have a glycine in their P_2 position. When we searched the available databases

for KPIs from different organisms, we were unable to find any other KPI having a glycine in this position. It was noticeable that the two domains of KPI8 both contained the P_1 Lys residues. The KPI8_domain2 with the P_2 Pro was active in trypsin inhibition but not the KPI8_domain1. As was shown by our mutagenesis experiment of KPI8, this P_2 Gly in domain1 did affect the inhibitory activity in a so far unknown manner. If the glycine was replaced by proline, the KPI domain became active showing high trypsin inhibitory activity.

The P_2 residue is among the amino acid residues that takes part in the contact between inhibitor and proteinase as shown by several crystallographic studies on other Kazal inhibitors. In the well-studied vertebrate ovomucoid Kazal-type inhibitor, all residues from P_6 to P_3' except the cysteine are hypervariable in spite of being important for the inhibitory activity (Lu et al., 2001). It has been frequently speculated that this hypervaribility ensures that inhibitors with different specificities vis-à-vis proteinase variants can arise. Studies using a very large data set consisting of turkey ovomucoid recombinant protein with different mutations in the above-mentioned residues including the P_2 residue, have shown that amino-acid replacements among these residues greatly affected the $\Delta G°$ values when tested against six different inhibitors (Lu et al., 2001). This means that exchanging one residue in this region of the inhibitor will have large effects on the K_i values of the inhibitor.

The unusual position of a glycine among the contact residues in the crayfish KPI2 and KPI8 would make the identification of potential target proteinases in the animal interesting. However, Kazal-like domains may serve other functions than direct inhibition of proteolysis. Rhodniin, from the blood-sucking insect *R. prolixus*, has, as is the case for KPI2 and KPI8, two Kazal domains. Detailed structural studies

have demonstrated that one domain of rhodniin is engaging the active site of the proteinase thrombin and is responsible for its inhibitory activity (van de Locht et al., 1995). The other domain is not directly involved with inhibiting proteolysis but is attaching to the fibrinogen-binding site of the thrombin. These double activities are likely to enhance the ability of rhodniin to interfere with the thrombin. Whether the KPI2 and KPI8 domains investigated here act as true inhibitors or, possibly, in other protein-protein interactions remain to be established, but it is striking that the inhibitor activity against the commercial proteinases was caused by only one of the two domains.

Since *P. leniusculus* is infected by the oomycete *A. astaci*, we decided to examine a possible interaction of these KPIs with *A. astaci* proteinases as well. Pathogenic fungi and oomycetes secrete extracellular proteinases and other extracellular enzymes in order to establish themselves. Proteinases secreted by these organisms and host-derived substances that become released by their activities have been shown to act as virulence factors (Gottar et al., 2006). Consequently, host-derived inhibitors such as proteinase inhibitors are important parts of the host defense arsenal. *A. astaci*, in spite of being a devastating pathogen on European crayfishes, lives in stable relationship as a benign parasite with the North American crayfish species used here, *P. leniusculus*. Parasite growth is counteracted by host immune reactions and unless the animal becomes immunocompromised by e.g. other pathogens it causes little harm (Cerenius et al., 2003). The parasite secretes several trypsin- and subtilisin-like proteinases, and the amounts of these can be substantially harmful when the parasite grows in a susceptible host (Bangyeekhun et al., 2001).

Gene expression of at least some of the responsible proteinase genes have been demonstrated experimentally by *in vitro* studies to be regulated by hitherto unidentified components of the crayfish plasma, indicative of parasite proteinases being important in the host-parasite interaction. For example, transcript levels of the major *A. astaci* trypsin-like proteinase, AaSP2, is more than 20 times higher in the presence of *P. leniusculus* plasma compared to other protein sources such as rabbit serum or skim milk (Bangyeekhun et al., 2001). The finding here that KPI2 acts as an inhibitor of extracellular proteinases from the parasite makes biological sense, since KPI2 is present in and secreted from semigranular hemocytes in relatively large amounts (Wu et al., 2008). These hemocytes reacts readily and specifically with β-1,3-glucans, the chief cell-wall constituent of fungi and oomycetes, and the inhibitor will be released upon glucan-triggered degranulation. This may be one way to restrict mycelial growth and, thus, spreading into the hemocoel. In the resistant host, mycelial growth is mainly restricted to the cuticle, and intrusions into the hemocoel are rarely observed. Specific interference with parasite-derived proteinases may be one way to prevent this parasite to use the hemolymph for its dissemination.

Recently, a five-domain Kazal-type serine proteinase inhibitor, SPI*Pm*2, identified from the hemocyte EST libraries of *P. monodon* and its proteinase inhibitory activities was reported (Somprasong et al., 2006; Tassanakajon et al., 2006). Owing to its proteinase inhibitory activity, the SPI*Pm*2 is believed to be involved in innate immunity in the shrimp (Supungul et al., 2002). The SPI*Pm*2 strongly inhibits subtilisin and elastase probably with the ratio of inhibitor to proteinase 1:2 and 1:1, respectively. It also weakly inhibits trypsin (Somprasong et al., 2006). The reactive P1 inhibitory specificity residues in domains 1-5 are Thr, Ala, Glu, Lys and Glu,

respectively. It is known that the inhibitory activities can be predicted from the P_1 residue. The SPIs with basic amino acids at P_1 position preferentially inhibit trypsin. Those with P_1 bulky hydrophobic residues tend to inhibit chymotrypsin like the L residue(s) in the four-domain Kazal inhibitor from the crayfish *Pacifastacus leniusculus*. The P_1 Gln residue in this crayfish inhibitor is supposedly responsible for subtilisin inhibition (Johansson et al., 1994). The three-domain Kazal inhibitor from *Bombyx mori* shows strong inhibition against subtilisin but not thrombin or chymotrypsin (Zheng et al., 2007); its P_1 are Thr, Ala and Gln. A heat-tolerant Kazal inhibitor with the P_1 Lys residue from the marine snail *Cenchritis muricatus* inhibits strongly both trypsin and human neutrophil elastase (González et al., 2007a). The 'nonclassical' Kazal-type elastase inhibitor with the P_1 Met residue from *Anemonia sulcata* inhibits strongly the porcine pancreatic elastase and moderately inhibits human leukocyte elastase (Hemmi et al., 2005).

From the above information on P_1 residue, it is tempting to speculate that the two Glu residues in SPI*Pm*2 are responsible for the inhibition of subtilisin, Thr or Ala residue for elastase and the Lys residue for trypsin. This speculation is also supported well with the work on ovomucoid third domain by Lu et al. (Lu et al., 1997). However, the SPIs with P_1 Thr residue from *Bombyx mori* and *Galleria mellonella* turn out to be subtilisin inhibitors (Nirmala et al., 2001a; Nirmala et al., 2001b). Thus, the assignment of inhibitory specificity to each domain is not satisfactory unless the domains are studied separately.

In this study, we had amplified and cloned each SPI domain into an *E. coli* expression vector and expressed the domain separately. The expression was not successful in the beginning probably because the SPI domain peptides were small and

easily degraded once they were synthesized in the cells. Using an expression vector pVR500, the SPI domains were, however, over-expressed successfully as fusion proteins with thioredoxin. After purification by using a nickel-NTA column, the fusion protein was cleaved with enterokinase. Only the SPI domains which contained the His·Tag were easily purified by using another nickel-NTA column.

The purified SPI domains of SPI*Pm2* were assayed for their inhibitory activities. We found that the SPI domain 1 with the P1 Thr residue was inactive against the three proteinase tested although the inhibition of subtilisin could be expected (Nirmala et al., 2001a; Nirmala et al., 2001b). The SPI domain 1 might be inactive domain in SPI*Pm*2 or active against other proteinases not tested. It has been shown that some multidomain Kazal SPIs have at least one inactive domain, for example domain 1 in the multidomain Kazal inhibitor LEKTI appears to be inhibitory inactive (Lauber et al., 2003). Surprisingly, the SPI domain 2 with the P_1 Ala residue was strongly active against subtilisin and slightly less active against porcine pancreatic elastase. The P_1 Ala residue is predicted to be the most specific for porcine pancreatic elastase but not subtilisin by the Laskowski algorithm (Lu et al., 2001). As expected, domains 3 and 5 with the P_1 Glu residues inhibited subtilisin while domain 4 with Lys residue weakly inhibited both subtilisin and trypsin.

The K_is for subtilisin of the strongly inhibitory domains (domains 2, 3 and 5) were in the range of 10^{-8} to 10^{-9} M slightly higher than that of SPI*Pm*2 (Table 3.1). The K_ms of the domains were also comparable to that of the intact inhibitor though the V_{max}s were lower. These results suggested that the separate domains were less suitable for proteinase inhibition. Similar situation was seen with elastase inhibition of SPI domain 2 where the K_i was higher, the K_M was lower, and the V_{max} was higher than

those of the intact inhibitor. With the SPI domains 2, 3 and 5 able to strongly inhibit subtilisin, it was not surprising that the SPI*Pm*2 was a strong inhibitor of subtilisin. Only SPI domain 2 also contributed to elastase inhibition.

Structural studies reveal several contact positions responsible for the interaction between Kazal domains and the proteinases, and the side chains of the P_1 amino acid residues lie neatly into the S_1 cavities of the proteinases (van de Locht et al., 1995; Read et al., 1983; Di Marco et al., 1997). There are twelve contact positions: P_6, P_5, P_4, P_3, P_2, P_1, P_1', P_2', P_3', P_{14}', P_{15}' and P_{18}' (Figure 1.3), responsible for the interactions between Kazal domains and the serine proteases. This means that although the inhibitory specificity is determined mainly by the P_1 amino acid residue, amino acid residues in other contact positions influence the potency of the binding as well as specificity of a serine proteinase inhibitor to its cognate proteinase. Mutagenesis of the P_2' residue of the domain 1 and domain 3 of SPI*Pm*2 significantly altered the inhibitory activity. It means that P_2' position of Kazal-type SPI may involve in binding efficiency against proteinase.

Although the actual biological function of SPI*Pm*2 in the black tiger shrimp is unknown, it is believed that the SPI*Pm*2 is involved in defense mechanism against microbial pathogens (Supungul et al., 2002). In particular, the strong subtilisin inhibitory activity suggested to us its activity against the bacteria that produces subtilisin (Christeller et al., 2005; Han et al., 2008). The effect of SPI*Pm*2 and its domains on the growth of Gram-positive bacteria, *B. subtilis*, *B. megaterium*, *S. aureus*, and Gram-negative bacteria, *V. harveyi* 639, *E. coli* JM109, was tested. As far as we know, only *B. subtilis* produced subtilisin. Interestingly, only the growth of *B. subtilis* was inhibited and the inhibition was bacteriostatic. The relatively stronger

inhibition was observed with the intact SPI*Pm*2 but not the domains. The domains 2 and 5 that strongly inhibited subtilisin inhibited the growth of *B. subtilis*. However, the SPI domain 3 that had comparable subtilisin inhibitory activity to SPI domain 2 had no growth inhibition effect while SPI domain 4 that had much less subtilisin inhibitory activity could slightly inhibit the growth of *B. subtilis*. The inhibition of growth might be due to the fact that the bacterial subtilisin was unable to digest protein in the medium and provide enough essential nutrients for the cells to grow. Nevertheless, the bacteriostatic action of SPI*Pm*2 on *B. subtilis* remained to be elucidated. One might speculate from the bacteriostatic activity that the SPI*Pm*2 might protect the shrimp from the potential pathogens that produced subtilisin-like proteinases.

By gene duplication, a multi-domain KPI genomic gene is expected to contain more than one nucleotide sequence units of Kazal domains separated by introns. A genomic gene organization of a KPI from the hemocyte cDNA library of oriental white shrimp *Fenneropenaeus chinensis* was elucidated recently (Kong et al., 2009). The KPI is a double-domain protein whose genomic gene consists of three exons and two introns. Within the introns are two-base microsatellite repeats, TA and TG. The first intron separates the coding sequence of the first Kazal domain including the signal peptide from the coding sequence of the second Kazal domain. The second intron separates the coding sequence of the second Kazal domain from a short coding sequence of the C-terminal amino acid sequence. This observation supports the gene duplication hypothesis. One can imagine that an ancestral Kazal domain gene duplicates itself from time to time. The new descendents evolve separately leading to

different amino acid sequences of Kazal domains. The same scenario is also observed with the genomic gene of SPI*Pm*2 from *P. monodon*

Besides the KPIs from different genes, different KPIs can also be derived from the same gene. The fruit fly, *Drosophila*, synthesizes five types of KPIs from a single gene (*KAZ1*) (Niimi et al., 1999). By using alternatively splicing, six or possibly more spliced mRNA variants are encoded. They are, in turn, translated into five different KPIs, namely α, β, γ, δ and ε. The α-type with its mitochondrial sorting signal is destined to function in the mitochiondria. The β- and δ-types are intracellular proteins with slightly different Kazal domains while the γ- and ε-types are secreted proteins as predicted from the N-terminal signal peptides.

Another example of possible alternatively splicing of the KPI pre-mRNA that gives rise to different KPIs is from the white shrimp, *F. chinensis* (Wang et al., 2009). The shrimp produce four different KPI mRNAs, *Fcspi*-1–4, in the hepatopancreas. Amino acid sequence analysis of the four inhibitors suggested that they might have been derived from the same transcript, which was subjected to alternative splicing. The *Fcspi*-1 mRNA is the longest mRNA containing nine Kazal domains. The *Fcspi*-2–4 inhibitors are shorter by 1–3 Kazal domains, respectively. The Kazal domains 3, 5 and 6 are probably removed by alternative splicing.

The potential role of several KPIs in invertebrate immunity can also be implied from their responses against microbial challenge. Semi-quantitative RT-PCR or quantitative real time RT-PCR analysis were performed and showed that the mRNA expression of invertebrate KPIs was up-regulated upon bacteria or viral challenges. Nevertheless, the actual functions of the up-regulated KPIs are to be confirmed by further investigation. A few examples are as follows. A mollusk KPI

(AISPI) mRNA from the bay scallop *Argopecten irradians* which encodes a six-domain KPI is up-regulated after *Vibrio anguillarum* injection (Zhu et al., 2006). A twelve-domain KPI gene from the Zhikong scallop *Chlamys farreri* (CfKZSPI) is highly expressed after *V. anguillarum* challenge (Wang et al. 2008). A double-headed KPI from the hemocyte cDNA library of the oriental white shrimp *Fenneropenaeus chinensis* is up-regulated in shrimp infected with the white spot syndrome virus (WSSV) (Kong et al., 2009). Likely, SPI*Pm*2 is up-regulated after WSSV challenge (data unpublished) and yellow head virus (Prapavorarat et al., 2010). The results lead to the question on how the SPI*Pm*2 involve in WSSV infection. The recombinant SPI*Pm*2 was produced for that question. The shrimp were injected with rSPI*Pm*2 and WSSV. The WSSV proliferation was determined. It found that SPI*Pm*2 had the anti-viral activity against WSSV. Previously, the recombinant vp28, enveloped protein of WSSV, was produced. Far-western bolt analysis of the recombinant vp28 showed that the recombinant vp28 could bind with SPI*Pm*2 (Sritunyalucksana et al., 2006). Possibly, SPI*Pm*2 might prevent the WSSV invasion into the host cell. When shrimp were infected by WSSV, it seemed that the SPI*Pm*2 protein level of all tissues was decreased, whereas, mRNA expression level of SPI*Pm*2 was increased after WSSV infection (data unpublished). Possibly, SPI*Pm*2 might be used for shrimp defense against WSSV. In addition, SPI*Pm*2 was found in the plasma of shrimp. It was suggested that SPI*Pm*2 was secreted for anti-WSSV. Because of secretion of SPI*Pm*2, the protein level of SPI*Pm*2 in tissues was decreased when shrimp was infected by WSSV. The anti-viral mechanism of SPI*Pm*2 was suggested that SPI*Pm*2 probably inhibited the essential proteinase for WSSV proliferation or invasion into the host cell.

CHAPTER V

CONCLUSIONS

Two hemocyte-specific Kazal type proteinase inhibitors, KPI2 and KPI8, inhibited the subtilisin and trypsin, respectively, but not the chymotrypsin and elastase. The KPI2 also weakly inhibited trypsin. Its domain 1 with the P_1 Arg weakly inhibited both the subtilisin and trypsin while the domain 2 with the P_1 Ser inhibited strongly the subtilisin but not the trypsin. The KPI8_domain2 with the P_1 Lys strongly inhibited trypsin while the KPI8_domain1 with also the P_1 Lys was inactive against the proteinases tested. We, thus, replaced the P_2 Gly32 of KPI8_domain1 with Pro. The inhibitory activity of the mutant was determined and compared with that of the wild type domain 1. As predicted, the mutant was active against trypsin. We have demonstrated that the two hemocyte-specific Kazal type proteinase inhibitors with an unusual amino acid configuration in their substrate-interacting pockets are effective against several proteinases and that the change in this pocket greatly affects inhibitor specificity. We observed that the proteinase activity from *Aphanomyces astaci* using the S-2222 and S-2586 but not the S-7388 were decreased by about 20% and 60%, respectively, when the extracellular proteinase was incubated with KPI2. The KPI8 was inactive against extracellular *A. astaci* proteinase. Whether these inhibitors are primarily aimed at endogenous targets or intruding microorganisms remains to be established.

The five-domain Kazal-type serine proteinase inhibitor SPI*Pm*2 with the domain P_1 residues Thr, Ala, Glu, Lys and Glu from the black tiger shrimp *Penaeus*

monodon is presumably involved in innate immune response. Domain 1 was found to be inactive. Domains 2, 3 and 5 inhibited subtilisin. Domain 2 inhibited also elastase. Domain 4 weakly inhibited subtilisin and trypsin. The intact SPI*Pm*2 inhibitor was found to possess bacteriostatic activity against the *Bacillus subtilis.* Domains 2, 4 and 5 contributed to this bacteriostatic activity. Mutagenesis of the P_2' residue of the domain 1 and domain 3 of SPI*Pm*2 significantly altered the inhibitory activity. It means that P_2' position of Kazal-type SPI may involve in binding efficiency against proteinase. To delineate the genomic organization of the SPI gene, the genomic DNA was amplified, sequenced and aligned with the cDNA clone. The result showed that the size of the SPI*Pm*2 gene was about 3.7 kb. This gene consisted of seven exons interrupted by six introns, which were between each domain of SPI*Pm*2. To determine the effect of SPIPm2 on WSSV replication, the shrimp were injected with rSPI*Pm*2 and WSSV. The WSSV proliferation was determined. It found that SPI*Pm*2 had the anti-viral activity against WSSV. The whereabouts of SPI*Pm*2 protein expression was determined from normal and WSSV-infected shrimp at 48 h. The result showed that SPI*Pm*2 was mainly found in hemocyte of normal shrimp. It was also found in gill, heart, epipodite, stomach and lymphoid, but the protein level was not high in those tissues. When shrimp were infected by WSSV, it seemed that the SPI*Pm*2 protein level of all tissues was decreased. Possibly, SPI*Pm*2 might be used for shrimp defense against WSSV. In addition, SPI*Pm*2 was found in the plasma of shrimp. It was suggested that SPI*Pm*2 was secreted for anti-WSSV. Because of secretion of SPI*Pm*2, the protein level of SPI*Pm*2 in tissues was decreased when shrimp was infected by WSSV.

REFERENCES

Aeschlimann D, and Pualsson, M. (1994). Transglutaminases: protein crosslinking enzynes in tissues and body fluids. *Thrombosis Haemostasis* **71**:402-415.

Aono H, Mori K. (1996). Interaction between hemocytes and plasma is necessary for hemolymph coagulation in the spiny lobster, *Panulirus japonicus*. *Comparative Biochemistry and Physiology - A Physiology* **113**(3):301-305.

Araujo RN, Campos IT, Tanaka AS, Santos A, Gontijo NF, Lehane MJ, Pereira MH. (2007). Brasiliensin: A novel intestinal thrombin inhibitor from *Triatoma brasiliensis* (Hemiptera: Reduviidae) with an important role in blood intake. *International Journal for Parasitology* **37**(12):1351–1358.

Ariki S, Koori K, Osaki T, Motoyama K, Inamori KI, Kawabata SI. (2004). A serine protease zymogen functions as a pattern-recognition receptor for lipopolysaccharides. *Proceedings of the National Academy of Sciences of the United States of America* **101**(4):953-958.

Aspán A, and Söderhäll, K. (1991). Purification of prophenoloxidase from crayfish blood-cells, and its activation by an endogenous serine proteinase. *Insect Biochemistry* **21**:363-373.

Aspán A, Huang T., Cerenius, L., Soderhall, K. (1995). cDNA cloning of prophenoloxidase from the freshwater crayfish *Pacifastacus leniusculus* and its activation. *Proc. Natl. Acad. Sci.* **92**:939-943.

Augustin R, Siebert S, Bosch TC. (2009). Identification of a Kazal-type serine protease inhibitor with potent anti-staphylococcal activity as part of Hydra's innate immune system. *Developmental and Comparative Immunology* **33**(7):830–837.

Bangyeekhun E, Cerenius L, Söderhäll K. (2001). Molecular cloning and characterization of two serine proteinase genes from the crayfish plague fungus, *Aphanomyces astaci*. *Journal of Invertebrate Pathology* **77**(3):206-216.

Bode W, Huber R. (2000). Structural basis of the endoproteinase-protein inhibitor interaction. *Biochimica et Biophysica Acta (BBA) - Protein Structure and Molecular Enzymology* **1477**(1-2):241-252.

Bode W. (1992). Natural protein proteinase inhibitors and their interaction with proteinases. *European Journal of Biochemistry* **204**(2):433-451.

Bolognesi M, Gatti G, Menagatti E, Guarneri M, Marquart M, Papamokos E, Huber R. (1982). Three-dimensional structure of the complex between pancreatic secretory trypsin inhibitor (Kazal type) and trypsinogen at 1.8 A resolution. Structure solution, crystallographic refinement and preliminary structural interpretation. *Journal of Molecular Biology* **162**(4):839–868.

Bradford MM. (1976). A rapid and sensitive method for the quantitation of microgram quantities of protein utilizing the principle of protein-dye binding. *Analytical Biochemistry* **72**:248-254.

Bruno S, Duschak VG, Ledesma B, Ferella M, Andersson B, Guarnera EA, Angel SO. (2004). Identification and characterization of serine proteinase inhibitors from *Neospora caninum*. *Molecular and Biochemical Parasitology* **136**(1):101–107.

Campos ITN, Silva MM, Azzolini SS, Souza AF, Sampaio CA, Fritz H, Tanaka AS. (2004). Evaluation of phage display system and leech-derived tryptase inhibitor as a tool for understanding the serine proteinase specificities. *Archives of Biochemistry and Biophysics* **425**(1):87–94.

Campos ITN, Amino R, Sampaio CAM, Auerswald EA, Friedrich T, Lemaire HG et al. (2002). Infestin, a thrombin inhibitor presents in Triatoma infestans midgut, a Chagas' disease vector: Gene cloning, expression and characterization of the inhibitor. *Insect Biochemistry and Molecular Biology* **32**(9):991-997.

Cao JX, Dai JQ, Dai ZM, Yin GL, Yang WJ. (2007). A male reproduction-related kazaltype peptidase inhibitor gene in the prawn, Macrobrachium rosenbergii : molecular characterization and expression patterns. *Marine Biotechnology (New York, N.Y.)* 9(1):45–55.

Cerenius L, Bangyeekhun E, Keyser P, Söderhäll I, Söderhäll K. (2003). Host prophenoloxidase expression in freshwater crayfish is linked to increased resistance to the crayfish plague fungus, Aphanomyces astaci. *Cellular Microbiology* **5**(5), 353-357.

Cerenius L, Liu H, Zhang Y, Rimphanitchayakit V, Tassanakajon A, Gunnar Andersson M, Söderhäll K, Söderhäll I (2010). High sequence variability among hemocyte-specific Kazaltype proteinase inhibitors in decapod crustaceans. *Developmental and Comparative Immunology* **34**(1):69–75.

Chen MY, Hu KY, Huang CC, Song YL. (2005). More than one type of transglutaminase in invertebrates? A second type of transglutaminase is involved in shrimp coagulation. *Developmental and Comparative Immunology* **29**(12):1003-1016.

Chera S, de Rosa R, Miljkovic-Licina M, Dobretz K, Ghila L, Kaloulis K, Galliot B. (2006). Silencing of the hydra serine protease inhibitor Kazal1 gene mimics the human SPINK1 pancreatic phenotype. *Journal of Cell Science* **119**(5):846–857.

Christeller JT. (2005). Evolutionary mechanisms acting on proteinase inhibitor variability. *FEBS Journal* **272**(22):5710-5722.

Cruciani RA, Barker JL, Zasloff M, Chen HC, Colamonici O. (1991). Antibiotic magainins exert cytolytic activity against transformed cell lines through channel formation. *Proc Natl Acad Sci U S A* **88**(9):3792-3796.

Destoumieux D, Bulet P, Loew D, Van Dorsselaer A, Rodriguez J, Bachere E. (1997). Penaeidins, a new family of antimicrobial peptides isolated from the shrimp *Penaeus vannamei* (Decapoda). *J Biol Chem* **272**(45):28398-28406.

Destoumieux-Garzon D, Saulnier D, Garnier J, Jouffrey C, Bulet P, Bachere E. (2001). Crustacean immunity. Antifungal peptides are generated from the C terminus of shrimp hemocyanin in response to microbial challenge. *J Biol Chem* **276**(50):47070-47077.

Dieguez-Uribeondo J, Cerenius L. (1998). The inhibition of extracellular proteinases from *Aphanomyces spp* by three different proteinase inhibitors from crayfish blood. *Mycological Research* **102**(7):820-824.

Di Marco S, Priestle JP. (1997). Structure of the complex of leech-derived tryptase inhibitor (LDTI) with trypsin and modeling of the LDTI-tryptase system. *Structure* **5**(11):1465–1474.

Fink E, Rehm H, Gippner C, Bode W, Eulitz M, Machleidt W, Fritz H. (1986). The primary structure of bdellin B-3 from the leech Hirudo medicinalis. Bdellin B-3 is a compact proteinase inhibitor of a ‘‘non-classical’’ Kazal type. It is present in the leech in a high molecular mass form. *Biological Chemistry Hoppe-Seyler* **367**(12):1235– 1242.

Friedrich T, Kröger B, Bialojan S, Lemaire HG, Höffken HW, Reuschenbach P, Otte M, Dodt J. (1993) A Kazal-type inhibitor with thrombin specificity from Rhodnius prolixus .*Journal of Biological Chemistry* **268**(22):16216–16222.

Fritz H, Sommerhoff C. (1999). Tryptase inhibitor. United States Patent No. 5,972,698.

González Y, Tanaka AS, Hirata IY, del Rivero MA, Oliva ML, Araujo MS, Chavez MA. (2007a). Purification and partial characterization of human neutrophil elastase inhibitors from the marine snail *Cenchritis muricatus* (Mollusca). *Comparative Biochemistry and Physiology - B Biochemistry and Molecular Biology* **146**(4):506–513.

González Y, Pons T, Gil J, Besada V, Alonso-del-Rivero M, Tanaka AS, Araujo MS, Chávez MA. (2007b). Characterization and comparative 3D modeling of CmPI-II, a novel 'nonclassical' Kazal-type inhibitor from the marine snail *Cenchritis muricatus* (Mollusca). *Biological Chem*istry **388**(11):1183–1194.

Gottar M, Gobert V, Matskevich AA, Reichhart JM, Wang C, Butt TM, Belvin M, Hoffmann JA, Ferrandon D. (2006). Dual detection of fungal infections in Drosophila via recognition of glucans and sensing of virulence factors. *Cell* **127**(7):1425-1437.

Greenberg CS, Birckbichler PJ, Rice RH. (1991). Transglutaminases: Multifunctional cross-linking enzymes that stabilize tissues. *Faseb Journal* **5**(15):3071-3077.

Gross PS, Bartlett TC, Browdy CL, Chapman RW, Warr GW. (2001). Immune gene discovery by expressed sequence tag analysis of hemocytes and hepatopancreas in the Pacific White Shrimp, Litopenaeus vannamei, and the Atlantic White Shrimp, L. setiferus. *Developmental & Comparative Immunology* **25**(7):565-577.

Han Y, Yu H, Yang X, Rees HH, Liu J, Lai R. (2008). A serine proteinase inhibitor from frog eggs with bacteriostatic activity. *Comparative Biochemistry and Physiology - B Biochemistry and Molecular Biology* **149**(1):58-62.

Hancock RE, Diamond G. (2000). The role of cationic antimicrobial peptides in innate host defences. *Trends Microbiol* **8**(9):402-410.

Hemmi H, Kumazaki T, Yoshizawa-Kumagaye K, Nishiuchi Y, Yoshida T, Ohkubo T, Kobayashi Y. (2005). Structural and functional study of an Anemonia elastase inhibitor, a "nonclassical" Kazal-type inhibitor from *Anemonia sulcata*. *Biochemistry* **44**(28):9626-9636.

Hergenhahn H, Aspan, A., and Söderhäll, K. (1987). Purification and characterization of a high-M_r proteinase inhbitor of pro-phenol oxidase activation from crayfish plasma. *Biochemical Journal* **248**:223-228.

Hoebe K, Janssen E, Beutler B. (2004). The interface between innate and adaptive immunity. *Nature Immunology* **5**(10):971-974.

Hoffmann JA, Kafatos FC, Janeway Jr CA, Ezekowitz RAB. (1999). Phylogenetic perspectives in innate immunity. *Science* **284**(5418):1313-1318.

Huang CC, Sritunyalucksana K, Soderhall K, Song YL, Yeh MS, Huang CJ et al. (2004). Molecular cloning and characterization of tiger shrimp (*Penaeus monodon*) transglutaminase. *Dev Comp Immunol* **28**(4):279-294.

Iwanaga S, Bok LL. (2005). Recent advances in the innate immunity of invertebrate animals. *Journal of Biochemistry and Molecular Biology* **38**(2):128-150.

Janeway Jr CA. (1998). Approching the asymptole evolution and revolution in immunology Colo. Spring Habour Symp. *Quant. Biol.* **54**:1-13.

Jering H, Tschesche H. (1976). Replacement of lysine by arginine, phenylalanine and tryptophan in the reactive site of the bovine trypsin-kallikrein inhibitor (Kunitz) and change of the inhibitory properties. *European Journal of Biochemistry* **61**(2): 453–463.

Jiravanichpaisal P, Lee BL, Soderhall K. (2006). Cell-mediated immunity in arthropods: Hematopoiesis, coagulation, melanization and opsonization. *Immunobiology* **211**(4):213-236.

Johansson MW, Keyser P, Söderhäll K. (1994). Purification and cDNA cloning of a four-domain Kazal proteinase inhibitor from crayfish blood cells. *European Journal of Biochemistry* **223**(2):389-394.

Kanost MR. (1999). Serine proteinase inhibitors in arthropod immunity. *Developmental and Comparative Immunology* **23**(4-5):291-301.

Kim Y-A, (2006). Haematopoiesis, Kazal Inhibitors and Crustins in a Crustacean, Uppsala, 1-48 pp.

Kong HJ, Cho HK, Park EM, Hong GE, Kim YO, Nam BH, Kim WJ, Lee SJ, Han HS, Jang IK, Lee CH, Cheong J, Choi TJ. (2009). Molecular cloning of Kazal-type proteinase inhibitor of the shrimp *Fenneropenaeus chinensis*. *Fish and Shellfish Immunology* **26**(1):109–114.

Kopácek P, Hall M, Soderhall K. (1993). Characterization of a clotting protein, isolated from plasma of the freshwater crayfish *Pacifastacus leniusculus*. *Eur J Biochem* **213**(1):591-597.

Krowarsch D, Cierpicki T, Jelen F, Otlewski J. (2003). Canonical protein inhibitors of serine proteases. *Cellular and Molecular Life Sciences* **60**(11):2427–2444.

Laskowski Jr M, Qasim MA. (2000). What can the structures of enzyme-inhibitor complexes tell us about the structures of enzyme substrate complexes?. *Biochimica et Biophysica Acta - Protein Structure and Molecular Enzymology* **1477**(1-2):324-337.

Laskowski M, Kato I. (1980). Protein inhibitors of proteinases. *Annu Rev Riochem* **49**:593-626.

Lauber T, Schulz A, Schweimer K, Adermann K, Marx UC. (2003). Homologous proteins with different folds: the three-dimensional structures of domains 1 and 6 of the multiple Kazal-type inhibitor LEKTI. *Journal of Molecular Biology* **328**(1):205-219.

Li Y, Qian YQ, Ma WM, Yang WJ. (2009a). Inhibition mechanism and the effects of structure on activity of Male Reproduction-Related Peptidase Inhibitor Kazal-Type (MRPINK) of *Macrobrachium rosenbergii*. *Marine Biotechnology* **11**(2):252-259.

Li XC, Wang XW, W ang ZH, Zhao XF, Wang JX. (2009b). A three-domain Kazal-type serine proteinase inhibitor exhibiting domain inhibitory and bacteriostatic activities from freshwater crayfish Procambarus clarkii. *Developmental and Comparative Immunology* **33**(12):1229–38.

Li Y, Ma WM, Dai JQ, Feng CZ, Yang F, Ohira T, Nagasawa H, Yang WJ. (2008). Inhibition of a novel sperm gelatinase in prawn sperm by the male reproduction-related Kazal-type peptidase inhibitor. *Molecular Reproduction and Development* **75**(8):1327–1337.

Lovato DV, Nicolau de Campos IT, Amino R, Tanaka AS. (2006). The full-length cDNA of anticoagulant protein infestin revealed a novel releasable Kazal domain, a neutrophil elastase inhibitor lacking anticoagulant activity. *Biochimie* **88**(2):673–681.

Lu SM, Lu W, Qasim MA, Anderson S, Apostol I, Ardelt W, Bigler T, Chiang YW, Cook J, James MN, Kato I, Kelly C, Kohr W, Komiyama T, Lin TY, Ogawa M, Otlewski J, Park SJ, Qasim S, Ranjbar M, Tashiro M, Warne N, Whatley H,

Wieczorek A, Wieczorek M, Wilusz T, Wynn R, Zhang W, Laskowski M. (2001). Predicting the reactivity of proteins from their sequence alone: Kazal family of protein inhibitors of serine proteinases. *Proceedings of the National Academy of Sciences of the United States of America* **98**(4):1410–1415.

Lu W, Apostol I, Qasim MA, Warne N, Wynn R, Zhang WL et al. (1997). Binding of amino acid side-chains to S1 cavities of serine proteinases. *Journal of Molecular Biology* **266**(2):441-461.

Martin GG, Omori JEHS, Chong C, Hoodbhoy T, McKrell N. (1991). Localization and roles of coagulogen and transglutaminase in hemolymph coagulation in decapod crustaceans. *Comparative Biochemistry and Physiology Part B: Biochemistry and Molecular Biology* **100**(3):517-522.

Masaki O, Nobuyuki O, Masahiko H, Hideo B, Ken-ichi Y. Serine protease inhibitor Kazal type 1 (SPINK1): beyond the trypsin inhibitor. *Current Enzyme Inhibition* **5**(2):110–116.

Mende K, Lange U, Nowak G. (2004). Three recombinant serine proteinase inhibitors expressed from the coding region of the thrombin inhibitor dipetalogastin. *Insect Biochemistry and Molecular Biology* **34**(9):971-979.

Mende K, Petoukhova O, Koulitchkova V, Schaub GA, Lange U, Kaufmann R, Nowak G. (1999). Dipetalogastin, a potent thrombin inhibitor from the blood-sucking insect. Dipetalogaster maximus cDNA cloning, expression and characterization. *European Journal of Biochemistry* **266**(2):583–90.

Millar DA, and Ratcliffe, N. A. (1994). Invertebrated. In: Turner, I.R.J. (Ed.), Immunology: A Comparative Approach, Chichester: Wiley, pp. 29-68.

Morris MT, Cheng WC, Zhou XW, Brydges SD, Carruthers VB. (2004). *Neospora caninum* expresses an unusual single-domain Kazal protease inhibitor that is discharged into the parasitophorous vacuole. *International Journal for Parasitology* **34**(6):693–701.

Morris MT, Coppin A, Tomavo S, Carruthers VB. (2002). Functional analysis of Toxoplasma gondii protease inhibitor 1. *Journal of Biological Chemistry* **277**(47):45259-45266.

Morris MT, Carruthers VB. (2003). Identification and partial characterization of a second Kazal inhibitor in *Toxoplasma gondii*. *Molecular and Biochemical Parasitol*ogy **128**(1):119–122.

Murakami T, Niwa M, Tokunaga F, Miyata T, Iwanaga S. (1991). Direct virus inactivation of tachyplesin I and its isopeptides from horseshoe crab hemocytes. *Chemotherapy* **37**(5):327-334.

Niimi T, Yokoyama H, Goto A, Beck K, Kitagawa Y. (1999). A Drosophila gene encoding multiple splice variants of Kazal-type serine protease inhibitor-like proteins with potential destinations of mitochondria, cytosol and the secretory pathway. *European Journal of Biochemistry* **266**(1):282–292.

Nirmala X, Kodrik D, Zurovec M, Sehnal F. (2001a). Insect silk contains both a Kunitz-type and a unique Kazal-type proteinase inhibitor. *European Journal of Biochemisry* **268**(7):2064-2073.

Nirmala X, Mita K, Vanisree V, Zurovec M, Sehnal F. (2001b). Identification of four small molecular mass proteins in the silk of *Bombyx mori*. *Insect Molecular Biolog y* **10**(5):437–45.

Nowak G, Schrör K. (2007). Hirudin--the long and stony way from an anticoagulant peptide in the saliva of medicinal leech to a recombinant drug and beyond. A historical piece. *Thrombosis Haemostasis* **98**(1):116–119.

O'Brien D, and McVey, J, 1993. Blood coagulation, inflammation, and defence. In: Sim, I.E. (Ed.), The natueal immune system, humoral factors, New York: IRL Press, pp. 257-280.

Patat SA, Carnegie RB, Kingsbury C, Gross PS, Chapman R, Schey KL. (2004). Antimicrobial activity of histones from hemocytes of the Pacific white shrimp. *Eur J Biochem* **271**(23-24):4825-4833.

Perazzolo LM, Barracco MA. (1997). The prophenoloxidase activating system of the shrimp *Penaeus paulensis* and associated factors. *Developmental and Comparative Immunology* **21**(5):385-395.

Pham TN, Hayashi K, Takano R, Itoh M, Eguchi M, Shibata H et al. (1996). A new family of serine protease inhibitors (Bombyx family) as established from the unique topological relation between the positions of bisulfide bridges and reactive site. *Journal of Biochemistry* **119**(3):428-434.

Prapavorarat A, Pongsomboon S, Tassanakajon A. (2010). Identification of genes expressed in response to yellow head virus infection in the black tiger shrimp, *Penaeus monodon*, by suppression subtractive hybridization. *Developmental and Comparative Immunology* **34**(6):611-617.

Pszenny V, Angel SO, Duschak VG, Paulino M, Ledesma B , Yabo MI, Guarnera E, Ruiz AM, Bontempi EJ. (2000). Molecular cloning, sequencing and expression of a serine proteinase inhibitor gene from *Toxoplasma gondii*. *Molecular and Biochemical Parasitology* **107**(2):241–249.

Quinton TM, Kim S, Derian CK, Jin J, Kunapuli SP. (2004). Plasmin-mediated activation of platelets occurs by cleavage of protease-activated receptor 4. *Journal of Biological Chemistry* 279(18):18434–18439.

Rawlings ND, Tolle DP, Barrett AJ. (2004). Evolutionary families of peptidase inhibitors. *Biochem J* **378**(Pt 3):705-716.

Rawlings ND, Morton FR, Kok CY, Kong J, Barrett AJ. (2008). MEROPS: the peptidase database. *Nucleic Acids Res* **36**:D320-325.

Read RJ, Fujinaga M, Sielecki AR, James MN. (1983). Structure of the complex of Streptomyces griseus protease B and the third domain of the turkey ovomucoid inhibitor at 1.8-A˚ resolution. *Biochemistry* **22**(19):4420–4433.

Rimphanitchayakit V, Tassanakajon A. (2010). Structure and function of invertebrate Kazal-type serine proteinase inhibitors. *Developmental and Comparative Immunology* **34**(4):377-386.

Salzet M. (2001). Vertebrate innate immunity resembles a mosaic of invertebrate immune responses. *Trends in Immunology* **22**(6):285-288.

Schechter I, Berger A. (1976). On the size of the active site in proteases. I. Papain. *Biochemical and Biophysical Research Communications* **27**(2):157–162.

Schlott B, Wöhnert J, Icke C, Hartmann M, Ramachandran R, Gührs KH, Glusa E, Flemming J, Görlach M, Grosse F, Ohlenschläger O. (2002). Interaction of Kazal-type inhibitor domains with serine proteinases: biochemical and structural studies. *Journal of Molecular Biology* **318**(2):533–546.

Shi XZ, Zhao XF, Wang JX. (2008). Molecular cloning and expression analysis of chymotrypsin-like serine protease from the Chinese shrimp, *Fenneropenaeus chinensis*. *Fish and Shellfish Immunology* **25**(5):589-597.

Shiao SH, Higgs S, Adelman Z, Christensen BM, Liu SH, Chen CC. (2001). Effect of prophenoloxidase expression knockout on the melanization of microfilariae in the mosquito *Armigeres subalbatus*. *Insect Molecular Biology* **10**(4):315-321.

Simonet G, Claeys I, Broeck JV. (2002a). Structural and functional properties of a novel serine protease inhibiting peptide family in arthropods. *Comparative Biochemistry and Physiology Part B: Biochemistry and Molecular Biology* **132**(1):247-255.

Slowinska M, Olczak M, Wojtczak M, Glogowski J, Jankowski J, Watorek W et al. (2008). Isolation, characterization and cDNA sequencing of a Kazal family proteinase inhibitor from seminal plasma of turkey (*Meleagris gallopavo*). *Comparative Biochemistry and Physiology - B Biochemistry and Molecular Biology* **150**(2):207-215.

Söderhäll K, Ajaxon R. (1982). Effect of quinones and melanin on mycelial growth of Aphanomyces spp. and extracellular protease of *Aphanomyces astaci*, a parasite on crayfish. *Journal of Invertebrate Pathology* **39**(1):105-109.

Söderhäll K, Cerenius L. (1998). Role of the prophenoloxidase-activating system in invertebrate immunity. *Curr Opin Immunol* **10**(1):23-28.

Sommerhoff CP, Söllner C, Mentele R, Piechottka GP, Auerswald EA, Fritz H. (1994) A Kazal-type inhibitor of human mast cell tryptase: isolation from the medical leech Hirudo medicinalis, characterization, and sequence analysis. *Biological Chemistry Hoppe-Seyler* **375**(10):685–694.

Somprasong N, Rimphanitchayakit V, Tassanakajon A. (2006). A five-domain Kazaltype serine proteinase inhibitor from black tiger shrimp Penaeus monodon and its inhibitory activities. *Developmental and Comparative Immunology* **30**(11):998–1008.

Sritunyalucksana K, Soderhall K. (2000). The proPO and clotting system in crustaceans. *Aquaculture* **191**(1-3):53-69.

Sritunyalucksana K, Wannapapho W, Lo CF, Flegel TW. (2006). PmRab7 is a VP28-binding protein involved in white spot syndrome virus infection in shrimp. *Journal of Virology* **80**(21):10734-10742.

Supungul P, Klinbunga S, Pichyangkura R, Jitrapakdee S, Hirono I, Aoki T, Tassanakajon A. (2002). Identification of immune-related genes in hemocytes of black tiger shrimp (*Penaeus monodon*). *Marine Biotechnology (New York, N.Y.)* **4**(5):487-494.

Supungul P, Klinbunga S, Pichyangkura R, Hirono I, Aoki T, Tassanakajon A. (2004). Antimicrobial peptides discovered in the black tiger shrimp *Penaeus monodon* using the EST approach. *Dis Aquat Organ* **61**(1-2):123-135.

Tassanakajon A, Klinbunga S, Paunglarp N, Rimphanitchayakit V, Udomkit A, Jitrapakdee S et al. (2006). *Penaeus monodon* gene discovery project: The generation of an EST collection and establishment of a database. *Gene* **384**(1-2):104-112.

Theopold U, Schmidt O, Soderhall K, Dushay MS. (2004). Coagulation in arthropods: defence, wound closure and healing. *Trends in Immunology* **25**(6):289-294.

Tian M, Benedetti B, Kamoun S. (2005). A second Kazal-like protease inhibitor from Phytophthora infestans inhibits and interacts with the apoplastic pathogenesis-related protease P69B of tomato. *Plant Physiology* **138**(3):1785-1793.

Tian M, Huitema E, Da Cunha L, Torto-Alalibo T, Kamoun S. (2004). A Kazal-like extracellular serine protease inhibitor from Phytophthora infestans targets the

tomato pathogenesis-related protease P69B. *Journal of Biological Chemistry* **279**(25):26370-26377.

Travis J, Potempa J, Maeda H. (1995). Are bacterial proteinases pathogenic factors? *Trends in Microbiology* **3**(10):405–407.

Van de Locht A, Lamba D, Bauer M, Huber R, Friedrich T, Kröger B, Höffken W, Bode W. (1995). Two heads are better than one: Crystal structure of the insect derived double domain Kazal inhibitor rhodniin in complex with thrombin. *EMBO Journal* **14**(21):5149-5157.

Visetnan S, Donpudsa S, Supungul P, Tassanakajon A, Rimphanitchayakit V. (2009). Kazal-type serine proteinase inhibitors from the black tiger shrimp *Penaeus monodon* and the inhibitory activities of SPI*Pm*4 and 5. *Fish and Shellfish Immunology* **27**(2):266–274.

Wang B, Zhao J, Song L, Zhang H, Wang L, Li C, Zheng P, Zhu L, Qiu L, Xing K. (2008). Molecular cloning and expression of a novel Kazal-type serine proteinase inhibitor gene from Zhikong scallop *Chlamys farreri*, and the inhibitory activity of its recombinant domain. *Fish and Shellfish Immunol*ogy **24**(5):629–637.

Wang ZH, Zhao XF, Wang JX. (2009). 'Characterization, kinetics, and possible function of Kazal-type proteinase inhibitors of Chinese white shrimp, *Fenneropenaeus chinensis*. *Fish Shellfish Immunology* **26**(6):885-897.

Whaley K, Lemercier, C., 1993. The complement system. In: Sim, I.E. (Ed.), The natural immune system, humoral factors, New York: IRL Press, pp. 121-150.

Wu C, Söderhäll, I, Kim YA, Liu H, Söderhäll K. (2008). Hemocyte-lineage marker proteins in a crustacean, the freshwater crayfish, *Pacifastacus leniusculus*. *Proteomics* **8**(20):4226-4235.

Yeh MS, Chen YL, Tsai IH. (1998). The hemolymph clottable proteins of tiger shrimp, *Penaeus monodon*, and related species. *Comp Biochem Physiol B Biochem Mol Biol* **121**(2):169-176.

Zhang X, Huang C, Qin Q. (2004). Antiviral properties of hemocyanin isolated from shrimp Penaeus monodon. *Antiviral Research* **61**(2):93-99.

Zheng Q-L, Chen J, Nie Z-M, Lv Z-B, Wang D, Zhang Y-Z. (2007). Expression, purification and characterization of a three-domain Kazal-type inhibitor from silkworm pupae (Bombyx mori). *Comparative Biochemistry and Physiology Part B: Biochemistry and Molecular Biology* **146**(2):234-240.

Zhu L, Song L, Chang Y, Xu W, Wu L. (2006). Molecular cloning, characterization and expression of a novel serine proteinase inhibitor gene in bay scallops (*Argopecten irradians*, Lamarck 1819). *Fish and Shellfish Immunology* **20**(3):320–331.

Appendices

Appendix A

SDS-Polyacrylamide Gel Electrophoresis (SDS-PAGE)

1. Preparation for polyacrylamide gel electrophoresis

- **30% (w/v) acrylamide, 0.8% (w/v) bis-acrylamide, 100 ml**

acrylamide	29.2	g
bis-acrylamide	0,8	g

Adjust volume to 100 ml with distilled water.

- **1.5 M Tris-HCl pH 8.8**

Tris (hydroxymethyl)-aminomethen 18.17 g

Adjust pH to 8.8 with 1 M HCl and adjust volume to 100 ml with distilled water.

- **2.0 M Tris-HCl (pH 8.8)**

Tris (hydroxymethyl)-aminomethen 24.2 g

Adjust pH to 8.8 with 1 M HCl and adjust volume to 100 ml with distilled water.

- **0.5 M Tris-HCl pH 6.8**

Tris (hydroxymethyl)-aminomethen 6.06 g

Adjust pH to 6.8 with 1 M HCl and adjust volume to 100 ml with distilled water.

- **1.0 M Tris-HCl pH 6.8**

Tris (hydroxymethyl)-aminomethen 12.1 g

Adjust pH to 6.8 with 1 M HCl and adjust volume to 100 ml with distilled water.

2. SDS-PAGE

- **18% Separating gel**

H_2O	1.013	ml
30% (w/v) Acrylamide solution	4.8	ml
1.5 M Tris (pH 8.8)	2.3	ml
10% SDS	0.08	ml
10% Ammonium persulfate	0.11	ml
TEMED	10	µl

- **5.0% Stacking gel**

H_2O	2.7	ml
30% (w/v) Acrylamide solution	0.67	ml
1.0 M Tris (pH 6.8)	0.5	ml
10% SDS	0.04	ml
10% Ammonium persulfate	0.04	ml
TEMED	5	µl

- **5x Sample buffer**

1 M Tris-HCl pH 6.8	0.6	ml
50% (w/v) Glycerol	5.0	ml
10% SDS	2.0	ml
2-mercaptoethanol	0.5	ml
1% Bromophenol blue	1.0	ml
Distilled water	0.9	ml

One part of sample buffer was added to four parts of sample. The mixture was heated 5 min. in boiling water before loading to the gel.

3. Electrophoresis buffer, 1 litre

(25 mM Tris, 192 mM glycine)

Tris (hydroxymethyl)-aminomethane	3.03	g
Glycine	14.40	g
SDS	1.0	g

Dissolve in distilled water to 1 litre. Do not adjust pH with acid or base (final pH should be 8.3).

Appendix B

Publications

1. Donpusa S, Tassanakajon A, Rimphanitchayakit V. Domain inhibitory and bacteriostatic activities of the five-domain Kazal-type serine proteinase inhibitor from black tiger shrimp *Penaeus monodon*. Developmental and comparative Immunology 2009; 27:266-274.

Developmental and Comparative Immunology 33 (2009) 481–488

Contents lists available at ScienceDirect

Developmental and Comparative Immunology

journal homepage: www.elsevier.com/locate/dci

Domain inhibitory and bacteriostatic activities of the five-domain Kazal-type serine proteinase inhibitor from black tiger shrimp *Penaeus monodon*

Suchao Donpudsa, Anchalee Tassanakajon, Vichien Rimphanitchayakit *

Shrimp Molecular Biology and Genomics Laboratory, Department of Biochemistry, Faculty of Science, Chulalongkorn University, Bangkok 10330, Thailand

ARTICLE INFO

Article history:
Received 20 August 2008
Received in revised form 15 September 2008
Accepted 18 September 2008
Available online 16 October 2008

Keywords:
Penaeus monodon
Black tiger shrimp
Kazal domain
Serine proteinase inhibitor

ABSTRACT

Serine proteinase inhibitors (SPIs) in multi-cellular organisms are important modulators of proteinase activities in various biological processes. A five-domain Kazal-type SPI SPI*Pm*2 from the black tiger shrimp *Penaeus monodon* is presumably involved in innate immune response. The SPI*Pm*2 with the domain P1 residues T, A, E, K and E was isolated from the hemocyte cDNA libraries and found to strongly inhibit subtilisin and elastase, and weakly inhibit trypsin. To unravel further the inhibitory activity of each domain, we subcloned, over-expressed and purified each individual SPI domain. Their inhibitory specificities against trypsin, subtilisin and elastase were determined. Domain 1 was found to be inactive. Domains 2, 3 and 5 inhibited subtilisin. Domain 2 inhibited also elastase. Domain 4 weakly inhibited subtilisin and trypsin. The intact SPI*Pm*2 inhibitor was found to possess bacteriostatic activity against the *Bacillus subtilis* but not the *Bacillus megaterium*, *Staphylococcus aureus*, *Vibrio harveyi* 639 and *Escherichia coli* JM109. Domains 2, 4 and 5 contributed to this bacteriostatic activity.

1. Introduction

Innate and adaptive immunity are important for multi-cellular organisms to protect themselves from the various potential pathogens. Invertebrates only have the innate immunity. The innate immune responses, carried out mostly by the hemocytes, can be divided into humoral and cellular defenses. These responses include phagocytosis, complement, antimicrobial peptides, coagulation and melanization [1,2]. Humoral defense usually involves components released from the hemocytes. These components include antimicrobial peptides, proteases and proteinase inhibitors [3].

The serine proteinase inhibitors (SPIs) are found widely in vertebrates, invertebrates and bacteria. They play important roles as modulators of several biological processes using proteinases, such as digestion, apoptosis, blood coagulation, prophenol oxidase activation, complement system, cellular remodeling, etc. [4–6]. They are also involved in metamorphosis [7], defense against invading organisms [8–11] or counter-defense the host protective proteases [12].

Among the at least 59 families of proteinase inhibitors, the Kazal, Kunitz, and pacifastin canonical inhibitors are relatively well characterized [13–15]. The Kazal-type SPIs are grouped into family I1. The Kazal-type SPIs typically contain one or more Kazal domains. Each domain of 50–60 amino acid residues has a characteristic three-dimensional structures derived from the formation of three intradomain disulfide bridges by six well-conserved cysteine residues [4,16]. The 'canonical' inhibition commences by tight binding of the SPI reactive site loop, into the active site of corresponding proteinase, competitively blocking and rendering the enzyme inactive [4]. The major inhibitory specificity determinant is the P1 amino acid residue which is the second amino acid residue after the second cysteine residue of the domain. A few other adjacent amino acid residues also influence the binding specificity [14,17].

Kazal-type SPIs are also found widely in all organisms. Besides those well-known Kazal-type SPIs like the LEKTI in human blood circulation [18] and the three-domain Kazal inhibitor in ovomucoid from chicken [19], more and more Kazal inhibitors have been identified in both vertebrates and invertebrates. For the recent examples in invertebrates, the SPIs containing four and five Kazal domains from *Litopenaeus vannamei* and *Penaeus monodon*, respectively, were identified from the hemocyte cDNA libraries [20,21]. A two-domain Kazal inhibitor, EPI1, from the oomycete plant pathogen *Phytophthora infestans*, was shown to inhibit subtilisin [12]. The 'nonclassical' Kazal-type elastase inhibitor was isolated from the sea anemone *Anemonia sulcata* [22]. The SPI called greglin specific for elastase/chymotrypsin from the ovary

* Corresponding author. Tel.: +66 2 2185436; fax: +66 2 2185418.
E-mail address: kpvr2@yahoo.com (V. Rimphanitchayakit).

0145-305X/$ – see front matter © 2008 Elsevier Ltd. All rights reserved.
doi:10.1016/j.dci.2008.09.009

gland of the desert locust *Schistocerca gregaria* was characterized [23]. The mollusk Kazal-type SPI, AISPI, was identified from the bay scallop *Argopecten irradians* [24]. The three heat-tolerant human neutrophil elastase inhibitors, CmPI–I, CmPI–II and CmPI–III, were isolated from a marine snail *Cenchritis muricatus* [25]. The male reproductive tract specific two-domain Kazal-type SPI gene was identified in *Macrobrachium rosenbergii* [26]. Most recently, the 12-domain Kazal-type SPI gene was cloned from the Zhikong scallop *Chlamys farreri* [27].

In *P. monodon*, several Kazal proteinase inhibitors were identified from the expressed sequence tag (EST) database (http://pmonodon.biotec.or.th/) particularly the hemocyte libraries [28]. The most abundant SPI is the five Kazal-domain SPI*Pm*2. It was over-expressed and its activity has been studied [21]. The recombinant SPI*Pm*2 exhibits strong inhibitory activity against subtilisin and elastase, weak inhibitory activity against trypsin, and no activity against chymotrypsin. It turns out that the inhibitory specificities cannot be assigned to all Kazal SPI domain of the SPI*Pm*2. It is then interesting to find out the inhibitory specificity of each Kazal domain. In this study, each domain of SPI*Pm*2 was individually over-expressed and tested for their inhibitory specificities. As compared to the intact recombinant SPI*Pm*2 inhibitor, their growth inhibition on bacteria were also elucidated and reported herein.

2. Materials and methods

2.1. Construction of the expression plasmid

For the sake of protein purification, a modified expression vector pVR500 was constructed from an expression vector pET-32a(+) by deleting the His·Tag and S·Tag between *Msc*I and *Kpn*I sites. The only His·Tag left was at the 3′ side of the reading frame and used for the protein purification as described below. The pET-32a(+) was digested with *Msc*I and *Kpn*I, treated with T4 DNA polymerase to blunt the DNA ends and relegated. The resulting pVR500 was sequenced to confirm the correct construction. By using the expression vector pVR500, the cloned gene was fused with the thioredoxin Trx·Tag at the N-terminal side and His·Tag at the C-terminal end.

PCR primers were designed for the PCR amplification of SPI domains from the pSPI*Pm*2-NS2, a pET22b(+) containing the SPI*Pm*2 gene [21]. The forward and reverse primers contain *Nco*I and *Xho*I sites at their 5′ terminal ends, respectively. The restriction sites were for the cloning of SPI domain into the expression vector. The primer sequences and their annealing sites are depicted in Fig. 1 and Table 1. The PCR reaction was carried out in a final volume of 30 μl containing 25 ng of DNA template, 0.45 μM of each primer, 0.2 mM of each dNTP and 0.45 units of *Pfu* polymerase (Promega). The PCR amplification was run for 30 cycles of 45 s at 94 °C, 45 s at 55 °C and 60 s at 72 °C. The PCR product was gel-purified, digested with *Nco*I and *Xho*I and cloned into the pVR500 vector at the same restriction sites. The sequences of the domain clones were verified by DNA sequencing. Each recombinant plasmid was transformed into an *Escherichia coli* Rosetta(DE3)pLysS for over-production of the recombinant protein.

2.2. Expression and purification of the recombinant proteins

The *E. coli* Rosetta(DE3)pLysS transformants were cultured under vigorous shaking at 37 °C. When the optical density at 600 nm of the culture reached 0.6–0.8, the expression was induced by adding IPTG to the final concentration of 1 mM and the incubation was continued for additional 3 h. The expression of five recombinant proteins was checked by sodium dodecyl sulfate polyacrylamide gel electrophoresis (SDS-PAGE).

Cells were harvested by centrifugation, resuspended in phosphate-buffered saline, pH 7.4 (1× PBS; 137 mM NaCl, 2.7 mM KCl, 10 mM Na_2HPO_4, 2 mM KH_2PO_4) and sonicated for 2–4 min. The cell lysate was centrifuged at 8000 rpm for 10 min at 4 °C to collect the supernatant. The soluble recombinant protein was purified using a Ni-NTA agarose column and eluted stepwise with the 1× PBS buffer pH 7.4 containing 500 mM imidazole. Consequently, the fractions containing the eluted protein were dialyzed against the enterokinase buffer (20 mM Tris–HCl, pH 8.0, 50 mM NaCl, 2 mM $CaCl_2$) followed by incubation with enterokinase at 23 °C for 16 h in order to cleave the SPI domain away from the Trx·Tag. The final step was to purify the SPI domain using a Ni-NTA agarose column as described above. The purified SPI domain was dialyzed against 50 mM carbonate buffer, pH 10, and analyzed using SDS-PAGE. The concentration of eluted protein was determined using the Bradford method [29].

The intact SPI*Pm*2 was prepared according to Somprasong et al. [21].

2.3. SDS-PAGE and Western blot analysis

Standard 15% SDS-PAGE was used to analyze and trace the expressed recombinant proteins upon expression and purification. The protein bands were visualized by staining with Coomassie Brilliant Blue.

Western blot analysis was used to confirm the identity of the expressed recombinant proteins. The proteins separated by the SDS-PAGE were electro-transferred onto a nitrocellulose membrane (Bio-Rad) in a semi-dry electrophoretic transfer cell (Trans-blot SD, Bio-Rad) at 10 V for 30 min. The membrane was then washed twice with Tris-buffered saline (TBS; 10 mM Tris–HCl, 150 mM NaCl, pH 7.5) at room temperature for 10 min, and incubated in a blocking buffer (3% BSA in TBS buffer) at room temperature for 1 h. The membrane was subsequently washed twice with TBS containing 0.05% (v/v) Tween20 at room temperature for 10 min and incubated with anti-His antibodies (Qiagen) at room temperature for 1 h. After washing with TBS, the secondary antibodies conjugated with horseradish peroxidase were then added. The recombinant protein was visualized as a reddish-brown band with the HRP staining solution [18 mg diaminobenzine (DAB) dissolved in Tris–saline (9% (w/v) NaCl in 1 M Tris–HCl, pH 8.0)] and 30% hydrogen peroxide.

2.4. MALDI-TOF mass spectrometry

MALDI-TOF mass spectrometry was used for an accurate molecular mass determination of the rSPI domains. It was performed in the commercial facility of the Proteomic Service Center, Bioservice Unit (BSU) (BIOTEC, Pathumthani, Thailand).

2.5. Inhibition assay

The inhibitory activity of each domain towards serine proteinases; trypsin (bovine pancreas, Sigma), subtilisin Carlsberg (*Bacillus licheniformis*, Sigma) and elastase (porcine pancreas, Pacific Science), was assayed using a procedure of Hergenhahn et al. [30]. The reaction mixture consisted of 50 mM Tris–HCl, pH 8; 146.8 and 293.6 μM of *N*-benzoyl–Phe–Val–Arg–*p*-nitroanilide (Sigma) for trypsin and subtilisin and 886.1 μM of *N*-succinyl–Ala–Ala–Ala–*p*-nitroanilide (Sigma) for elastase; and 0.02, 0.04 and 0.08 μM of subtilisin, trypsin and elastase, respectively, in a total

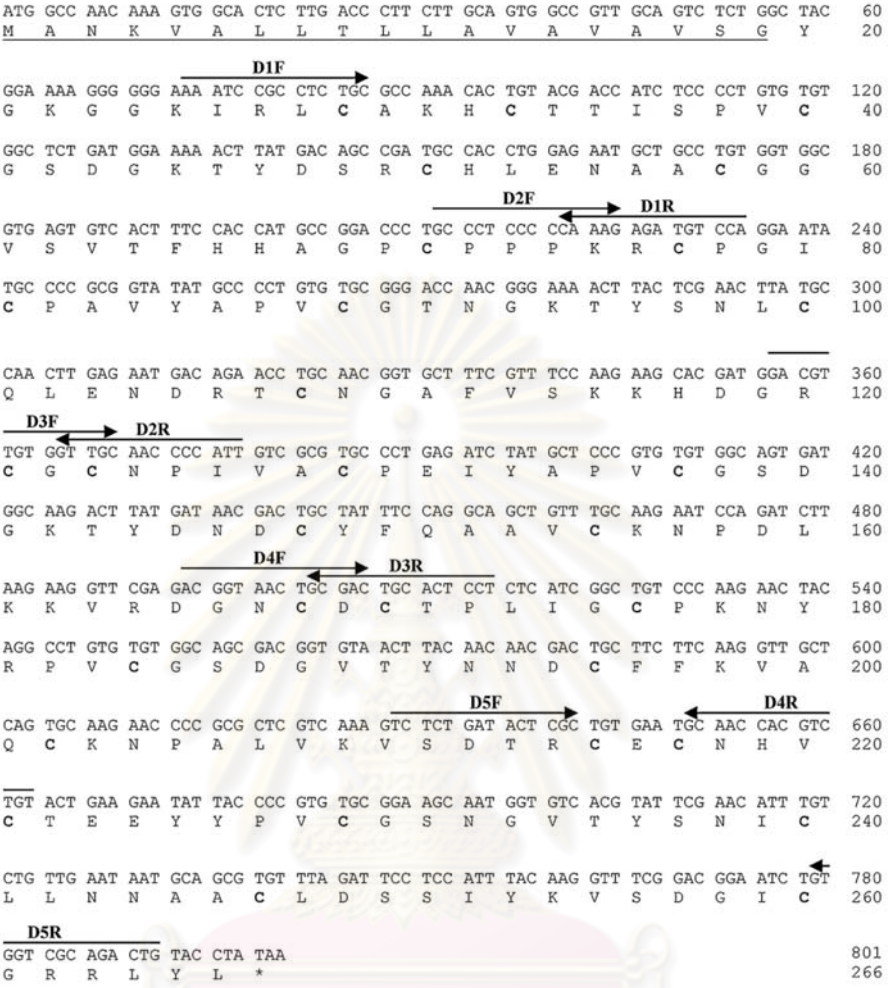

Fig. 1. The nucleotide and amino acid sequences of SPI*Pm*2. The annealing sites of primers used to amplify each inhibitory domain for the cloning into an expression vector. The SPI domains 1–5 are represented by D1–D5. The F and R letters indicate forward and reverse direction as also represented by the directions of arrows. The cysteine residues and signal sequence are bold-faced and underlined, respectively.

Table 1
Nucleotide sequences of primers for PCR amplification of the Kazal domains.

Primer[a]	Sequence (5′–3′)[b]
1F	AAAGCCATGGAAATCCGCCTCTGC
1R	GGCACTCGAGTGGACATCTCTTTG
2F	GCCGCCATGGGCCCTCCCCCAAAG
2R	GGCACTCGAGAATGGGGTTGCAAC
3F	AAGCCCATGGGACGTTGTGGTTGC
3R	AGCCCTCGAGAGGAGTGCAGTCGC
4F	AAGGCCATGGACGGTAACTGCGAC
4R	ATTCCTCGAGACAGACGTGGTTGC
5F	CTCGCCATGGTCTCTGATACTCGC
5R	CGACCTCGAGCAGTCTGCGACCAC

[a] F and R are forward and reverse, respectively.
[b] Restriction sites are underlined.

volume of 100 μl. The final concentrations of SPI*Pm*2 inhibitory domains in the reaction mixtures were listed in Table 2. The reaction was incubated at 30 °C for 15 min and then terminated by adding 50 μl of 50% acetic acid. The absorbance of *p*-nitroaniline formed was measured at 405 nm. The percentages of remaining activity were calculated and plotted against the molar ratios of inhibitor domain to proteinase.

2.6. Kinetics of serine proteinase inhibition

The experiment was composed of four sets of reactions for different concentrations of each inhibitory domain. Each set consisted of four concentrations of substrate in the presence of fixed amounts of serine proteinase and three different concentrations of SPI*Pm*2 inhibitory domain. For subtilisin: 10 nM of

Table 2
The final concentrations of SPI*Pm*2 inhibitory domains (D) in the inhibition assay reactions.

	Concentration of inhibitory domain (μM)	
	Subtilisin reactions	Elastase (D2) and trypsin (D4) reactions
D1	0, 0.013, 0.026, 0.051, 0.103, 0.205, 0.410, 0.820	
D2	0, 0.002, 0.004, 0.007, 0.014, 0.028, 0.056, 0.112, 0.224, 0.449, 0.897	0, 0.009, 0.017, 0.034, 0.068, 0.136, 0.272, 0.544, 1.089, 2.178
D3	0, 0.027, 0.055, 0.109, 0.219, 0.438, 0.875	
D4	0, 0.013, 0.026, 0.053, 0.105, 0.210, 0.420, 0.840	0, 0.013, 0.025, 0.050, 0.100, 0.200, 0.400, 0.800, 1.600, 3.200
D5	0, 0.028, 0.056, 0.113, 0.226, 0.452, 0.904	

subtilisin; 0, 0.11, 0.22, 0.44 and 0.88 mM *N*-benzoyl–Phe–Val–Arg–*p*-nitroanilide; 0, 0.003, 0.006 and 0.013 μM domain 2; 0, 0.014, 0.028 and 0.056 μM domain 3 or 0, 0.045, 0.090 and 0.181 μM domain 5 were used. For elastase: 77.2 nM of elastase; 0, 0.22, 0.44, 0.89 and 1.77 mM *N*-succinyl–Ala–Ala–Ala–*p*-nitroanilide; 0, 0.011, 0.021 and 0.043 μM domain 2 were used.

The reactions were made a total volume of 100 μl with 50 mM Tris–HCl, pH 8, and initiated by the addition of proteinase. After incubating at 30 °C for 15 min, they were stopped by adding 50 μl of 50% acetic acid. The absorbance of *p*-nitroaniline formed was measured at 405 nm. The amount of *p*-nitroaniline was calculated using a millimolar extinction coefficient of 9.96. The activity was calculated as nmol of *p*-nitroaniline/min. The activities were plotted against the concentrations of substrates as a substrate saturation curve and a Lineweaver–Burk plot. The apparent K_Ms at different concentrations of inhibitor and V_{max} were determined. The apparent K_Ms were re-plotted against the concentrations of inhibitor. The latter plotting was constructed for the calculation of inhibition constant (K_i).

2.7. Bacterial growth inhibition assay

Bacteriostatic activity of SPI*Pm*2 and its domains was assayed based on the procedure by Han et al. [31] on Gram-positive bacteria, *Bacillus subtilis*, *Bacillus megaterium*, *Staphylococcus aureus*, and Gram-negative bacteria, *Vibrio harveyi* 639, *E. coli* JM109. For each bacterium, the assay was done in duplicate. An overnight culture of bacterium was diluted a 100-fold, and grew in a shaking incubator in the presence of 0, 3.5 and 7 μM of SPI*Pm*2 or 7 μM of each domain at 30 °C for *B. megaterium* and *V. harveyi* 639 and 37 °C for *B. subtilis*, *S. aureus* and *E. coli* JM109. The bacterial growth was measured by monitoring the optical density at 595 nm from 0 to 18 h.

3. Results

3.1. Construction of the expression plasmids for SPI*Pm*2 domains

In an attempt to study each domain of the SPI*Pm*2 separately, five PCR primer pairs were designed for the amplification of the domains such that there would be *Nco*I and *Xho*I sites at the 5′ and 3′ sides of the PCR products. A few amino acid residues were left on both sides of each SPI domain as well (Fig. 1). Initially, the PCR products were cloned into the pET-28a(+). The SPI domains were not detectable probably due to their small sizes which were vulnerable to cellular degradation. The pET-32a(+) was then chosen since the SPI domain sequence would fused with the thioredoxin tag and expressed as fusion protein. To simplify the purification of SPI domains, the His·Tag at the 5′ side in pET-32a(+) was removed along with the S·Tag leaving the His·Tag at the 3′ side intact. The resulting expression vector, pVR500 was, then, used for the cloning of SPI domain sequences. The SPI domain sequences were fused to the 5′ thioredoxin tag and 3′ His·Tag. The recombinant clones were sequenced to verify the correct SPI domain sequences. The recombinant expression plasmids obtained were named pSPI*Pm*2-D1 to pSPI*Pm*2-D5 for domains 1–5, respectively.

3.2. Expression and purification of the domain inhibitors

Each expression plasmid was transformed into an *E. coli* Rosetta(DE3)pLysS for protein expression. The thioredoxin tag-SPI domain fusion proteins were found to be soluble. They were purified using the Ni-NTA agarose column and digested with enterokinase to cleave the SPI domains from the thioredoxin tag. Since only the SPI domains were fused to the His·Tag, they were conveniently purified with the Ni-NTA agarose column.

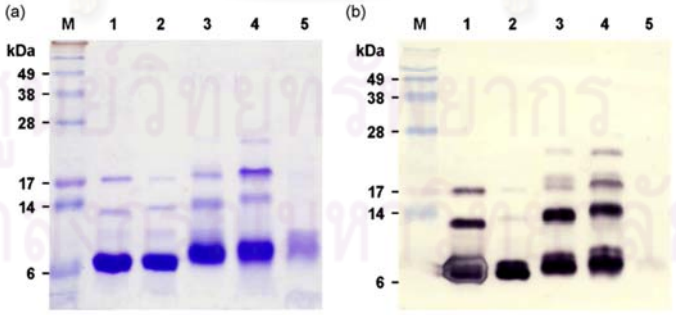

Fig. 2. SDS-PAGE and (a) Western blot analysis (b) of the purified SPI domains. A 15% polyacrylamide gel was used. Lane M is the size marker. Lanes 1–4 are 1.8 μg SPI domains 1–4, respectively. Lane 5 is 0.9 μg SPI domain 5.

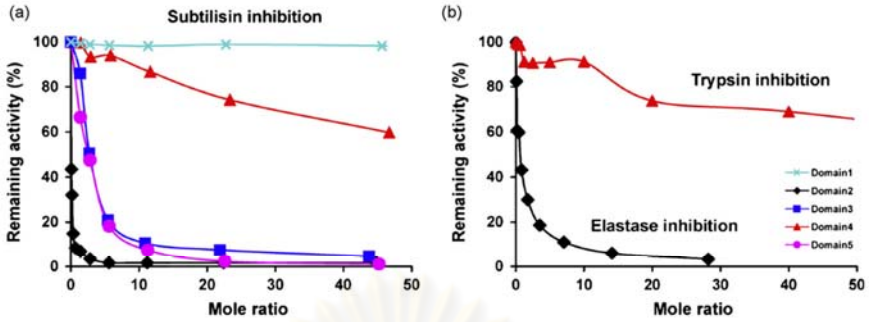

Fig. 3. Inhibition assays of the SPI domains against subtilisin (a), trypsin (b) and elastase (b). All five SPI domains were tested against subtilisin at various mole ratio of inhibitor to protease. Symbols ×, ◆, ■, ▲ and ● are for domains 1–5, respectively. Only domains 2 and 4 were active against elastase and trypsin, respectively.

Analysis of the recombinant SPI domains using 15% SDS-PAGE revealed 2–3 more minor bands of proteins besides the major band in each SPI domain sample (Fig. 2a). Western blot analysis indicated that these bands were actually the SPI domains whose sizes were corresponding to dimer or trimer of the SPI domains (Fig. 2b). The molecular masses of the SPI domains 1–5 were determined by MALDI-TOP mass spectrometry to be 6977.09, 7148.63, 7038.239, 7453.13 and 7253.52, respectively, which were agreed well with the calculated ones. The SPI domains on SDS-PAGE, however, gave anomalous mobility probably due to their small sizes so that the mobility was not related only to the size but also the amino acid sequences. Relatively to other SPI domains, the SPI domain 5 was notably less detectable with Western blot analysis.

3.3. Inhibition assays and kinetics

The SPI domains were tested against subtilisin, trypsin and elastase. All but SPI domain 1 inhibited subtilisin with variable activity (Fig. 3a). Domain 1 has no inhibitory activity against subtilisin. Domains 2, 3 and 5 strongly inhibited subtilisin while domain 4 weakly inhibited subtilisin. Only domains 2 and 4 were active against elastase and trypsin, respectively (Fig. 3b). Domain 2 strongly inhibited elastase while domain 4 weakly inhibited trypsin.

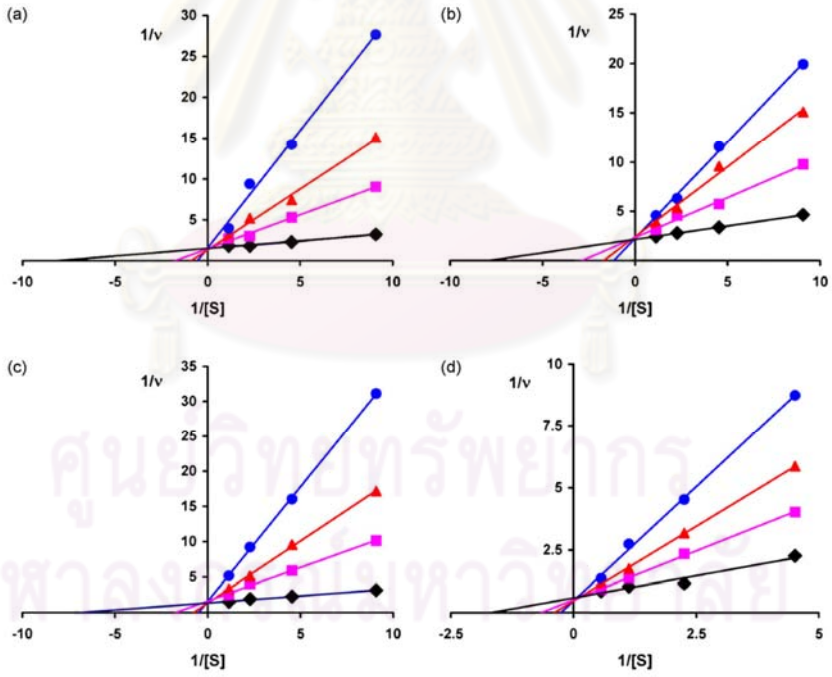

Fig. 4. Lineweaver–Burk plots of proteinase inhibition assays. The inhibition of subtilisin activity was assayed with domain 2 (a), domain 3 (b) and domain 5 (c). The inhibition of elastase activity was assayed with domain 2 (d).

Table 3
The values of V_{max}s, K_Ms and K_is for subtilisin and elastase.

	Subtilisin				Elastase	
	Domain 2	Domain 3	Domain 5	SPI*Pm*2[a]	Domain 2	SPI*Pm*2[a]
V_{max} (nmol/min)	0.6818	0.4373	0.6781	1.25	1.9877	1.49
$K_M \times 10^{-3}$ (M)	0.1611	0.1588	0.1755	0.22	0.7073	1.73
$K_i \times 10^{-9}$ (M)	1.2547	12.0303	16.4019	0.52	8.9873	3.27

[a] Data from Somprasong et al. [21].

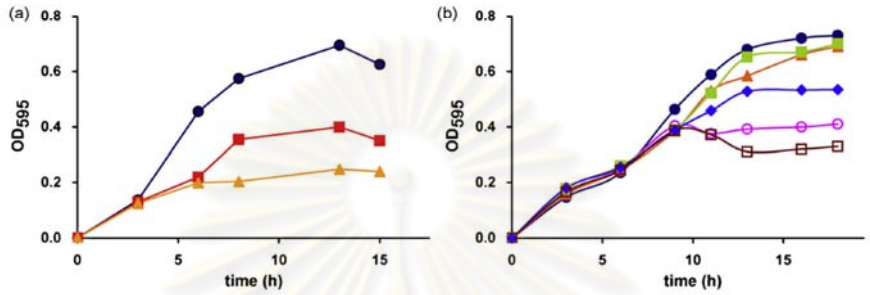

Fig. 5. Bacteriostatic activity of SPI*Pm*2 and its five domains on *Bacillus subtilis*. (a) The *B. subtilis* cultures were grown in the absence (●) and presence of 3.5 μM (■) and 7.0 μM (▲) SPI*Pm*2. (b) The *B. subtilis* cultures were grown in the absence (●) and presence of 7 μM SPI domain 1 (▲), domain 2 (○), domain 3 (■), domain 4 (◆) and domain 5 (□).

The strong inhibitory domains 2, 3 and 5 were assayed for their kinetic parameters against subtilisin and only domain 2 against elastase. Fig. 4 shows the Lineweaver–Burk plots of proteinase inhibition of the SPI domains. The apparent K_Ms obtained from the plots were used to calculate the inhibition constants (K_is). The values of V_{max}s, K_Ms and K_is are summarized in Table 3 as well as those of the SPI*Pm*2. The three SPI domains were shown to be strong inhibitors with the K_is in the range of 10^{-8} to 10^{-9} M. The V_{max}s and K_Ms were both varied with the SPI domains as compared to those of SPI*Pm*2.

3.4. Bacterial growth inhibition assay

Since the SPI*Pm*2 strongly inhibits subtilisin, an enzyme produced by several bacteria particular *B. subtilis*, the effect of inhibitor on the growth of Gram-positive bacteria, *B. subtilis*, *B. megaterium*, *S. aureus*, and Gram-negative bacteria, *V. harveyi* 639, *E. coli* JM109, was tested. The diluted culture of bacteria was grown in the presence of SPI*Pm*2 and the growth was monitored. It was found that only the growth of *B. subtilis* (Fig. 5a) but not *B. megaterium*, *S. aureus*, *V. harveyi* 639 and *E. coli* JM109 (data not shown) was inhibited. Greater growth inhibition was observed with higher concentration of SPI*Pm*2. The growth inhibitory activity was bacteriostatic since the cells continued to grow at slower pace or stopped growing. Testing the growth of *B. subtilis* with the SPI domains, domains 2 and 5 exerted stronger inhibition on growth while domains 4 had lower activity and domains 1 and 3 were relatively neutral (Fig. 5b). The SPI domains exhibited lesser growth inhibitory effect than the intact SPI*Pm*2, and the inhibition took effect quite late in the growing culture.

4. Discussion

Recently, a five-domain Kazal-type SPI, SPI*Pm*2, identified from the hemocyte EST libraries of *P. monodon* and its proteinase inhibitory activities were reported [21,28]. Being identified from the hemocyte cDNA library and expressed mainly in the shrimp hemocytes, the SPI*Pm*2 is believed to be involved in innate immunity in the shrimp [32,33]. The SPI*Pm*2 strongly inhibits subtilisin and elastase probably with the ratio of inhibitor to proteinase 1:2 and 1:1, respectively. It also weakly inhibits trypsin [21]. The reactive P1 inhibitory specificity residues in domains 1–5 are T, A, E, K and E, respectively. It is known that the inhibitory activities can be predicted from the P1 residue. The SPIs with basic amino acids at P1 position preferentially inhibit trypsin. Those with P1 bulky hydrophobic residues tend to inhibit chymotrypsin like the L residue(s) in the four-domain Kazal inhibitor from the crayfish *Pacifastacus leniusculus*. The P1 Q residue in this crayfish inhibitor is supposedly responsible for subtilisin inhibition [34]. The three-domain Kazal inhibitor from *Bombyx mori* shows strong inhibition against subtilisin but not thrombin or chymotrypsin [10]; its P1 are T, A and Q. A heat-tolerant Kazal inhibitor with the P1 R residue from the marine snail *C. muricatus* inhibits strongly both trypsin and human neutrophil elastase [25]. The 'nonclassical' Kazal-type elastase inhibitor with the P1 M residue from *A. sulcata* inhibits strongly the porcine pancreatic elastase and moderately inhibits human leukocyte elastase [22].

From the above information on P1 residue, it is tempting to speculate that the two E residues in SPI*Pm*2 are responsible for the inhibition of subtilisin, T or A residue for elastase and the K residues for trypsin. This speculation is also supported well with the work on ovomucoid third domain by Lu et al. [35]. However, the SPIs with P1 T residue from *B. mori* and *Galleria mellonella* turn out to be subtilisin inhibitors [8,36]. Thus, the assignment of inhibitory specificity to each domain is not satisfactory unless the domains are studied separately.

In this study, we had amplified and cloned each SPI domain into an *E. coli* expression vector and expressed the domain separately. The expression was not successful in the beginning probably because the SPI domain peptides were small and easily degraded once they were synthesized in the cells. Using an expression vector pVR500, the SPI domains were, however, over-expressed success-

fully as fusion proteins with thioredoxin. After purification by using a nickel-NTA column, the fusion protein was cleaved with enterokinase. Only the SPI domains which contained the His·Tag were easily purified by using another nickel-NTA column.

The purified SPI domains of SPI*Pm2* were assayed for their inhibitory activities. We found that the SPI domain 1 with the P1 T residue was inactive against the three proteinase tested although the inhibition of subtilisin could be expected [8,35]. The SPI domain 1 might be inactive domain in SPI*Pm2* or active against other proteinases not tested. It has been shown that some multidomain Kazal SPIs have at least one inactive domain, for example domain 1 in the multidomain Kazal inhibitor LEKTI appears to be inhibitory inactive [37]. Surprisingly, the SPI domain 2 with the P1 A residue was strongly active against subtilisin and slightly less active against porcine pancreatic elastase. The P1 A residue is predicted to be the most specific for porcine pancreatic elastase but not subtilisin by the Laskowski algorithm [17]. As expected, domains 3 and 5 with the P1 E residues inhibited subtilisin while domain 4 with K residue weakly inhibited both subtilisin and trypsin.

The K_is for subtilisin of the strongly inhibitory domains (domains 2, 3 and 5) were in the range of 10^{-8} to 10^{-9} slightly higher than that of SPI*Pm2* (Table 3). The K_Ms of the domains were also comparable to that of the intact inhibitor though the V_{max}s were lower. These results suggested that the separate domains were less suitable for proteinase inhibition. Similar situation was seen with elastase inhibition of SPI domain 2 where the K_i was higher, the K_M was lower, and the V_{max} was higher than those of the intact inhibitor. With the SPI domains 2, 3 and 5 able to strongly inhibit subtilisin, it was not surprising that the SPI*Pm2* was a strong inhibitor of subtilisin. Only SPI domain 2 also contributed to elastase inhibition. The inhibitory activity of SPI domain 2 led us to hypothesize that the SPI domain 2 played a major role in the SPI*Pm2* inhibition against subtilisin and elastase.

Although the actual biological function of SPI*Pm2* in the black tiger shrimp is unknown, it is believed that the SPI*Pm2* is involved in defense mechanism against microbial pathogens [32]. In particular, the strong subtilisin inhibitory activity suggested to us its activity against the bacteria that produces subtilisin [11,31]. The effect of SPI*Pm2* and its domains on the growth of Gram-positive bacteria, *B. subtilis*, *B. megaterium*, *S. aureus*, and Gram-negative bacteria, *V. harveyi* 639, *E. coli* JM109, was tested. As far as we know, only *B. subtilis* produced subtilisin. Interestingly, only the growth of *B. subtilis* was inhibited and the inhibition was bacteriostatic. The relatively stronger inhibition was observed with the intact SPI*Pm2* but not the domains. The domains 2 and 5 that strongly inhibited subtilisin inhibited the growth of *B. subtilis*. However, the SPI domain 3 that had comparable subtilisin inhibitory activity to SPI domain 2 had no growth inhibition effect while SPI domain 4 that had much less subtilisin inhibitory activity could slightly inhibit the growth of *B. subtilis*. The inhibition of growth might be due to the fact that the bacterial subtilisin was unable to digest protein in the medium and provide enough essential nutrients for the cells to grow. Nevertheless, the bacteriostatic action of SPI*Pm2* on *B. subtilis* remained to be elucidated. One might speculate from the bacteriostatic activity that the SPI*Pm2* might protect the shrimp from the potential pathogens that produced subtilisin-like proteinases.

Acknowledgments

This work was supported by a research grant from the Commission on Higher Education. A Ph.D. student fellowship to Mr. Suchao Donpudsa for the Strategic Scholarships Fellowships Frontier Research Networks from the Commission on Higher Education is greatly appreciated. We also thank the Chulalongkorn University 90th Anniversary Fund to Mr. Suchao Donpudsa and the support from Chulalongkorn University to the Shrimp Molecular Biology and Genomics Laboratory under the Ratchadaphisek Somphot Endowment.

References

[1] Cerenius L, Söderhäll K. The prophenoloxidase-activating system in invertebrates. Immunol Rev 2004;198:116–26.
[2] Jiravanichpaisal P, Lee BL, Söderhäll K. Cell-mediated immunity in arthropods: hematopoiesis, coagulation, melanization and opsonization. Immunobiology 2006;211(4):213–36.
[3] Iwanaga S, Lee BL. Recent advances in the innate immunity of invertebrate animals. J Biochem Mol Biol 2005;38(2):128–50.
[4] Laskowski Jr M, Kato I. Protein inhibitors of proteinases. Annu Rev Biochem 1980;49:593–626.
[5] Bode W, Huber R. Natural protein proteinase inhibitors and their interaction with proteinases. Eur J Biochem 1992;204(2):433–51.
[6] Laskowski M, Qasim MA. What can the structures of enzyme–inhibitor complexes tell us about the structures of enzyme substrate complexes? Biochim Biophys Acta 2000;1477(1–2):324–37.
[7] Kress H, Jarrin A, Thüroff E, Saunders R, Weise C, Schmidt am Busch M, et al. A Kunitz type protease inhibitor related protein is synthesized in *Drosophila prepupal* salivary glands and released into the moulting fluid during pupation. Insect Biochem Mol Biol 2004;34(8):855–69.
[8] Nirmala X, Mita K, Vanisree V, Zurovec M, Sehnal F. Identification of four small molecular mass proteins in the silk of *Bombyx mori*. Insect Mol Biol 2001;10(5):437–45.
[9] Morris MT, Coppin A, Tomavo S, Carruthers VB. Functional analysis of *Toxoplasma gondii* protease inhibitor 1. J Biol Chem 2002;277(47):45259–66.
[10] Zheng QL, Chen J, Nie ZM, Lv ZB, Wang D, Zhang YZ. Expression, purification and characterization of a three-domain Kazal-type inhibitor from silkworm pupae (*Bombyx mori*). Comp Biochem Physiol B Biochem Mol Biol 2007;146(2):234–40.
[11] Christeller JT. Evolutionary mechanisms acting on proteinase inhibitor variability. FEBS J 2005;272(22):5710–22.
[12] Tian M, Kamoun S. A two disulfide bridge Kazal domain from *Phytophthora* exhibits stable inhibitory activity against serine proteases of the subtilisin family. BMC Biochem 2005;6:15.
[13] Kanost MR. Serine proteinase inhibitors in arthropod immunity. Dev Comp Immunol 1999;23(4–5):291–301.
[14] Simonet G, Claeys I, Franssens V, De Loof A, Broeck JV. Genomics, evolution and biological functions of the pacifastin peptide family: a conserved serine protease inhibitor family in arthropods. Peptides 2003;24(10):1633–44.
[15] Rawlings ND, Tolle DP, Barrett AJ. Evolutionary families of peptidase inhibitors. Biochem J 2004;378(Pt 3):705–16.
[16] van de Locht A, Lamba D, Bauer M, Huber R, Friedrich T, Kröger B, et al. Two heads are better than one: crystal structure of the insect derived double domain Kazal inhibitor rhodniin in complex with thrombin. EMBO J 1995;14(21):5149–57.
[17] Lu SM, Lu W, Qasim MA, Anderson S, Apostol I, Ardelt W, et al. Predicting the reactivity of proteins from their sequence alone: Kazal family of protein inhibitors of serine proteinases. Proc Natl Acad Sci USA 2001;98(4):1410–5.
[18] Mägert HJ, Ständker L, Kreutzmann P, Zucht HD, Reinecke M, Sommerhoff CP, et al. LEKTI, a novel 15-domain type of human serine proteinase inhibitor. J Biol Chem 1999;274(31):21499–502.
[19] Kato I, Schrode J, Kohr WJ, Laskowski Jr M. Chicken ovomucoid: determination of its amino acid sequence, determination of the trypsin reactive site, and preparation of all three of its domains. Biochemistry 1987;26(1):193–201.
[20] Jiménez-Vega F, Vargas-Albores F. A four-Kazal domain protein in *Litopenaeus vannamei* hemocytes. Dev Comp Immunol 2005;29(5):385–91.
[21] Somprasong N, Rimphanitchayakit V, Tassanakajon A. A five-domain Kazal-type serine proteinase inhibitor from black tiger shrimp *Penaeus monodon* and its inhibitory activities. Dev Comp Immunol 2006;30(11):998–1008.
[22] Hemmi H, Kumazaki T, Yoshizawa-Kumagaye K, Nishiuchi Y, Yoshida T, Ohkubo T, et al. Structural and functional study of an *Anemonia* elastase inhibitor, a "nonclassical" Kazal-type inhibitor from *Anemonia sulcata*. Biochemistry 2005;44(28):9626–36.
[23] Brillard-Bourdet M, Hamdaoui A, Hajjar E, Boudier C, Reuter N, Ehret-Sabatier L, et al. A novel locust (*Schistocerca gregaria*) serine protease inhibitor with a high affinity for neutrophil elastase. Biochem J 2006;400(3):467–76.
[24] Zhu L, Song L, Chang Y, Xu W, Wu L. Molecular cloning, characterization and expression of a novel serine proteinase inhibitor gene in bay scallops (*Argopecten irradians*, Lamarck 1819). Fish Shellfish Immunol 2006;20(3):320–31.
[25] González Y, Tanaka AS, Hirata IY, del Rivero MA, Oliva ML, Araujo MS, et al. Purification and partial characterization of human neutrophil elastase inhibitors from the marine snail *Cenchritis muricatus* (Mollusca). Comp Biochem Physiol A Mol Integr Physiol 2007;146(4):506–13.
[26] Cao JX, Dai JQ, Dai ZM, Yin GL, Yang WJ. A male reproduction-related Kazal-type peptidase inhibitor gene in the prawn. *Macrobrachium rosenbergii*: molecular characterization and expression patterns. Mar Biotechnol (NY) 2007;9(1):45–55.

[27] Wang B, Zhao J, Song L, Zhang H, Wang L, Li C, et al. Molecular cloning and expression of a novel Kazal-type serine proteinase inhibitor gene from Zhikong scallop *Chlamys farreri*, and the inhibitory activity of its recombinant domain. Fish Shellfish Immunol 2008;24(5):629–37.
[28] Tassanakajon A, Klinbunga S, Paunglarp N, Rimphanitchayakit V, Udomkit A, Jitrapakdee S, et al. *Penaeus monodon* gene discovery project: the generation of an EST collection and establishment of a database. Gene 2006;384:104–12.
[29] Bradford MM. A rapid and sensitive method for the quantitation of microgram quantities of protein utilizing the principle of protein–dye binding. Anal Biochem 1976;72:248–54.
[30] Hergenhahn HG, Aspan A, Söderhäll K. Purification and characterization of a high-Mr proteinase inhibitor of pro-phenol oxidase activation from crayfish plasma. Biochem J 1987;248(1):223–8.
[31] Han Y, Yu H, Yang X, Rees HH, Liu J, Lai R. A serine proteinase inhibitor from frog eggs with bacteriostatic activity. Comp Biochem Physiol B Biochem Mol Biol 2008;149(1):58–62.
[32] Supungul P, Klinbunga S, Pichyangkura R, Jitrapakdee S, Hirono I, Aoki T, et al. Identification of immune-related genes in hemocytes of black tiger shrimp (*Penaeus monodon*). Mar Biotechnol (NY) 2002;4(5):487–94.
[33] Jarasrassamee B, Supungul P, Panyim S, Klinbunga S, Rimphanichayakit V, Tassanakajon A. Recombinant expression and characterization of five-domain Kazal-type serine proteinase inhibitor of black tiger shrimp (*Penaeus monodon*). Mar Biotechnol (NY) 2005;7(1):46–52.
[34] Johansson MW, Keyser P, Söderhäll K. Purification and cDNA cloning of a four-domain Kazal proteinase inhibitor from crayfish blood cells. Eur J Biochem 1994;223(2):389–94.
[35] Lu W, Apostol I, Qasim MA, Warne N, Wynn R, Zhang WL, et al. Binding of amino acid side-chains to S1 cavities of serine proteinases. J Mol Biol 1997;266(2):441–61.
[36] Nirmala X, Kodrík D, Zurovec M, Sehnal F. Insect silk contains both a Kunitz-type and a unique Kazal-type proteinase inhibitor. Eur J Biochem 2001;268(7):2064–73.
[37] Lauber T, Schulz A, Schweimer K, Adermann K, Marx UC. Homologous proteins with different folds: the three-dimensional structures of domains 1 and 6 of the multiple Kazal-type inhibitor LEKTI. J Mol Biol 2003;328(1):205–19.

BIOGRAPHY

Mr. Suchao Donpudsa was born on November 17, 1982 in Nonthaburi. He graduated with the degree of Bachelor of Science from the Department of Biochemistry, Faculty of Science, Chulalongkorn University in 2004. He has studied for the degree of Doctor of Science at the Department of Biochemistry, Chulalongkorn University since 2004.

He had published his works in the research journals on the topics of “Domain inhibitory and bacteriostatic activities of the five-domain Kazal-type serine proteinase inhibitor from black tiger shrimp *Penaeus monodon*”.